AN INVESTIGATION OF THE ANTIFUNGAL AND ANTITUMOR ACTIVITY OF AJOENE

A thesis submitted in partial fulfilment of the requirements for the

Degree

of Master of Biological Sciences

in the University of Canterbury

by Mandy Yang

University of Canterbury

2013

Table of Contents

Acknowledgements

This work was carried out at the School of Biological Sciences, University of Canterbury, New Zealand.

This Master's thesis was supposed to be started in 2011, but it was postponed due to the Christchurch earthquake and the complications which I experienced during my pregnancy. Restarting of the thesis was kindly supported by my supervisor Doctor Ashley Garrill in 2012. As a new Mother and a Master's student, it was always challenging to take care of both the little one and my thesis. Fortunately, I received consistent warm support from the school and my family, so that I could achieve my targets and complete the project with satisfaction.

I wish to express my sincere gratitude to my supervisors Doctor Ashley Garrill and Doctor Kenny Chitcholtan. Working under their supervision has been my pleasure. They are knowledgeable mentor to me and they guided me in every aspect of the thesis. I have been gaining not only knowledge but also inspiration from them during the supervision period.

I would like to thank my co-supervisors Doctor David Collings and Doctor Andy Pratt. Doctor David Collings provided help in imaging, materials for antibodies, and advice for my project. Doctor Andy Pratt guided me all the way through the garlic extraction with his professional chemistry knowledge. He spent a lot of time on teaching me the experimental skills on chemical extraction and on trouble shooting of my extraction experiments. I want to thank him from the bottom of my heart.

I would also like to thank our laboratory technicians and managers, Craig Galilee, Jackie Healey and Manfred Ingerfeld. They provided professional technical support whenever we demanded.

Finally to my esteemed colleagues, I received kind help and friendship from Tiffany Tan, Emma Swadel, Gloria Adjapong, Abishek Muralidhar, Freddie Prebble and Wafaa Hassan.

In a word, the help from all of you is very much appreciated.

Abstract

The garlic extract ajoene is considered to have antimicrobial and antitumor effects against a variety of cell types, and it is suggested to have the potential to be used as an antifungal or antitumor drug clinically. The underlying mechanism of its inhibitory effects is still uncertain. In this project, the effects of ajoene on the growth of fungal and oomycete cells were studied on *Candida albicans*, *Neurospora crassa* and *Achlya bisexualis*. Endometrial cancer is the most common gynecologic cancer. A 3D spheroid model of endometrial cancer cells were for the first time used to investigate the antitumor effects of ajoene and selected antitumor agents. Ajoene was extracted from fresh garlic by chromatographic methods and the outcome of the extractions was verified with Mass spectrometry and NMR spectroscopy. Ajoene was then tested on the yeast form or germ tubes of *C. albicans*, and the cell division and germ tube formation was analyzed. *N. crassa* and *A. bisexualis* were treated with ajoene on plates or on glass slides to measure the hyphae radial extension or individual hyphal extension. 3D endometrial adenocarcinoma cell (Ishikawa) spheroids were treated with ajoene, paclitaxel, targeted drugs everolimus, sorafenib, gefitinib and canertinib alone or in combinations. The growth activity, metabolic activity, cell proliferation, apoptotic activity and the cytoskeletons were analyzed after the treatments.

Cell division of *C.albicans* was inhibited by ajoene at 5µg/ml or higher concentrations. The length of *C.albicans* germ tubes was significantly shorter in ajoene treated groups than the untreated ones. Radial extension and individual hyphal extension of *N. crassa* and *A. bisexualis* were both inhibited by ajoene. Ajoene did not show any antitumor effects on the 3D cell model of Ishikawa cells. No synergistic effect was detected between ajoene and paclitaxel or ajoene and everolimus. The targeted drugs Canertinib and everolimus showed an inhibitory effect on growth activity of the spheroids, but no synergy with paclitaxel. In conclusion, ajoene was able to inhibit various forms of fungal and oomycete growth, but any antitumor activity of ajoene did not show on 3D culture of endometrial cancer cells.

Abbreviations

MAPK: mitogen-activated protein kinase

Bcl-2: B-cell lymphoma/leukemia-2

Apaf-1: apoptotic protease activating factor 1

Akt: serine/threonine specific protein kinase

P-Akt: phosphorylated Akt

PTEN: phosphatase and tensin homologue

MIC: minimum inhibitory concentration

ROS: reactive oxygen species

HPLC: high performance liquid chromatography

TLC: thin layer chromatography

UV: ultra violet

MS: mass spectrometer

NMR: Nuclear magnetic resonance

DMSO: dimethylsulfoxide

PBS: phosphate buffer saline

EGFR: epidermal growth factor receptor

mTOR: mammalian target of rapamycin

VEGF: vascular endothelial growth factor

ECM: extra- cellular matrix proteins

HER-2: human epidermal growth factor receptor 2

FKBP12: FK506-binding protein 12;

mTORC1: mammalian target of rapamycin complex 1;

mTORC2: mammalian target of rapamycin complex 2;

PDK: phosphoinositide-dependent kinase;

PCNA: proliferating cell nuclear antigen

PARP: poly (ADP-ribose) polymerase

PI3K: phosphatidylinositol 2 kinase;

PIP_2: phosphatidylinositol 4,5-bisphosphate;

PIP_3: phosphatidylinositol (3,4,5)-trisphosphate

SDS: sodium dodecyl sulfate

SDS-PAGE: sodium dodecyl sulfate polyacrylamide gel electrophoresis

RIPA buffer: radioimmunoprecipitation assay buffer

GAPDH: glyceraldehyde 3-phosphate dehydrogenase

PVDF: polyvinylidene difluoride

BSA: bovine serum albumin

Chapter 1- Introduction

Natural therapeutic products

Many natural products are used in traditional herbal medicine or are believed to be beneficial to health. The therapeutic effects of these natural products are increasingly proven by modern science. For example, leaves of *Wedelia chinensis* are traditionally used in infections and skin diseases. Ethanol and hexane extract of *Wedelia chinensis* leaf were tested on bacterial and fungal species with a disc diffusion method, and the extract showed strong inhibitory effects on bacterial strains including *Staphylococcus aureus* and *Salmonella typhimurium*, and fungal stains including *Aspergillus niger* and *Candida albicans* (Das, Jeyanthi, & Sharmila, 2013). *Blechnum orientale* leaves are believed to have good medical value for treating diarrhoea and stomach problems. The pet-ether, chloroform, methanol and aqueous extract of *Blechnum orientale* fronds were incubated with several bacterial strains in 96 well plates and with fungal strains in tubes, and the minimum inhibitory concentrations were determined after the incubation. The four extracts were able to inhibit the growth of *Pseudomonas aeruginosa*, *Escherichia coli* and *C.albicans* (Deepa, Parashurama, Krishnappa, & Nataraja, 2013).

In Brazil, plants from the *Mikania* genus have been widely used in the treatment of respiratory disorders and many inflammatory diseases. Interestingly, hexane and ethanol extracts of *Mikania laevigata* were tested on two cancer cells lines. For the human Larynx carcinoma cell line HEp-2 and cervix adenocarcinoma cell line HeLa, and an non-tumor cell line MRC-5, the extracts of *Mikania laevigata* were found to selectively inhibit the proliferation of the cancer cells (Rufatto, Finimundy, Roesch-Ely, & Moura, 2013). Another example of a plant with antitumor activity is rosemary. The extract of dried *Rosmarinus officinalis* (Rosemary) leaves have been incubated with human colon cancer cells SW620 and DLD-1 in 96 well plates, and the rosemary induced cell death was detected by various assays (González-Vallinas et

al., 2013). Moreover, the green tea extract EGCG and grape extract resveratrol were both found to have antitumor effects on various cancer cell types *in vitro* and *in vivo*, suggesting the potential of treating cancers with nutraceuticals. (Zlotogorski et al., 2013).

Garlic extract, allicin and ajoene

Of the therapeutic plant extracts, garlic is one of the oldest plants used for treatment of diseases and as a heath supplement (Bhandari, 2012). Nowadays, scientists are trying to verify the therapeutic effects of garlic by scientific researches and it has been confirmed to have antibacterial, antifungal, antivirus, immunostimulating and antioxidant activities. The biological activities are thought to be due to the abundant active sulfur containing compounds that are found in garlic (Iciek, Kwiecień, & Włodek, 2009). There are at least 33 sulfur containing compounds in garlic, these include water soluble ones such as *S*-allylcysteine, and oil soluble ones such as allicin (allyl 2-propenethiosulfinate) (Bhandari, 2012; Iciek et al., 2009). Allicin does not exist in intact garlic bulbs. It is produced during the crushing of garlic.

Allicin has been confirmed to be the most biologically active compound among the sulfur containing compounds in garlic. It has antimicrobial activities towards a variety of microorganisms, such as the bacterial strains *Escherichia coli* and *Staphyloccocus aureus* (Ankri & Mirelman, 1999), and fungal strains *C.albicans* and *Trichophyton rubrum* (Aala, Yusuf, Jamal, & Khodavandi, 2010; Guo et al., 2010). Unfortunately, allicin is very unstable at normal body temperature (Freeman & Kodera, 1995). Therefore, allicin may not be responsible for therapeutic effects of garlic and the instability of allicin has limited its use as a potential treatment of diseases.

Ajoene (4,5,9-thrithiadodeca-1,6,11-triene 9-oxide), which is one of the degradation products of allicin, is suggested to be more stable and have

antithrombotic, antifungal and antitumor activities (Block et al., 1984; Erkoc, Sumerb, & Erkoc, 2003; Naganawa et al., 1996). It is a mixture of two isomers, Z-ajoene and E-ajoene, and it can be obtained from garlic by mixing garlic with edible oils.

Antifungal activities of ajoene

Fungal infections in healthy humans are mostly caused by a limited number of fungal species. The majority of fungal species that cause disease will do so mostly on immunocompromised individuals. For example, *Candida* infections and mould infections, such as *Aspergillus* infections and some environmental filamentous fungi, are common major causes of severe infections on susceptible bodies, unfortunately a lot of the moulds are resistant to commonly used antifungal drugs (Araujo, Pina-Vaz, & Rodrigues, 2010). Ajoene has shown inhibitory effects against a broad spectrum of fungal species *in vitro*, *in vivo* and in clinical trials, and it has a potential to be used as a novel antifungal drug in the clinic. In 1987, Yoshida's group incubated *A. niger* and *C.albicans* with ajoene or allicin on Sabouraud medium and the fungal growth was assessed by measuring the dry weight of the culture after incubation. The authors found that ajoene exhibited stronger antifungal effects against these two microorganisms than allicin. The effects of ajoene on hyphae of *A.niger* were further observed by scanning and transmission electronic microscopy. The authors suggested that ajoene was able to induce hyphae surface depression and the detachment between cell membrane and cell wall (S. Yoshida et al., 1987).

Maluf's group infected mice with *Paracoccidioides brasiliensis*, and the mice were then treated with synthesized ajoene by intraperitoneal injection. After the treatment, ajoene reduced the levels of anti-*P. brasiliensis* antibodies and reversed the symptoms of *P. brasiliensis* infection which included granulomas in the spleen, liver and abdominal cavity (Maluf et al., 2008).

Ajoene has also shown its ability to be effective against fungal infection in humans. The fungus *Cladophialophora carrionii* causes chromoblastomycosis in

humans. The disease is one of the most common mycosis in tropical areas, and causes localized lesions on skin and subcutaneous tissues. The lesions can be classified into several types, nodular, tumorous, verrucous, plaque and scarring. The severe cases of the infection may cause a combination of more than one types of lesions and spreading of the fungus into the blood or lymphatic vessels. Perez-Blanco et al. (2003) treated two groups of patients who had localized lesions by applying gel containing 0.5% ajoene or gel containing 1% 5-fluorouracil on the skin, and the cure rate was comparable between these two groups. The ajoene treated group had less skin damage and lower rates of relapse (Pérez-Blanco, Valles, Zeppenfeldt, & Apitz-Castro, 2003).

Antitumor activities of ajoene

Besides antifungal activity, ajoene is also believed to have antitumor activity. Cancer is one of the most public concerning diseases (Milner & Romagnolo, 2010). It is ranked as the second cause of health loss (after cardiovascular disease) in the world (Soeberg, 2012). The antitumor activity of ajoene has been tested on many cancer cell lines *in vitro* and solid tumors *in vivo*. For example, it is able to cause cell death to human promyelocytic leukemia HL-60 cell line by inducing reactive oxygen species and activation of apoptosis (Dirsch, Gerbes, & Vollmar, 1998). Li et al. (2002) used Z-ajoene for treating nasopharyngeal carcinoma cell line, promyelocytic leukemia HL-60 cell line, and several other cells lines *in vitro*, the growth of the cancer cells were inhibited significantly, and the HL-60 cancer cells were arrested at G2/M phase of their cell cycle. The authors then tested the *in vitro* effects of ajoene on tubulin, and the tubulin assembly was blocked by ajoene in a dose dependent manner (Li et al., 2002). Taylor's group induced melanoma tumor on mice by injection of melanoma cells, and ajoene was injected afterwards to treat the metastatic and primary tumors. The number of metastases in lung and the size of the primary tumor were both reduced significantly by ajoene (Taylor et al., 2006). Furthermore, twenty one patients with skin cancer basal cell carcinoma were treated with ajoene by applying ajoene

cream on their affected skin, and the local application of ajoene reduced the tumor size in 17 of the 21 patients (Tilli et al., 2003).

Growth patterns of fungal cancer cells

The underlying mechanism of the antifungal and antitumor activity of ajoene is still uncertain. Fungal cells and tumor cells are two distinct cell types, and they employ various growth patterns.

Apical growth of fungal and oomycete cells

Fungal cell growth can be divided into two types, the apical form of growth and the yeast form of growth. Apical growth (tip growth) is the extension of the predominant vegetative cell form of fungi, the hypha. It is a form of growth displayed in oomycete hyphae, root hair cells, algal zygotes and pollen tubes. The apical growth of hyphae can be described as the continuous extension of the plastic and deformable tip (the extension zone), with locally synthesized cell wall components. When the hypha is growing, the formed hyphal part ages and does not grow, and the growth only occurs on the tip or at a branching point. When a hypha extends, the viscoelastic cell wall at the hypha tip is synthesized at the same rate as the extension. Materials required for the new wall synthesis are continuously delivered to the tip of hypha by vesicles and other cytoplasmic components. The cytoplasm is drawn towards the tip while the hypha grows (Deacon, 2009).

Analysis of the ultrastructure of fungal hyphae further confirmed the pattern of apical growth (Fig.1.1). The arrangement of fungal organelles from the tip to the base of a hypha shows a clear polarity. The tip end contains a cluster of vesicles and they are moved to the tip when hypha extends. The vesicles contain materials for cell wall synthesis including chitin and glucan synthase, and the cluster of vesicles is termed the SpitzenkÖrper. Sub-apical to this, there is a mitochondria rich zone which is thought to be responsible for providing the energy for movement of nutrients to the tip.

Further back is the branched tubular vacuoles zone which may be responsible for transporting the metabolites (Deacon, 2009).

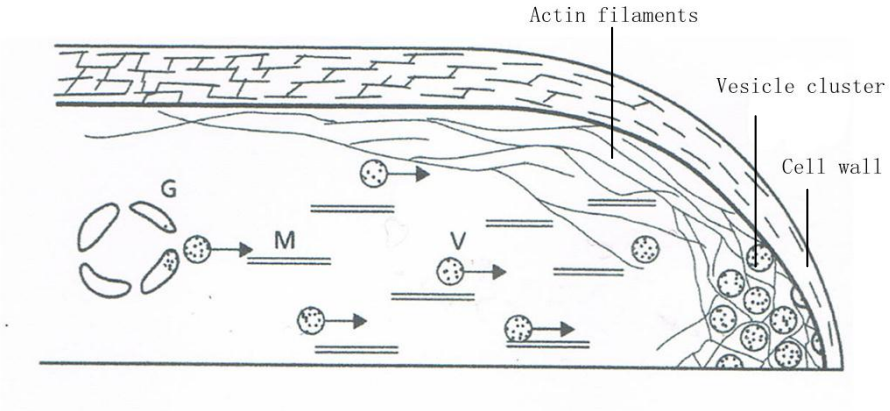

Figure 1.1. Hypha extension model of filamentous organisms. Vesicles are transported to the cell apex and form a cluster that function in wall synthesis. The cell wall at the cell apex is considered to be softer and with less crosslinks than the wall further back.

M: microtubule associated motor proteins

V: Vesicles which are transported to the hyphal tip by cytoskeleton.

The image is reproduced from Deacon, J. W. (Deacon, 2009)

The driven force of the tip growth is suggested to be related to turgor pressure at the tip and possibly cytoskeletal components (microtubules and actin filaments) (Deacon, 2009). Turgor pressure is the internal hydrostatic pressure which provides a force that drives cellular expansion. Turgor is created by osmosis that occurs in response to the concentrations of osmotically active substances being higher within the cell than in the surrounding environment. During the process of cell growth, the cell expands as a result of water flow and the cell wall is continuously restructured to response to the volume and pressure change. In order to regulate and maintain the turgor pressure under a changing extracellular environment, the osmolyte synthesis and ion accumulation are possibly regulated by osmotic mitogen-activated protein kinase (MAPK) pathway (Lew, 2011). However, there are some evidence that turgor does not play a role as the driven force of growth in some hyphal cells. For example, oomycetes *Achlya bisexualis* and *Saprolegnia ferax* have been found to be able to grow without a measureable turgor (Money & Harold, 1993); and a *slime* variant of *Neurospora crassa* was found to be able to grow in the absence of cell wall (Emerson, 1964). Thus, for these hyphal cells, it is suggested that cell growth may be mainly driven by cytoskeletal components (Deacon, 2009).

Role of the cytoskeleton in apical growth

Microtubules and actin filaments are components of the cytoskeleton which exist in all eukaryotic cells. They have important roles in cell growth, division, shape maintenance, vesicle transport and movement. Microtubules are composed of multiple protofilaments, which are formed by tubulin heterodimers joining head to tail. The protofilaments are assembled to form the helical cylinder wall that makes a microtubule. As the tubulin subunits are α and β tubulin heterodimers, the assembled microtubules are polarized, with the β end termed the plus end and α end termed the minus end. The microtubules are dynamic, which means the length, location and number of them can be changed easily by addition or disassociation of tubulin subunits to/from the microtubules. The addition of subunits tends to take place at the plus end and the disassociation of subunits tends to take place at the minus end. Actin

filaments are formed by two parallel protofilaments that twist around each other. The actin subunits which form actin protofilaments are monomers. Similar to microtubules, actin subunits also join head to tail to generate a polarized actin filament, and the addition of subunits tends to happen at the plus end (Alberts et al., 2002).

In polarized apical growth, dynamic microtubules and actin filaments are thought to be crucial for establishing and maintaining cell polarity for the growth process, and also are required for delivering the vesicles for polarized cell extension. Microtubules are thought to deliver the "cell end marker" proteins to cell pole, in order to organize the actin cytoskeleton for subsequent transport of vesicles to the cell end (Fischer, Zekert, & Takeshita, 2008). It is also possible that in low turgor cells, the actin cytoskeleton could provide a protrusive force at the tip (Heath & Steinberg, 1999).

Yeast form growth in fungi

In the other form of fungal growth, yeast growth, the fungal cells employ a repeated "budding" (or fission) process to produce single cells. The young cell is called a daughter cell and the cell which it originates from is called the mother cell. In the beginning, daughter cells bud from a designated position on the mother cell by channeling of the cell wall components to the bud tip. DNA synthesis and duplication of the mother nucleus is processed by mitosis (the process of mitosis will be explained in the later paragraphs) when the budding process starts. When the wall components are uniformly formed for the daughter cell by the mother, one of the nuclei enters the daughter cell, and cytokinesis starts to separate them into two single cells. The budding process is also a form of polarized growth (Fig.1.2). When mother cell develops the first bud, it emerges at one of the poles of the mother cell, and initially the bud grows in a polar manner towards the upper pole of the daughter cell. After the first daughter cell is separated from the mother cell, there is a scar left on the first budding point. The point for the next bud will be adjacent to the scar, and there will be a mark and a ring of septin proteins placed on the new point before the second budding, so that the actin filaments and septum can be directed to this point rapidly for the second budding. During the whole process, many of the cellular components

arrange asymmetrically. Some yeast cells grow in the way of fission, which means that the yeast cells are cylindrical and they extend in both ends. The cells divide when they reach a critical volume (Deacon, 2009).

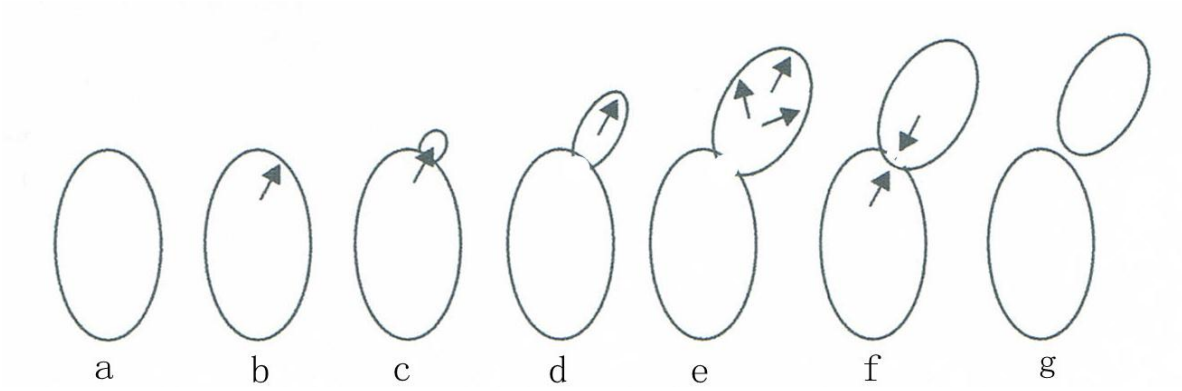

Figure 1.2. The polarized budding process of yeast.

a. A yeast cell. **b.** The mother cell is preparing for budding on the planed budding point. **c.** Emergence of the bud tip on the budding point. **d.** Initially the bud grows towards its upper pole. **e.** As the bud grows to a critical size, wall expansion happens in all directions of the bud. **f.** A septin ring is formed between the daughter and mother cells. **g.** The daughter cell is separated from the mother cell.

The drawing is reproduced from Deacon, J. W. (Deacon, 2009)

Role of cytoskeleton in yeast form growth

Microtubules and actin filaments are important in yeast cell polarity and the processes of budding and fission. In addition, during mitosis of cells, microtubules and actin filaments are assembled specially. After the chromosomes are replicated, the microtubules and accessory proteins are assembled to form bipolar mitotic spindles, and they separate the chromosomes and allocate one copy to each daughter cell. Then the actin filaments and myosins form a contractile ring or cell plate that facilitates cell division (Alberts et al., 2002).

Germ tube formation

Some fungi, such as *C. albicans*, can grow in both a yeast and a hyphal form. These fungi are called dimorphic fungi and the dimorphism allows them to adapt to various environmental conditions (Ruiz-Herrera, 2012). The transition of cell growth from a budding to a hyphal form is recognized by a phenomenon called germ tube formation, as a young hypha like tube extended from yeast cell (Munin, Giroldo, Alves, & Costa, 2007).

Fig. 1.3 shows the cell cycle that underlies the germ tube formation. The germ tube extends through a band of septin proteins. The polarisome and Spitzenkörper initially drive the polarized extension of the germ tube. When the germ tube extends to a certain length, a septin ring forms and the spindle body, which is responsible for the separation of chromosomes, is duplicated at this time. The septin ring then travels down and the nuclei travels up together with short spindles to the position of septin ring. The movement of nuclei is facilitated by microtubules. After the chromosomes are condensed, the spindles elongate to drag the chromosomes apart, one to the newly formed germ tube, the other to the basal cell. Finally, the septin ring constricts the cells and there is a septum formed between the hypha and basal cell to separate the two cells. However, the two cells are still attached (Gladfelter & Berman, 2009).

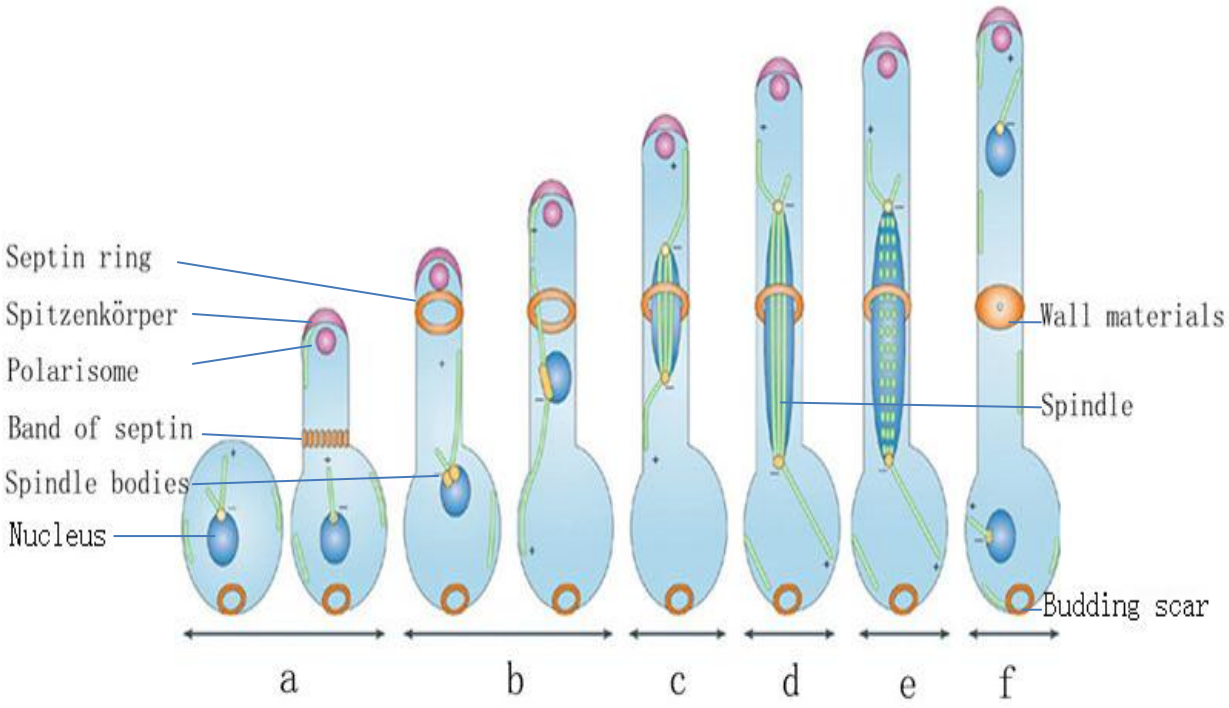

Figure 1.3. The process of germ tube formation and cell division.

a. The cell prepares for germ tube formation by DNA replication and reproduction of cytoplasmic components. The septin band forms at the boundary between the germ tube and basal cell. **b.** The septin ring and new spindle body form. The septin ring and nuclei travel towards each other. **c.** Nuclei travel to the position of septin ring. **d. and e.** Spindles drag the chromosomes apart and the nuclei are separated, and the spindles are dissolved after the process. **f.** Cells are separated by septin ring and the wall materials form between the new hypha and basal cells.

The figure is reproduced from Gladfelter & Berman (2009). (Gladfelter & Berman, 2009)

Animal cell growth

Cell cycle in normal and cancer cells

Somatic animal cells including cancer cells reproduce by division. The time of the process from the start point when a cell is generated from its mother cell to its own division is termed the cell cycle. The cell cycle can be divided into two periods, interphase and mitosis. Interphase covers almost 90% of the cell cycle, and it is a period for synthesis and growth. It can be further divided into 3 phases, G_1 (first gap), S (synthesis) and G_2 (second gap). Chromosomes of the cell are replicated in S phase and the proteins and cytoplasmic components are reproduced during the whole interphase (Alberts et al., 2002).

Mitosis (M) is the period during which the cell divides, and it is further divided into prophase, prometaphase, metaphase, anaphase, telophase and cytokinesis. During prophase and prometaphase, the replicated chromosomes condense and are released from the nuclear envelope. Then in the later phases, the microtubules formed mitotic spindles attach the kinetochores of the chromosomes and pull the chromosomes to the spindle poles. In telophase, the chromosomes de-condense and a new nuclear envelope forms, so that each nucleus contains one copy of the genome. In the final stages of division, actin filaments and myosin constrict the middle of the cell and clave the cell into two daughter cells (Bolsover, Shephard, White, & Hyams, 2011).

Cancer cells have the feature of continuous division and an absolute proliferative rate. In normal cells, the cell cycle is regulated by cell cycle regulators during interphase. Normal cells can respond to extracellular signals through the regulators at G_1 phase and exit from the cell cycle by entering G_0 (resting) phase. In contrast, cancer cells have a perturbed G_1 checkpoint control, and cell cycle exit is prevented by overriding the regulators and pathways, such as mutation on cell cycle regulation gene *P53*. Therefore, cancer cells are unable to exit the cell cycle (Sherr, 1996).

Cell death in normal and cancer cells

In animal organs, homeostasis is maintained through the elimination of unnecessary cells by cell death. Apoptosis is one important type of cell death, and it is characterized by cytoplasmic shrinkage, membrane blebbing, chromatin condensation, nuclear fragmentation, DNA fragmentation, and the formation of apoptotic bodies with cytoplasmic content. There is no inflammation involved in this type of cell death. Caspases, which are cysteine-dependent aspartic acid-specific proteases, are the most important compounds responsible for apoptosis. During apoptosis, caspases cleave vital cellular substrates, therefore inducing cell death (Reimann & Schmitt, 2007).

The activation of apoptosis is suggested to be mainly achieved by either extrinsic or intrinsic signals. The extrinsic signal is released by the activation of cytoplasmic membrane based death receptors and their downstream caspases. DNA damage and cytotoxic drugs induce intrinsic signals that are mediated by the mitochondria. The B-cell lymphoma/leukemia-2 (Bcl-2) protein regulators destabilize the mitochondria, and then the mitochondria release cytochrome-c and subsequently cause the oligomerization of apoptotic protease activating factor 1 (Apaf-1) and formation of apoptosome. The apoptosome can then activate caspases and induce proteolysis to the cell (Reimann & Schmitt, 2007).

Continuous proliferation and suppressed apoptosis are common events in cancer progression. To achieve these, cancer cells have altered survival signaling pathways such as deregulated expression of the survival factors, activating mutations of survival signal inducer Akt (a serine/threonine specific protein kinase), or mutation on Akt suppression associated *PTEN*. Some cancer types are found to be able to overexpress some anti-apoptotic proteins and stabilize the mitochondria. Moreover, loss of Apaf-1 is also suggested in some tumors as a way of apoptosis suppression (Evan & Vousden, 2001).

Aim of the study and cell models selected

Aims and cells

As stated previously, the underlying mechanism of the effects of ajoene on fungal and tumor growth is still unsure. The mostly supported hypotheses are microtubule assembly inhibition and oxidative stress induction, or both (Dirsch et al., 1998; Li et al., 2002; Scharfenberg, Wagner, & Wagner, 1990). Disulfide bonds in ajoene are believed to be the central structure responsible for its biological activity (Kaschula et al., 2012).

In the present project, ajoene's antifungal and antitumor activities were studied. In order to investigate the effects of ajoene on yeast and hyphal forms growth, ajoene was used to treat yeast and germ tube form *C. albicans*, and hyphae of *A. bisexualis* and *Neurospora crassa*. Its antitumor activity was tested by treating human endometrial adenocarcinoma cancer with ajoene *in vitro*.

Endometrial cancer

Human endometrial is the seventh most common malignant disorder worldwide, and is the commonest cancer of the female genital tract in developed countries (Amant, Moerman, Neven, & Timmerman, 2005). Most cases are diagnosed when vaginal bleeding after the menopause is reported. For patients who are diagnosed at an early stage of endometrial cancer, hysterectomy (surgical removal of tumor) is curative. However, advanced stage and high grade endometrial cancers have a poor prognosis (Leslie, Thiel, & Yang, 2012).

There are different means of classification in endometrial cancer. The disease can be divided into several stages according to the histopathology, or two subtypes based on the underlying pathogenesis. Type-I is normally a lower grade cancer and it is believed to be estrogen related (Leslie et al., 2012). The structure and cells of the human endometrium change in response to fluctuations of estrogen and progesterone during the menstrual cycle. Long term exposure to estrogen induces endometrial hyperplasia, and increases the chance of development of type-I endometrial cancer

(Amant et al., 2005). The type-I endometrial cancer is frequently found to have mutations of the cell proliferation marker Akt suppressor PTEN. The type-II endometrial cancer is poorly differentiated and often high grade, and it has been suggested to be estrogen-independent. The mutations frequently associated with type-II endometrial cancer are of the cell cycle regulator p53 (Leslie et al., 2012).

Chemotherapy is used for the treatment of the metastatic stage of the disease. Drugs clinically used for chemotherapy are still limited to cytotoxic drugs which induce apoptosis in the cells (Markman, 2007). Targeted therapy using growth factor inhibitors has also shown beneficial effects in clinical trials, but is still under investigation (Leslie et al., 2012). In this study, ajoene was tested on a 3D endometrial cancer cell culture not only by the use of it alone, but also in combination with cytotoxic and targeted drugs. The aim of using the combination was to detect any additional or synergistic effects between these drugs.

3D cancer cell culture

The cancer cell culture we used in this study was 3D spheroid model. When cancer cells are cultured on an adherent surface, they form 2D monolayers which adhere to the surface. By contrast, cancer cells undergo spontaneous homotypic aggregation on non-adherent surfaces (Chitcholtan, Asselin, Parent, Sykes, & Evans, 2013). These multicellular structured tumor spheroids are believed to be closely associated with solid tumors. Intercellular adhesion within the spheroids is achieved by interactions between cadherin proteins. Adjacent cells in the spheroids can be connected by gap connections, which allow exchange of cytoplasmic components between the cells. It is suggested that in a 3D spheroid culture, intercellular signaling pathways are able to regulate cell survival and apoptosis resistance. Although the model has only been used in *in vitro* tumor experiments recently, the 3D spheroid culture is believed to be more accurately mimic the *in vivo* growth and microenvironments of tumors (Bates, Edwards, & Yates, 2000).

In the following chapters, the detailed extraction of ajoene, antifungal experiments and antitumor experiments will be explained and discussed separately.

Chapter 2 - Garlic extraction

Introduction

Ajoene (4,5,9-thrithiadodeca-1,6,11-triene 9-oxide, $C_9H_{14}OS_3$, scheme 2.1) was firstly discovered and extracted from garlic by Block's research group in 1986. It is a mixture of two isomers, E isomer and Z isomer (Block, Ahmad, Catalfamo, Jain, & Apitz-Castrozd, 1986). Garlic contains a considerable high amount of alliin (S-allylcysteine S-oxide) and an enzyme allinase, which can convert alliin to allicin (allyl 2-propenethiosulfinate) at room temperature (Block et al., 1984). Block's group reported that allicin would then undergo a slow decomposition at room temperature and yield ajoene. To test their hypothesis, they obtained ajoene by extraction from fresh garlic and also by synthesizing it from allicin. In their methods of extraction, they mixed garlic with methanol and extracted it with organic solvents based on the polarity of the compound of interest, and the final separation was achieved by flash chromatography (Block et al., 1986).

Since the discovery of ajoene, there are numerous reports that suggest antithrombotic and antimicrobial activities of ajoene (Block et al., 1984; Naganawa et al., 1996; San-Blas, San-Blas, Gil, Marino, & Apitz-Castro, 1989). Increasing numbers of scientific communities have shown particular interests in the biological activity of ajoene and attempted to extract and purify it from garlic. Yoshida and co-workers for example extracted ajoene from garlic and tested it on various microbial organisms (S. Yoshida et al., 1987). It was suggested that ajoene could be extracted by mixing garlic with rape seed oil and this was further purified with HPLC (H. Yoshida et al., 1998). Recently, scientists also managed to extract ajoene from garlic by mixing garlic with ethanol or animal lipids (Kay et al., 2010; Shin et al., 2012). Currently, there is no analytical grade ajoene or allicin commercially available for research purposes. Therefore, in this project, ajoene was extracted from fresh local garlic using the methods described by Block's research group. The results presented

here were obtained from four independent experiments.

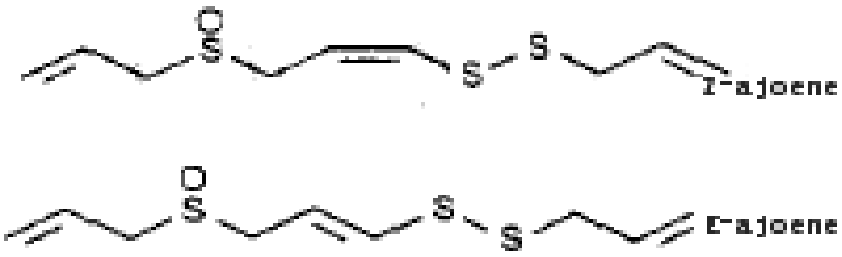

Scheme 2.1. The skeletal structures of Z and E isomers of ajoene (Block et al., 1986).

Materials

Fresh New Zealand garlic was obtained from the local supermarket Count Down on Riccarton Road, Christchurch. Analytical grade organic solvents including methanol, ether, pentane, methylene chloride and ethyl acetate were purchased from Ajax Chemicals Limited (New Zealand). Silica gel 60, which had a 230-400 mesh, was purchased from Sigma-Aldrich Limited (New Zealand).

Methods

For each extraction, six hundred grams (600 g) of fresh New Zealand garlic was peeled and mashed. The mashed garlic was soaked in 1 L of methanol and then placed on an orbited shaker set at 70rpm at 20°C for 72 hours. The methanol was removed every 24 hours during the incubation. The removed methanol was combined to give 3 L of methanol, which was then filtered to remove any solid materials, and the filtrate was then concentrated with a rotary evaporator to obtain the amount of 100 ml. The concentrated soluble material was then purified with ether, pentene and methylene chloride to remove unwanted compounds, and finally the partial purified solution, which was the methylene chloride extract, was subjected to silica/ ethyl acetate flash chromatography for further separation.

Silica gel 60 was placed in a 15cm x 2cm column and packed with ethyl acetate. The partial purified crude extract was loaded on the silica gel and eluted with ethyl acetate under pressure. Twenty four to 30 fractions of eluate were collected and tested with thin layer chromatography (TLC). The presence of active compounds was observed under ultra violet (UV) light. The active fractions which had same retention time on silica gel/ethyl acetate TLC were combined and tested using mass spectrometry (MS, acquisition parameters are shown in appendix 2.1) and NMR spectroscopy to detect the presence of ajoene. The fraction which contained ajoene was evaporated to remove any solvent. The ajoene oil was diluted to 5 mg/ml with 10% DMSO (dimethylsulfoxide) and stored at -20°C (Dirsch et al., 1998). The stock

solution was further diluted with phosphate buffer saline (PBS) before being used for *in vitro* manipulations.

Results and discussion for each extraction

In this project, I extracted ajoene from four independent attempts. The results of these extractions were somewhat variable as described below.

First extraction

In this extraction, after washing with organic solvents, 0.32 g of crude material was subjected to silica gel/ethyl acetate flash chromatography. Twenty four tubes of fractions were collected from flash chromatography. The fractions which quenched UV light were tested on TLC, and the eluates showing the same retention time were combined. The TLC plate of the active fractions from this extraction was shown in Fig.2.1. Based on the similarity of retention times on the TLC plate, the fractions tube 4 and 5 were combined and tube 7 was combined with tube 8. Fraction tube 10 was combined with 11. Fraction tube 12 was combined with 13, 14 and 15. These combinations were then tested using MS and NMR spectroscopy. Ajoene was detected in the combined fractions 7- 8. The MS for fractions 7- 8 is shown in Fig.2.2 and the NMR spectroscopy data is shown in Fig.2.3.

The mass spectrometer created charged particles (ions which are H^+ and Na^+ forms of ajoene) from ajoene molecules. The ions were then analyzed by measuring the mass/charge ratio to provide information about the molecular weight of the compound (University of Arizona). The molecular weight of ajoene is 234.4, and H^+ and Na^+ forms of ajoene were detected in fractions 7-8 with a molecular weight of 235.0277 and 257.0099. Therefore, the composition of this compound was confirmed by MS to be consistent with the composition of ajoene.

NMR spectroscopy measures the resonant frequencies of the nuclei in the compounds and provides structural information about the compound. The distinct peaks of *cis* and *trans* ajoene were identified by NMR and common peaks were also

displayed on the result (Fig 2.3). The NMR data was consistent with the NMR data of ajoene in literature. Therefore, the structure of the compound in fractions 7-8 represented a mixture of E and Z isomers of ajoene.

Based on these results, ajoene appeared to be present in the fractions that had moderate elution rates (Fig 2.1). There were still some impurities as shown in NMR spectroscopy result (Fig 2.3), but they were unlikely to affect the activity of the ajoene. Therefore, the solute in tubes 7-8, which had a final weight of 10mg, was diluted with DMSO and used in subsequent antifungal and antitumor experiments. The garlic extract from first extraction will be termed "1GE" in the following chapters.

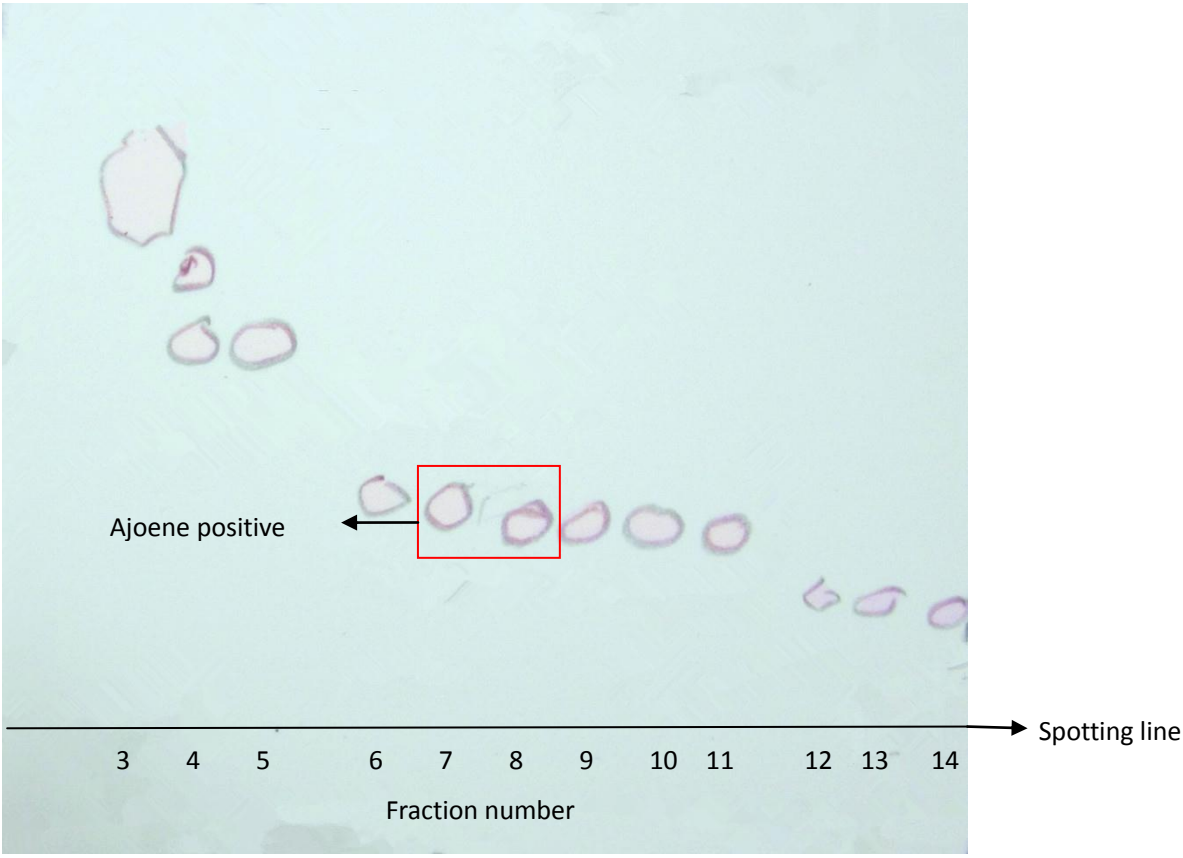

Figure 2.1. TLC plate of the fractions collected from flash chromatography for the first garlic extraction. On this plate, Fractions 4 and 5; fractions 7 and 8; fractions 10 and 11; and fractions 12, 13, 14 and 15 were combined respectively and tested using MS. Fractions 7-8 combination was found to contain ajoene based on the MS data.

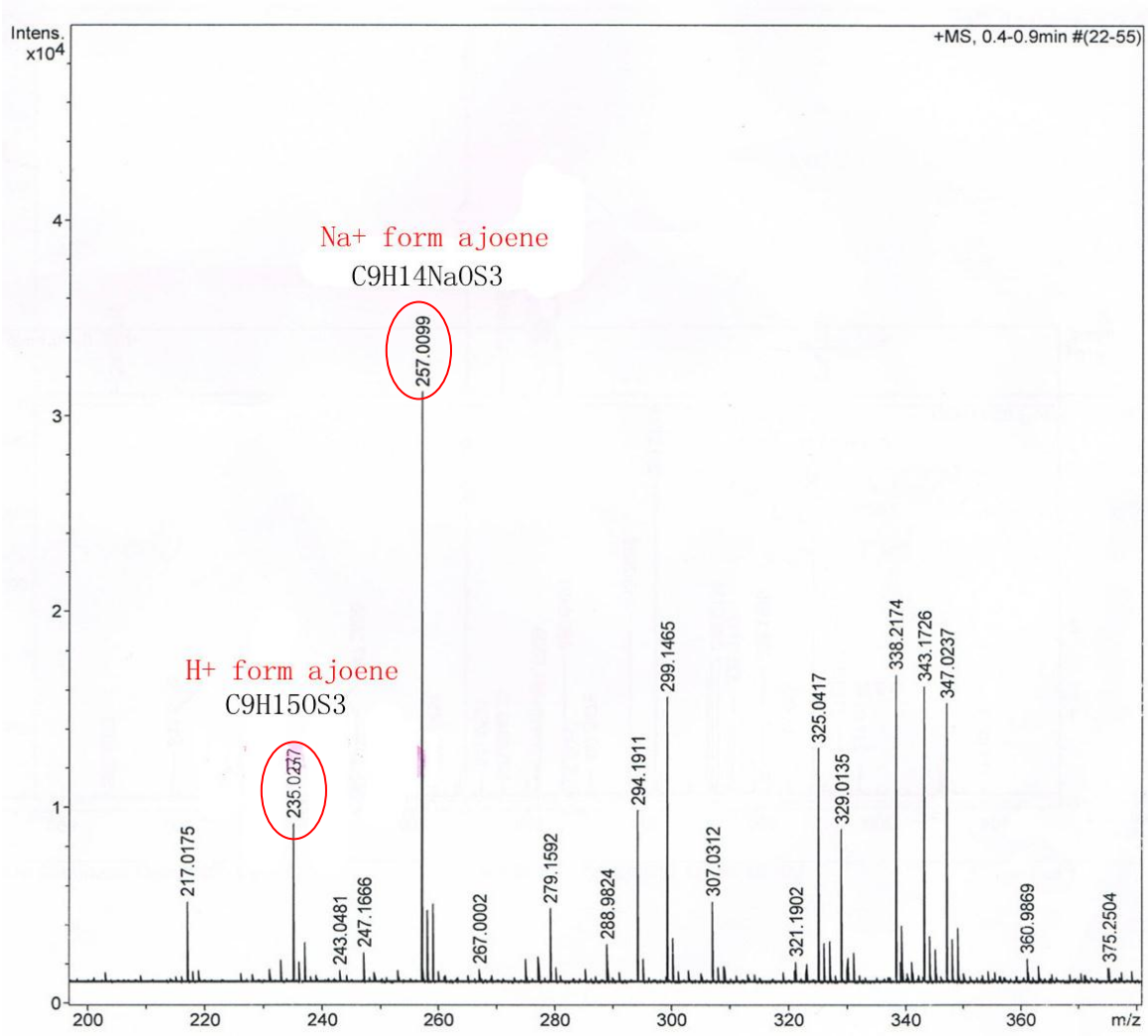

Figure 2.2. Mass spectrum of fractions 7-8 of the first extraction. Ajoene was detected in H^+ and Na^+ form. The detection of ajoene was based on the molar mass of the compounds. The molar mass of ajoene is 234.4. In mass spectrometry, ajoene molecule was ionized in H^+ or Na^+ form, the molar mass 235.0277 and 257.0099 agreed with the H^+ and Na^+ form of ajoene.

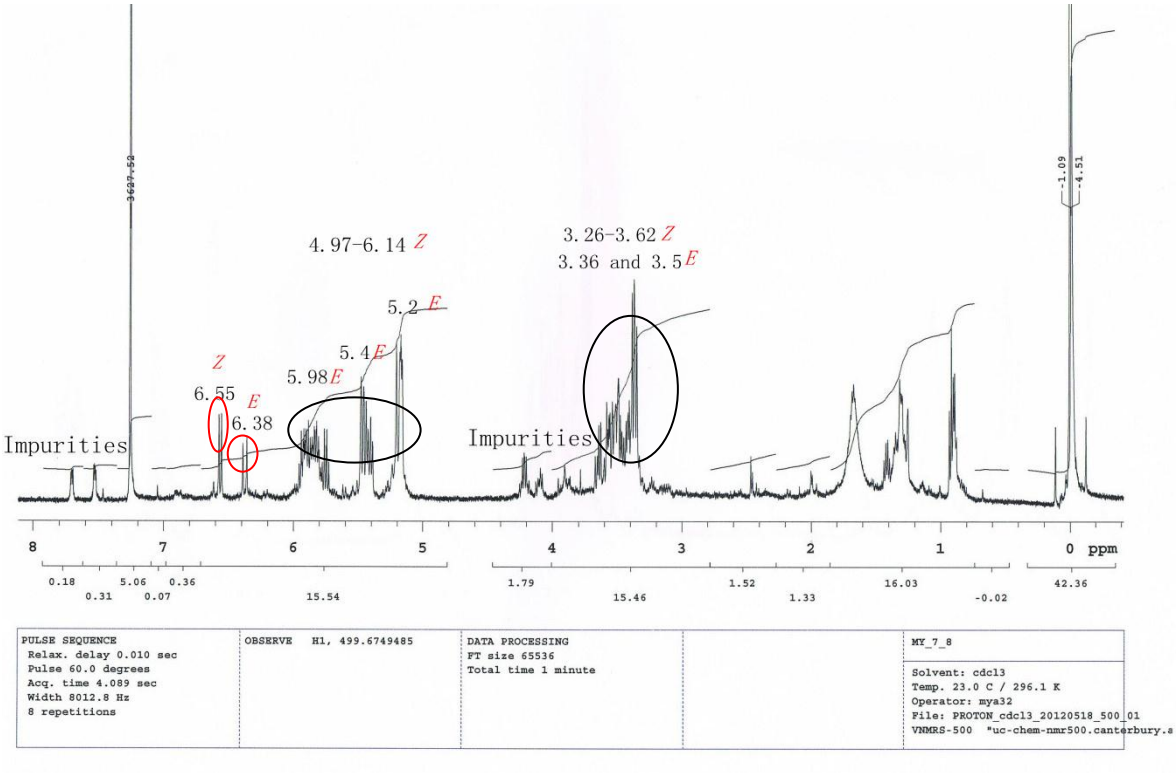

Figure 2.3. NMR spectroscopy data of tube 7-8 fractions. Two isomers of ajoene were detected by NMR. The Z isomer and E isomer had common peaks at 5-6 ppm and 3.2-3.6 ppm (black circles), and distinct peak for the double bond of which 6.55 ppm for Z and 6.38 ppm for E isomers (red circles). This data was consistent with the literature from Block's group on extraction of ajoene from garlic (Block et al., 1986). Therefore, the structure of the compound in our garlic extract was confirmed to be consistent with the structure of ajoene.

Second extraction

After washing with organic solvents, the methylene chloride extract was spotted on to a TLC plate to test the components before it was subjected to flash chromatography. This TLC plate of the crude material from this extraction is shown in Fig.2.4. 0.44 g of crude material was subjected to silica gel/ethyl acetate flash chromatography. Thirty fractions were collected after elution. The fractions were tested with TLC but there was no moderate elution rate compound detected. After washing the column with 1:9 methanol/ethyl acetate, an additional 30 tubes were collected and the contents of fractions 4-6, 9, 10, 11-12, 13, 19-24 were tested with MS. No ajoene was detected in any of these fractions. However, there was some material that had a moderate travelling rate showed on the TLC plate before flash chromatography (Fig.2.4). The size of column used in the first extraction was 15 cm in height and 2 cm in width as detailed, whereas the column used in the second extraction was 40 cm in height and 1.5 cm in width. The pressure used for the second column was much lower than the first extraction. According to Van Deemter's curve, the influence of diffusion to the result of separation will be increased largely if the flow rate is too slow (Van Deemter & Zuiderweg, 1956). The extremely slow rate also resulted in an interruption of flow during the night which could also have caused failure of elution of the compound. It is possible that the moderate elution rate material was trapped in the column and it was not eluted off, even after the increasing of the polarity of the mobile phase.

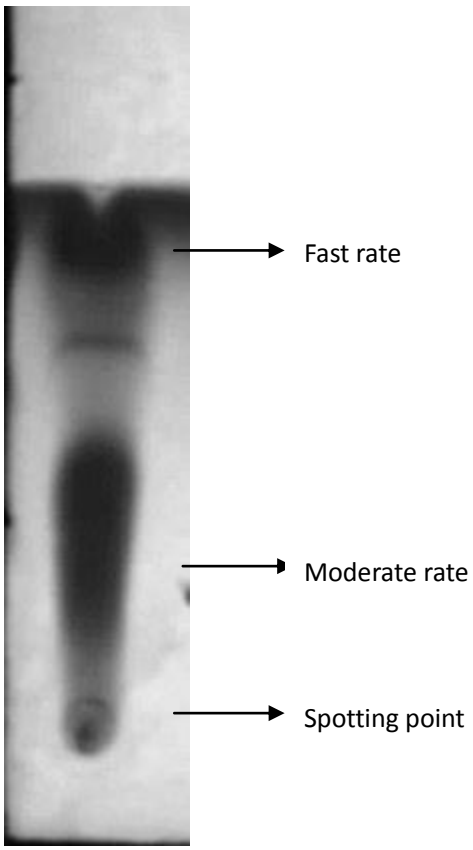

Figure 2.4. TLC plate of the methylene chloride extract from the second extraction. A small amount of the extract was spotted on the TLC and the TLC was run with ethyl acetate. The plate showed that there were fast, moderate and slow materials on TLC. But the moderate material was not detected by MS after the chromatography.

Third extraction

After washing with organic solvents, 0.78 g of crude material was subjected to silica gel/ethyl acetate flash chromatography. Thirty fractions were collected after elution. All fractions which quenched UV light were tested on TLC and eluates which had same retention time were combined. The TLC plate is shown in Fig.2.5. Fractions 3 to 17 were tested using MS. Ajoene was detected from fractions 5 to 7 and from fractions 8-12. The Mass spectrum reports of positive tubes are shown in Fig.2.6 to Fig.2.10.

Based on the TLC (Fig.2.5) and MS data (Fig.2.6-2.10), fraction 5 can be seen to have a small amount of ajoene and the concentration of ajoene increased in the subsequent tubes and then was absent in fraction 13. This result agreed with the TLC pattern of the moderate travelling rate material marked red on Fig.2.5. Therefore, we could confirm ajoene's position on TLC plate based on these results (Fig.2.5). This was used as a quick indicator for the presence of ajoene on the TLC plate of the next extraction.

The final weight of the yellow oil in fractions 5-7 was 0.12g after evaporating the solvent. The yellow oil was then diluted with DMSO and used in antifungal and antitumor experiments. This extract will be termed "3GE" in the following chapters.

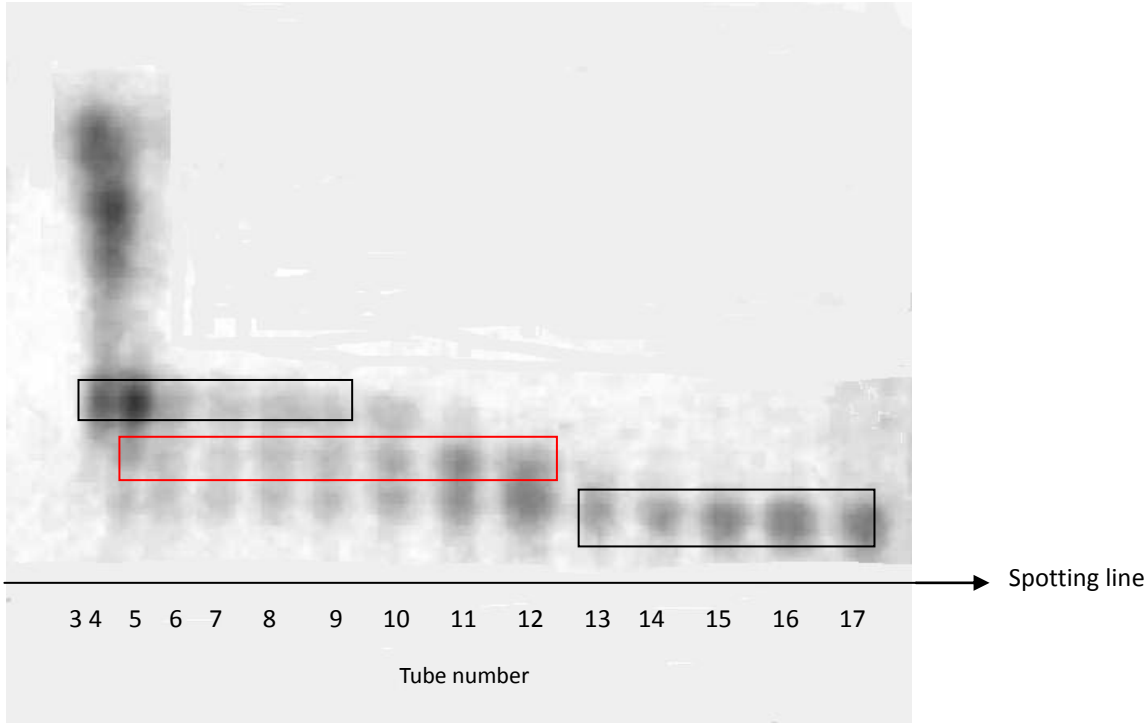

Figure 2.5. The TLC plate of the fractions collected from flash chromatography for the third garlic extraction. On this plate, fractions 5-7, 8-12, and 13-17 appeared to have compounds which travelled at the same rate on silica gel. These fractions were combined and tested using MS. The MS data showed that the 7-8 fractions had most of the ajoene.

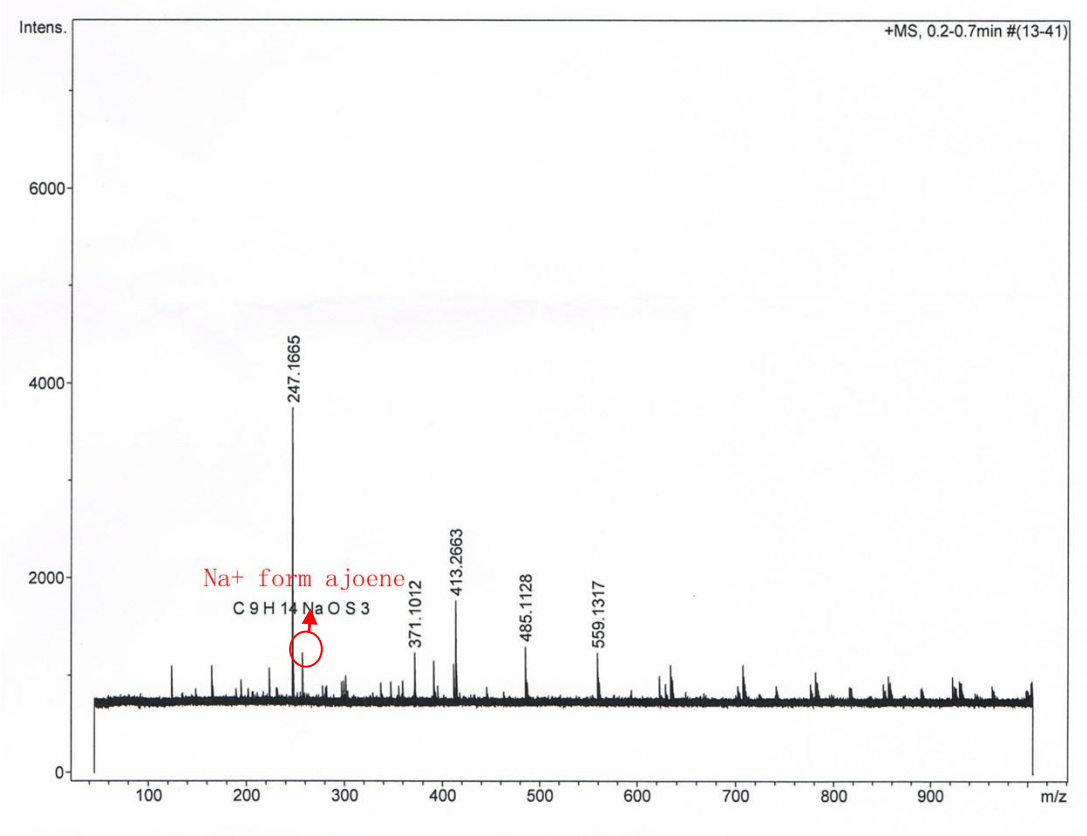

Figure 2.6. Mass spectrum of fraction 5 of the third extraction. Ajoene was detected in the Na^+ form (shown in red circle, $C_9H_{14}NaOS_3$) in a small amount.

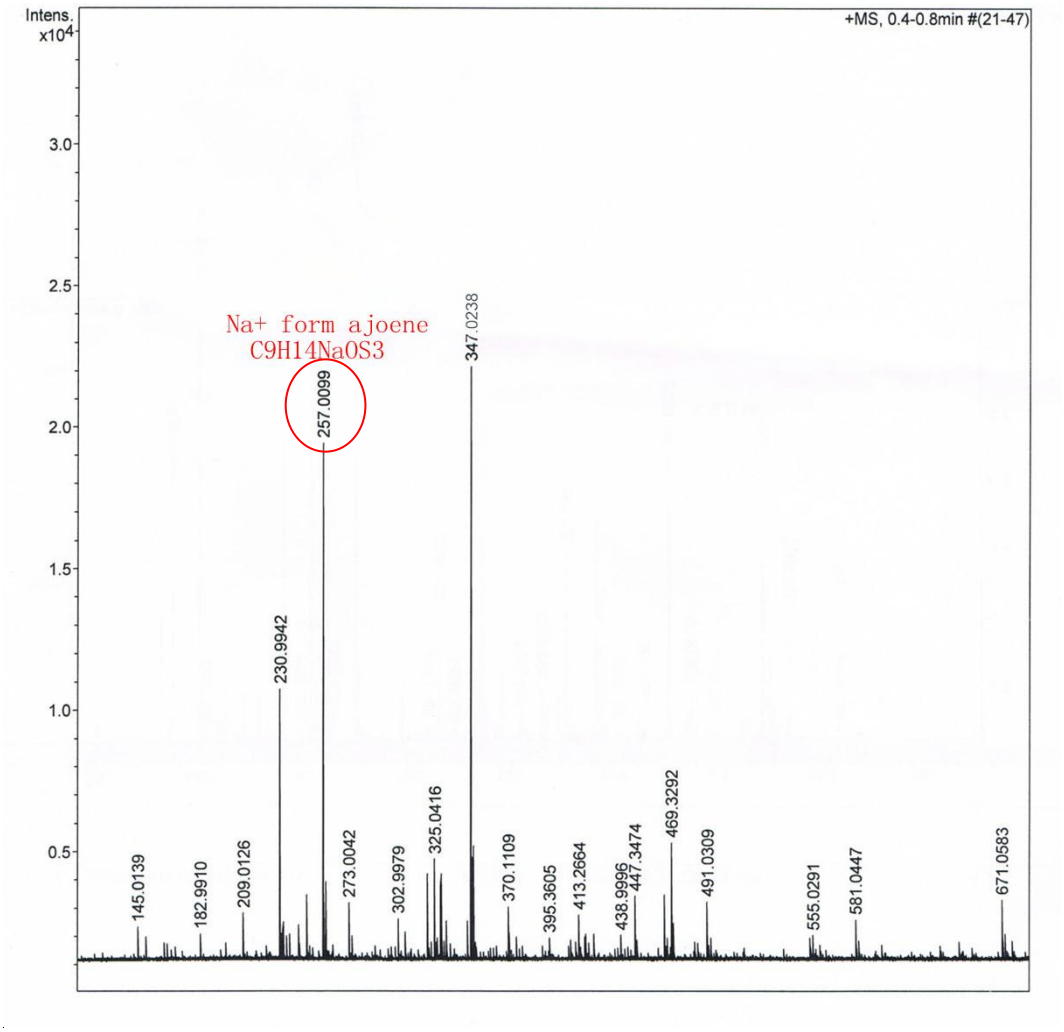

Figure 2.7. Mass spectrum of fraction 7 from the third extraction. Ajoene was detected in the Na^+ form (molar mass 257.0099).

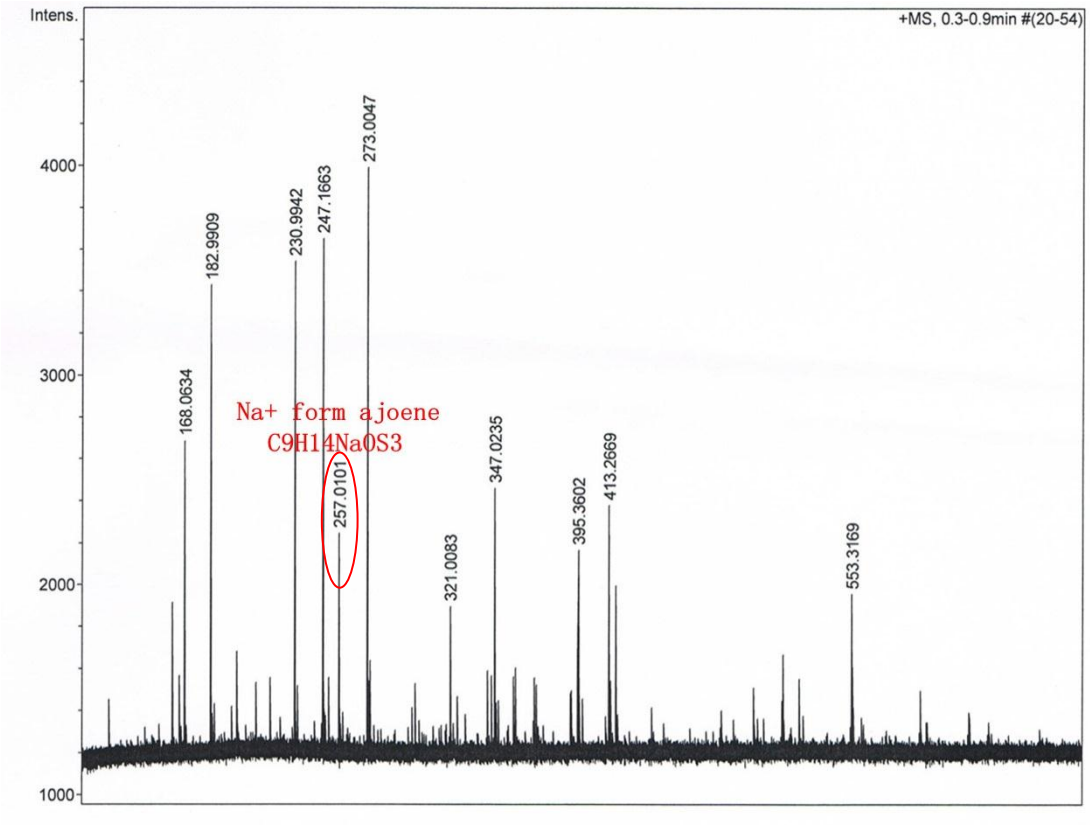

Figure 2.8. Mass spectrum of fraction 9 from third extraction. Ajoene was detected in the Na^+ form (red circle molar mass 257.0101).

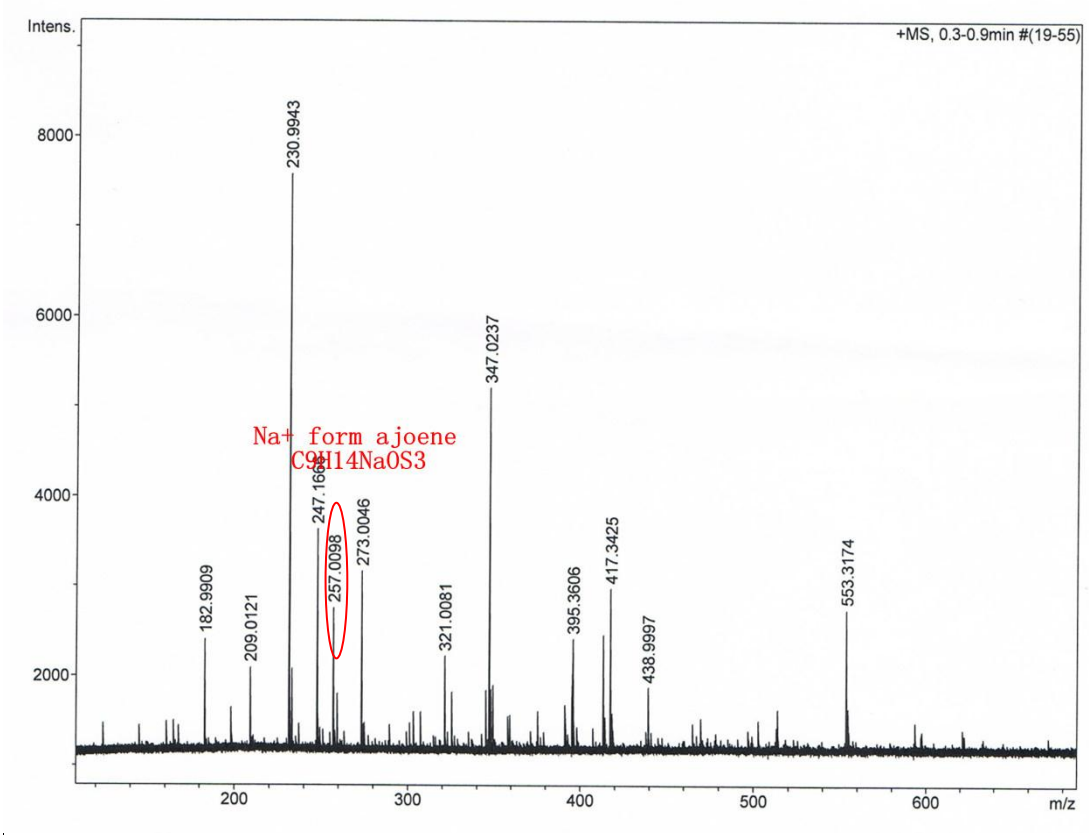

Figure 2.9. Mass spectrum of fraction 11 from third extraction. Ajoene was detected in the Na^+ form (red circle, molar mass 257.0098).

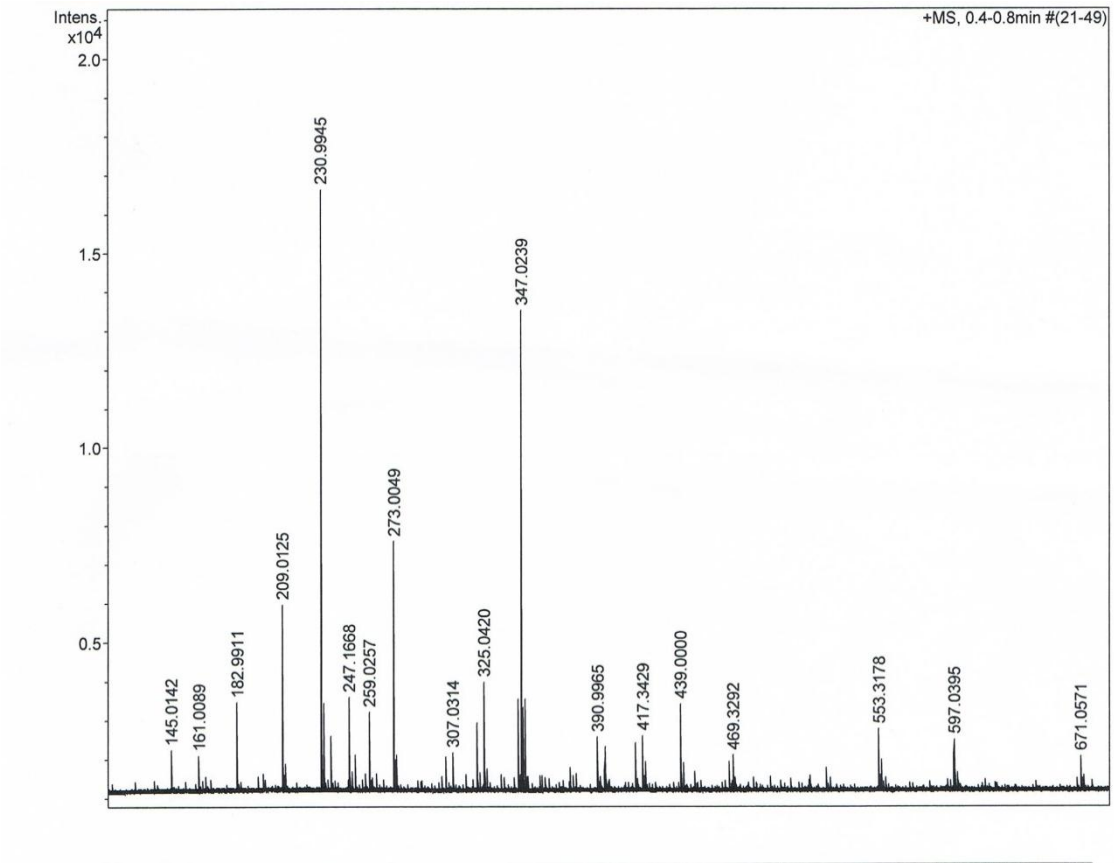

Figure 2.10. Mass spectrum of fraction 13 from the third extraction. Ajoene was not detected.

Fourth extraction

After washing with organic solvents, 0.56 g of crude material was subjected to silica gel/ethyl acetate flash chromatography. Twenty four fractions were collected after elution. Again all fractions which quenched UV light were tested on TLC and eluates which had the same retention time were combined. The TLC plate for this extraction is shown in Fig.2.11. As mentioned in the previous extraction, ajoene's position on the TLC plate was confirmed and it was predicted that it should be present in fractions 7-10 in this extraction (Fig.2.11). Therefore, fractions 7-9 and fraction 10 were tested for ajoene using MS. Ajoene was detected from fractions 7 to 9. The Mass spectrum of fractions 7 - 9 is shown in Fig.2.12. The final weight of the yellow oil in fractions 7-9 was 0.0973g after evaporating the solvent. This extract will be termed "4GE" in the following chapters.

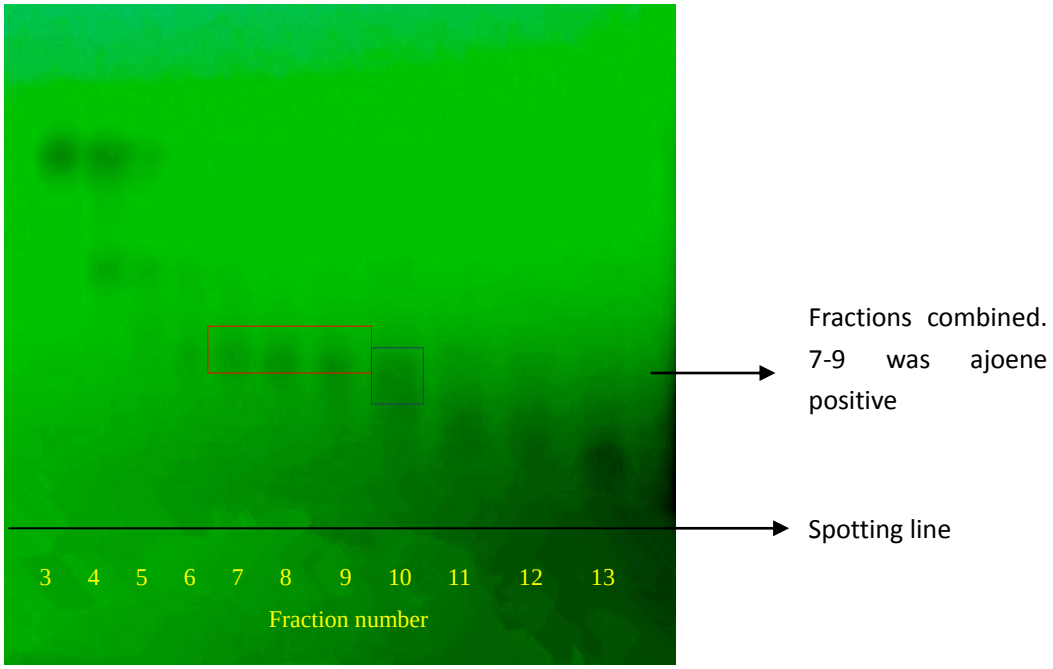

Figure 2.11. The TLC plate of the fractions collected from flash chromatography for the fourth garlic extraction. Fractions 7-9 and fraction 10 were tested on MS. 7-9 was ajoene positive based on the following MS data.

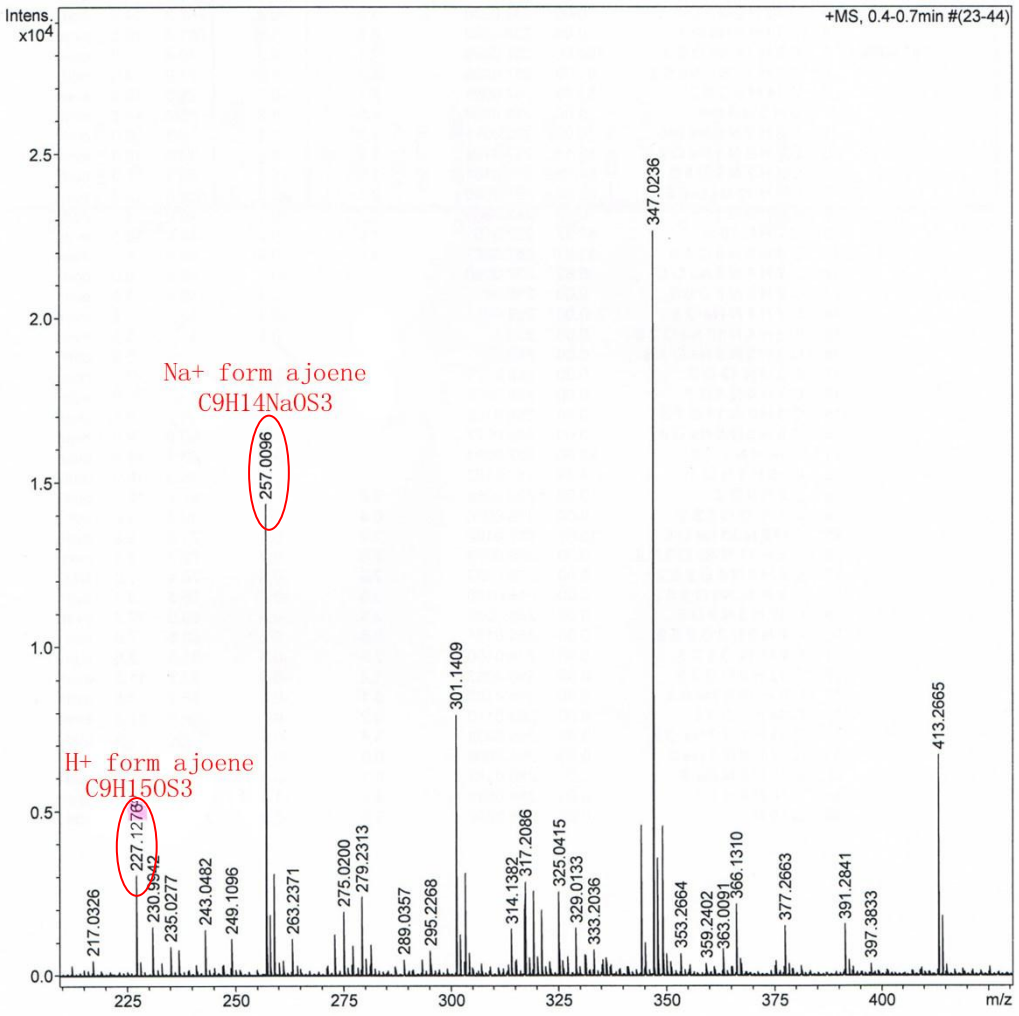

Figure 2.12. Mass spectrum of fractions 7-9 of the fourth extraction. Ajoene was detected in both H^+ (molar mass 227.1276) and Na^+ (molar mass 257.0096) form.

Conclusion

In the four independent extractions, we managed to extract ajoene from garlic in the first, third and fourth extraction. The identity of ajoene in the garlic extracts was confirmed by mass spectrometry (MS) and Nuclear magnetic resonance (NMR) spectroscopy. The NMR spectroscopy result suggested that the ajoene in the extracts was a mixture of E and Z isomers. The purity of ajoene in each garlic extract was reasonably high as shown in the MS and NMR results.

Appendix

Appendix 2.1

Acquisition Parameter of Mass spectrometry	
Source type	ESI
Ion polarity	Positive
Set nebulizer	1.0 Bar
Focus	Not active
Set capillary	4000 V
Set dry heater	200 ^{o}C
Scan begin	50 m/z
Set end plate offset	-500 V
Set dry gas	8.0 I/min
Scan End	1000 m/z
Set collision cell RF	1800.0 Vpp
Set divert value	Waste

Chapter 3 - Antifungal activity of ajoene

Introduction

Garlic has been shown to have antifungal effects towards a variety of different species of fungi (Ledezma et al., 1996). Its antifungal effects are suggested to be due to the large number of active sulfur containing compounds that are found in garlic extract (Iciek et al., 2009). Of these, allicin, which is produced during the crushing of garlic cloves, is believed to be mostly responsible for the antimicrobial activity of garlic (Cavallito & Bailey, 1944). In later research, allcin is found to have antifungal activities against a broad spectrum of microorganisms both *in vitro* and *in vivo*. These species include *Candida spp.*, *Cryptococcus spp.*, *Trichophyton spp.* and *Aspergillius spp* (Aala et al., 2010; Gruhlke et al., 2010; Khodavandi et al., 2011; Shadkchan et al., 2004; Yamada & Azuma, 1977).

However, in terms of its use to tackle fungal infections, the pitfall of the active compound allicin is that it is very unstable at the normal human body temperature. This means that there is only a trace amount of allicin found in human blood at a temperature of 37^{o}C several minutes after addition of allicin to the blood in volumetric flask (Freeman & Kodera, 1995). At room temperature, as mentioned in the previous chapter, allicin readily converts to ajoene when it is mixed with edible oil or alcohol (Block et al., 1986). The degradation product ajoene of allicin is more stable than allicin and the pharmacological activity of ajoene is therefore much more likely to be preserved (Ilić et al., 2011). Since its discovery, ajoene's antifungal effects have been demonstrated on many fungal species. It has shown very strong antifungal activity on *Aspergillus niger* and *Candida albicans* (S. Yoshida et al., 1987). San-Blas *et al.* (1989) tested ajoene on the dimorphic fungus *Paracoccidioides brasiliensis* and found that it inhibited both the yeast and mycelial phase growth (San-Blas et al., 1989) and later in 1997 the same group suggested that the inhibition was probably due to inhibition of phosphatidylcholine synthesis and disruption of the fatty acid

composition of the fungal plasma membrane (San-Blas et al., 1997). Naganawa et al. (1996) found that ajoene had a microbicidal effect on yeast when the concentration of ajoene was increased to 30 μg/ml. Since the fungi were only killed effectively during cultivation, they suggested that the antifungal function of ajoene was effective on growing cells (Naganawa et al., 1996). More recently, clinical trials were carried out to test ajoene's potential as an antifungal drug. The antifungal activity of ajoene and the antifungal drug 5-fluorouracil has been compared for the treatment of *Cladophialophora carrionii* chromoblastomycosis on patients. Chromoblastomycosis is a localized chronic fungal infection, usually causing papules on skin and subcutaneous tissues. Further development of this infection may cause the spreading of the fungus into blood or lymphatic vessels. The authors suggested that the cure rate was similar between the 5-fluorouracil and ajoene treatment but the ajoene treated group seemed to have a lower chance of relapse and skin damage (Pérez-Blanco et al., 2003). Moreover, Ledezma et al. (2000) tested 1% ajoene in an inert hydrosoluble gel on soldiers with *Tinea pedis* and the efficacy of treatment was 100%. The efficacy of ajoene treatment was higher than the drug terbinafine, a synthetic allylamine antifungal drug mainly used for treating dermatophytosis (Ledezma et al., 2000).

The dimorphic fungus *Candida albicans* grows in both a yeast and a mycelial form, and it has significant contribution to oral and genital infections in humans (Gow & Gadd, 1995). The overgrowth and opportunistic infection of the fungus results in candidiasis which is often observed in immunocompromised individuals such as AIDS and cancer patients (Calderone & Clancy, 2012; Tylicki et al., 2012). When *C. albicans* is cultivated on agar plate at 37^{o}C, it grows in yeast form, when cells are grown in a medium similar to physiological environment of a human host, they grow as "true" hyphae which are often at the site of invasion (Berman & Sudbery, 2002).

The budding of yeast and polarized extension of hyphae are two distinct patterns of fungal growth, and the cytoskeleton is thought to play a crucial role both in budding and in polarized cell growth. In polarized cell growth of fungi, the microtubules and actin filaments are crucial for establishing and maintaining cell

polarity for the process of budding, fission or filamentous growth, but are also required for delivering the vesicles for polarized cell extension. That is, microtubules deliver the “cell end marker” proteins to cell pole, in order to organize the actin cytoskeleton for the transportation of vesicles to the cell end (Fischer et al., 2008).

During mitosis of eukaryotic cells, microtubules and actin filaments are assembled specially in M phase of the cell cycle. After the chromosomes are replicated, the microtubules and accessory proteins are assembled to form bipolar mitotic spindles, these function to separate the chromosomes and allocate one copy to each daughter cell. Then the actin filaments and myosins form a contractile ring or cell plate that facilitates cell division (Alberts et al., 2002).

As mentioned above, ajoene is able to inhibit the growth of both yeast and mycelial form of *P. brasiliensis* (San-Blas et al., 1989). The underlying mechanism is still unclear. The inhibition of yeast and mycelial growth by ajoene may or may not be achieved by same target. *Achlya bisexualis* is one of the *Achlya* species which normally cause aquatic animal diseases (Fuangsawat, Abking, & Lawhavinit, 2011). *A.bisexualis* and *Neurospora crassa* are model microorganisms frequently used for research into filamentous growths. In this chapter, the antifungal effects of ajoene were tested on the dimorphic fungus *C. albicans* and on filamentous cells of *N. crassa* and *A. bisexualis*, in order to investigate any inhibitory activity of ajoene on both yeast and mycelial form of growth.

Materials

Strains of *Candida albicans* C57, *Neurospora crassa* and *Achlya bisexualis* were obtained from the collection of the University of Canterbury. Growth media PYG (components shown in Appendix 3.1) media was used for growth and maintenance of *Neurospora crassa* and *Achlya bisexualis*. PDB and PDA (potato dextrose broth and agar, components shown in Appendix 3.2) were used for growth and maintenance of *Candida albicans* C57. Human blood serum for germ tube formation was obtained from Christchurch Hospital, New Zealand. Ninety six well microplates for *C. albicans* incubation were from BD Falcon limited, New Zealand.

Methods

C. albicans treatment and cell division assessment

A colony of *C. albicans* on fresh PDA plate was inoculated in 15 ml of PDB and the broth was incubated at 37 ºC for 24 hours. The cell number in the broth was determined with a haemocytometer after the incubation. Based on the cell counting, the original broth was diluted to $5x10^4$ cells/ml and 200 µl of the diluted cell solution was added to each well of a 96 well microplate.

1GE (ajoene from first garlic extraction) was diluted to 1mg/ml before its use in experiments. 1GE at the concentrations of 5, 10, 20, 40, 60 and 80 µg/ml were used to treat *C. albicans* and there were 5 replicates of cells in each concentration group. The volume of 1GE used for each group is listed in Appendix 3.3.

The plate was incubated at 37 ^oC for 24 hours, and the cell density which was taken to represent the amount of cell division of *C. albicans* was monitored by the absorbance of solution in the wells at 530 nm.

C. albicans germ tube length comparison

A colony of *C. albicans* on a fresh PDA plate was added to 2 ml of human blood serum and mixed thoroughly. The serum was then divided into two equal parts and added into 2 sterile eppendorf tubes. 35 µl of 1mg/ml 1GE was added to one of the tubes so that the final concentration of ajoene in the serum was 35µg/ml. Both tubes were then incubated at 37 ^{o}C for 3 hours. After incubation, the serum in each of the tubes was observed under the microscope. Fifty germ tubes were measured for each group and the average results were averaged.

A.bisexualis and *N.crassa* treatment and hyphae extension assessments

Radial extension of the whole culture

Growth media which contained 5, 10 or 20 µg/ml of 1GE was made by adding 1GE to melting PYG media containing 2% agar and 2.5 ml of the media was poured into each of the 55mm x 15mm Petri dishes. The volumes of 1GE used in each group of plates are listed in appendix 3.4. Fresh cultures of *A. bisexualis* and *N. crassa* were inoculated with a cork borer on the center of plates. The *N. crassa* plates were incubated at 22 ºC for 24 hours and the *A. bisexualis* plates were incubated at 22 ºC for 48 hours. The diameters of colonies were measured after incubation.

Individual hyphal extension

Growth media was prepared by laying a piece of sterile cellophane over PYG agar. Fresh cultures of *N. crassa* and *A. bisexualis* were inoculated on the cellophane on the plate. The *N. crassa* plates were incubated at 22 ºC for 24 hours and the *A.bisexualis* plates were incubated at 22 ºC for 48 hours for further analysis.

After incubation, a perfusion slide was made by spotting nail polish on a glass slide and the filamentous cell culture on cellophane was cut and placed on the slide between the spots and immersed in liquid PYG medium. The culture was then covered with a coverslip and extension of an individual hypha was observed under microscope. Hyphal growth rate was measured by observed the growing distance of

individual hypha over a specified time. After the measurement, the medium on slide was then replaced by perfusion with PYG medium which contained 20 μg/ml of 1GE. The extension rate of the same hypha was measured again after the replacement of medium.

Statistical analysis

Data were statistically analyzed with Prism statistical software using Student's *t*-test and $P<0.05$ was used to determine statistical significant. All data were presented as mean+SEM.

Results

Results listed below were the average results of 3 independent experiments, and the detailed statistical data was shown in Appendix 3.5.

Effect of ajoene on C. albicans cell division

The turbidity (Absorbance) in wells of the 96 well plate was used to indicate the cell number of *C. albicans* after incubation and hence the ability of the culture to divide. When *C. albicans* was incubated with ajoene, there was a significant decline in cell division with 5 µg/ml ajoene. The inhibitory effect of ajoene increased as the concentration of ajoene was increased. The MIC_{50} (Minimum inhibitory concentration for inhibiting 50% of the cell division) was estimated to be 15 µg/ml and MIC_{90} (Minimum inhibitory concentration for inhibiting 90% of the cell division) was estimated to be 35 µg/ml. The comparisons of average absorbance between the groups are shown in Fig.3.1

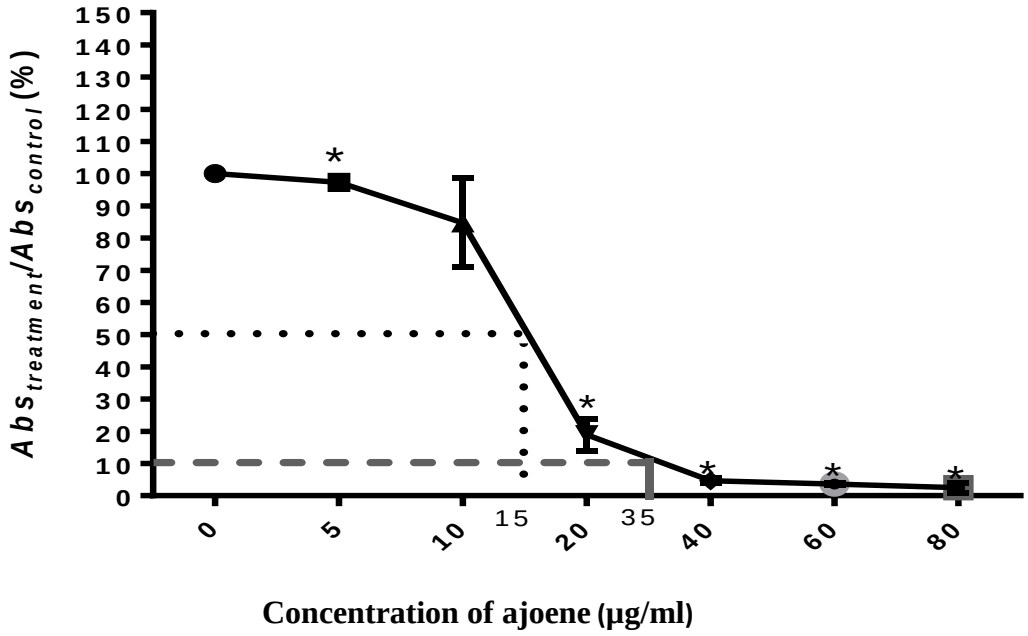

Figure 3.1. Relative absorbance of medium of *C. albicans* after incubation with or without ajoene. As the concentration of ajoene increased, the absorbance (turbidity) decreased in a dose dependent manner. The absorbance of the 5, 20, 40, 60, 80 µg/ml ajoene treated wells were significantly lower than the control wells ($P < 0.05$, t test). Data was normalized to the absorbance of the control well, thus the data on y axis is the percentage calculated by dividing the average absorbance of each group with the average absorbance of control group. The MIC_{50} was estimated to be 15 µg/ml and MIC_{90} was estimated to be 35 µg/ml.

Effect of ajoene on C. albicans germ tube length

Three individual experiments were completed and 50 germ tubes in each group were measured in each experiment. Due to the limited amount of 1GE, only one concentration 35 μg/ml, which was the MIC_{90} of ajoene on *C.albicans* cell division, was used in treating *C. albicans* germ tubes. After 3 hours of incubation in serum with or without ajoene, germ tubes of *C. albicans* formed and the average length of the germ tubes in 35 μg/ml ajoene treated groups were more than 50% shorter than these of the control groups. The relative lengths of germ tubes in control and ajoene treated groups are shown in Fig.3.2.

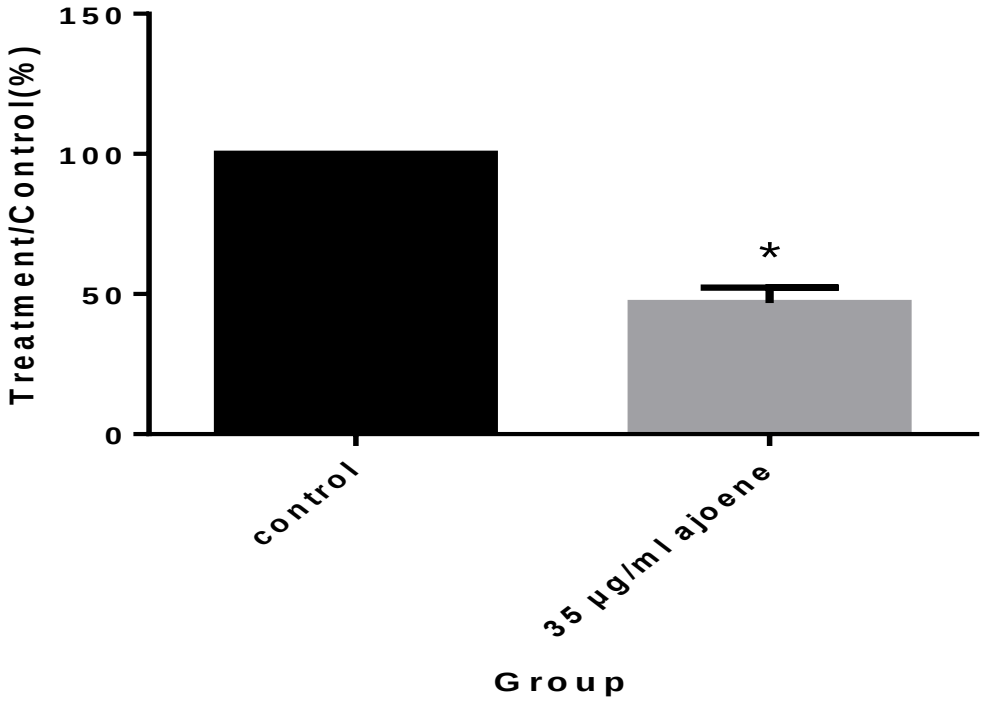

Figure 3.2. Comparison of the length of *C. albicans* germ tubes in serum with or without ajoene. Again data was normalized to the length of the control groups. The germ tubes formed in serum contained 35 μg/ml ajoene were significantly shorter than the ones in normal serum ($P<0.05$, *t* test).

Effect of ajoene on radial extension of N. crassa mycelia

When *N. crassa* was inoculated on the PYG plates with or without ajoene, radial extension of the fungal mycelia became visible in 24 hours in all groups. The size of *N. crassa* mycelia was obtained by taking the average diameter from the diameters at 3 different angles. Average diameters of the *N. crassa* mycelia treated with ajoene at a 5 μg/ml or higher concentrations were significantly lower than that of the control groups. The diameter of 5 μg/ml ajoene treated *N. crassa* mycelia was about 46% shorter than that of the control groups. Data and comparisons are shown in Fig.3.3. The images of culture plates after incubation are shown below in Fig.3.4.

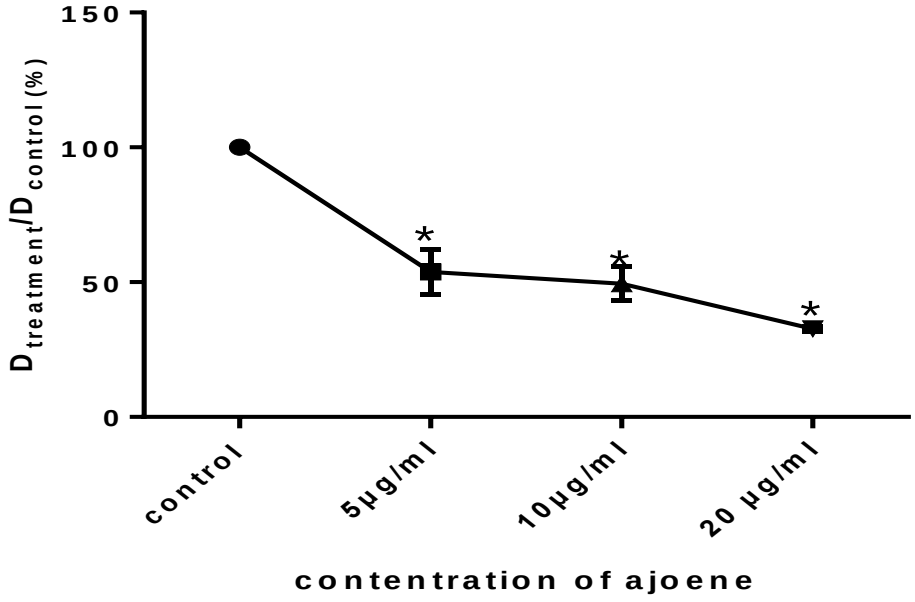

Figure 3.3. The average colony diameter of *N. crassa* after incubation with or without ajoene. As the concentration of ajoene was increased, the diameters of the fungal colony decreased in a dose dependent manner. The diameters of the ajoene treated mycelia were all significantly smaller than the control ones ($P < 0.05$, t test). Again data was normalized to the diameter of the control colony, thus the figures on y axis are the percentages calculated by dividing the average diameter of each group with the average diameter of control group.

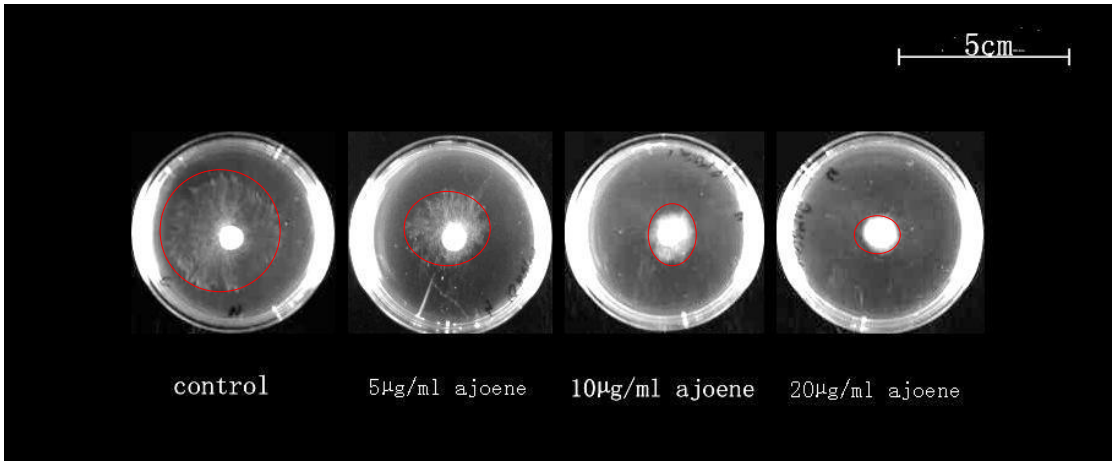

Figure 3.4. Images of *N. crassa* culture plates taken after 24 hours of incubation. The photos clearly indicate that the colony size decreased significantly due to addition of ajoene in growth media. Red circles indicate the edges of the mycelia.

Effect of ajoene on hyphal extension of N. crassa

N. crassa hyphae on cellophane on a glass slide were allowed to grow for 30 to 60 minutes. The extension rate was calculated by measuring the distance of an individual hypha's extension in a certain time. The same hypha was measured before and after the addition of ajoene to the PYG medium. The average extension rates (μm/min) were obtained from 3 independent experiments.

The average rate of *N. crassa* hyphal extension in PYG medium containing 20 μg/ml ajoene was 92.46% slower than that in normal PYG medium. The comparison of relative extension rate between control and ajoene treated groups is shown in Fig.3.5.

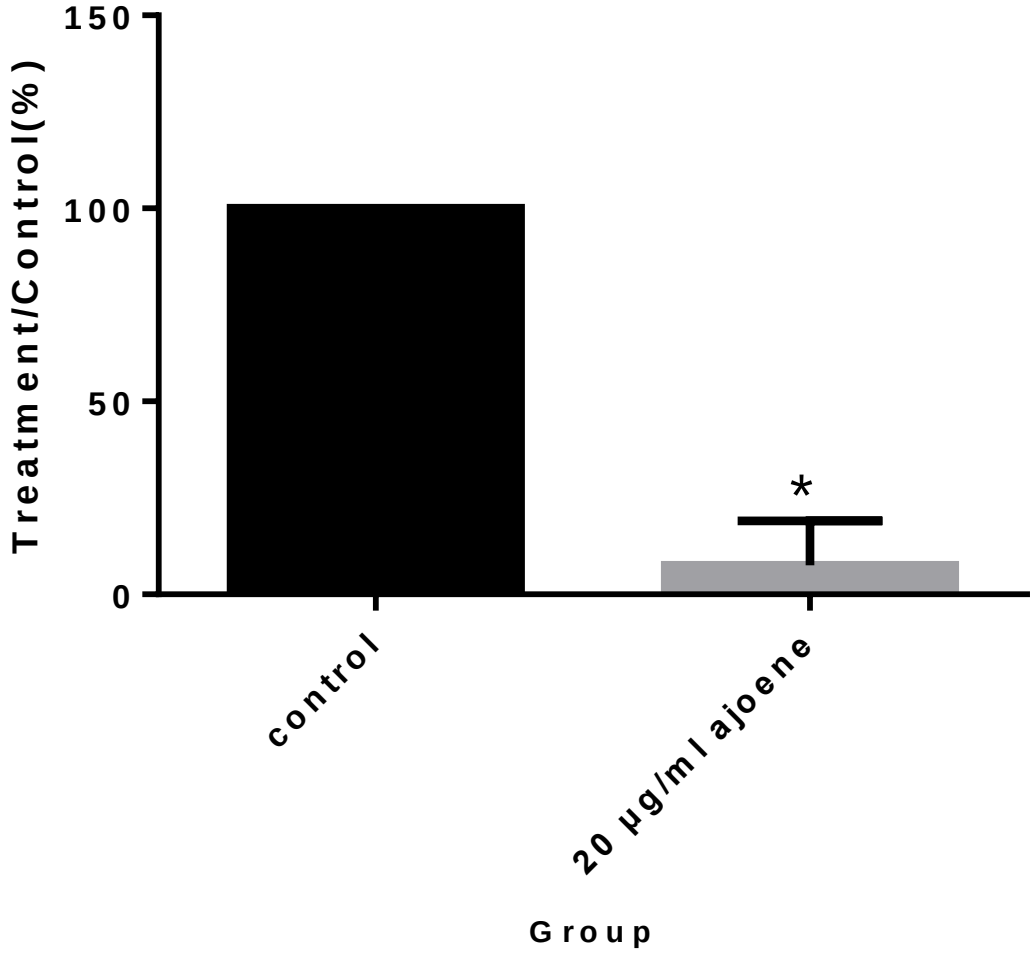

Figure 3.5. Growth rate of individual *N. crassa* hypha in PYG broth and in PYG broth which contained 20 µg/ml ajoene. The results were normalized by dividing the result of ajoene treated group with the control group. The figure shows that hypha grew significantly slower in ajoene treated medium than in normal medium ($P<0.05$, *t* test).

Effect of ajoene on radial extension of A. bisexualis mycelia

When *A. bisexualis* was inoculated on the PYG plates with or without ajoene, radial extension of the mycelia became visible in 48 hours in all groups. Again size of *A. bisexualis* colony was obtained by taking the average diameter from the diameters of 3 different angles. Average diameters of the *A. bisexualis* mycelia treated with ajoene at a 5 μg/ml or higher concentrations were significantly lower than that of the control groups. However, the inhibitory effect of ajoene on *A. bisexualis* was less than on *N. crassa*. The average mycelia diameter in 5 μg/ml ajoene treated groups was about 13.7% shorter than the control groups. Data and comparisons are shown in Fig.3.6. The images of culture plates after incubation are shown below in Fig.3.7.

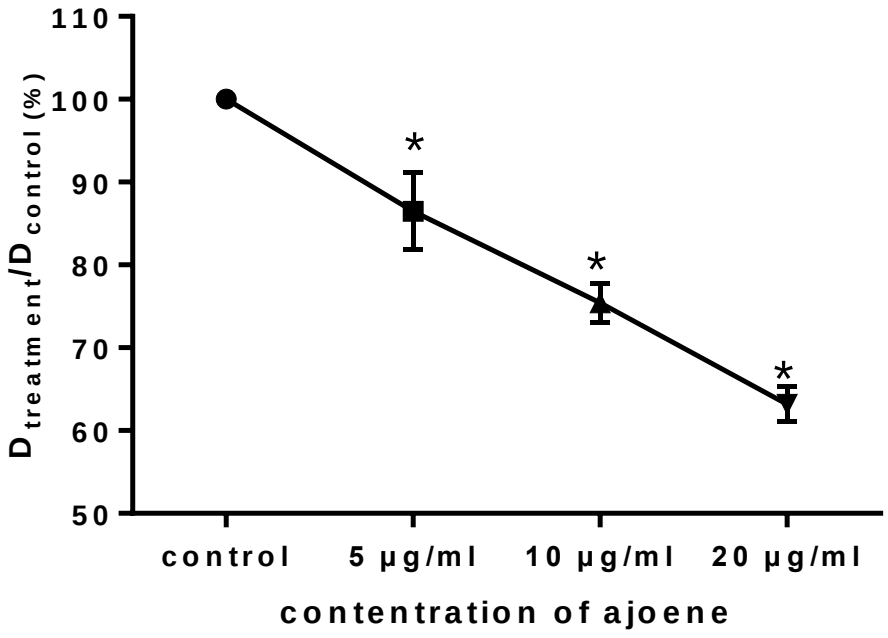

Figure 3.6. Average relative colony diameter of *A. bisexualis* after incubation with or without ajoene. The diameters of *A. bisexualis* colony decreased in a dose dependent manner. Results in the ajoene treated mycelia were all significantly lower than control wells ($P < 0.05$, t test). Again, data was normalized to the diameter of the control colony.

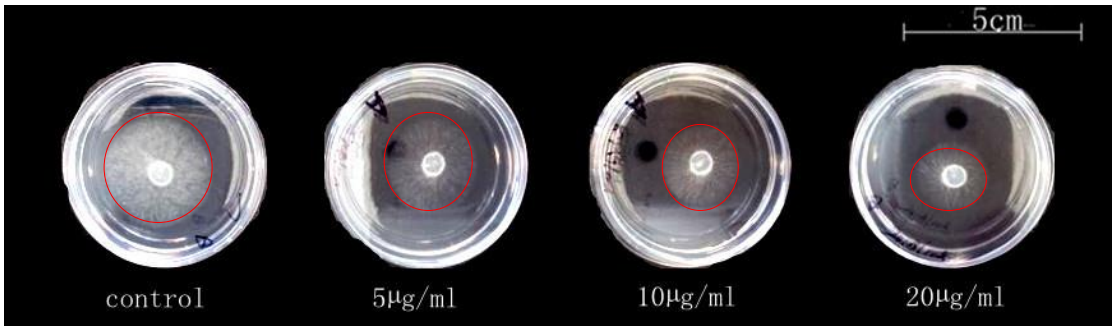

Figure 3.7. Images of *A. bisexualis* culture plates taken after 48 hours of incubation. The photos clearly indicate that the colony size decreased significantly due to addition of ajoene in growth media. Red circles indicate the edges of mycelia.

Effect of ajoene on hyphal extension of A. bisexualis

As for *N. crassa*, the hyphal extension rate of *A. bisexualis* was calculated by measuring the distance an individual hypha extended in a certain time. The same hypha was measured before and after the addition of ajoene to the PYG medium. The average extension rates (μm/min) were obtained from 3 independent experiments.

The average rate of *A. bisexualis* hyphal extension in PYG medium contained 20 μg/ml ajoene was significantly slower than that in normal PYG medium. Again, the effect of ajoene on *A. bisexualis* individual hyphal extension was milder than that on *N. crassa*. The relative extension rates of *A. bisexualis* are shown in Fig.3.8.

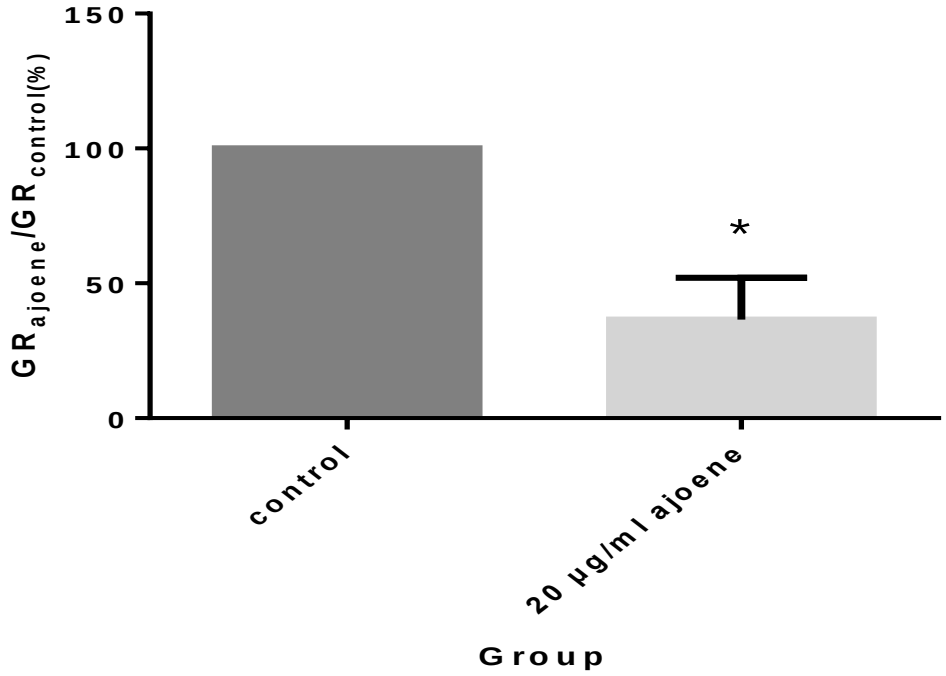

Figure 3.8. Individual *A. bisexualis* hypha growth rate in PYG broth and in PYG broth which contained 20 μg/ml ajoene. Again results were normalized by dividing the result of ajoene treated group with the control group. The figure shows that hypha grew significantly slower in ajoene treated medium than in normal medium ($P<0.05$, *t* test).

Discussion

The results above indicated that the yeast form of *C. albicans* showed significant decline in a cell number, even at low concentration of ajoene (5µg/ml). The MIC_{50} was estimated to be 15µg/ml and MIC_{90} was estimated to be 35µg/ml. The MIC_{90} value is higher than the MIC_{95} in previous study of Yoshida et al. which was 7.6 µg/ml (S. Yoshida et al., 1987), This is likely to be because of the lower purity of ajoene and different methods used in this project.

When *C. albicans* was incubated in serum, germ tube formed after the incubation. Germ tubes are the slender hyphae which emerge from a germinating spore (Carlile, 1995). The concentration of ajoene used in the germ tube tests was that which gave the MIC_{90} for division of the yeast form of *C. albicans*. The germ tube length of *C. albicans* had more than a 50% decline in the 35µg/ml ajoene treated groups.

The yeast form of *C. albicans* is thought to be important for dissemination through the blood stream, and the ability of switching from yeast form to hyphae form was suggested to be associated with the virulence of *C. albicans* (Berman & Sudbery, 2002; Gow, Brown, & Odds, 2002). A *cph1/cph1 efg1/efg1* double mutant *C. albicans*, which failed to switch from yeast to filamentous forms, was unable to cause damage to microphages (Lo et al., 1997). The germ tube, the initial stage of the formation of *C.albicans* hyphae, was considered to be one of the important virulence factors and essential for tissue adhesion (Wellmer & Bernhardt, 1997). The length of germ tube has been found to be correlated with tissue invasion and tissue damage (Kretschmar et al., 1999). In the present study, ajoene was able to inhibit both yeast division and germ tube extension. While ajoene has been tested on *C. albicans* previously (Carrero, Romero, & Apitz-Castro, 2009; S. Yoshida et al., 1987), to the best of my knowledge this is the first time that ajoene has shown inhibitory effects on both yeast and germ tubes of *C. albicans*.

The mechanism of the inhibitory effect of ajoene on *C. albicans* cell division is still under debate. San-Blas‘s group reported that ajoene was able to reduce the phosphatidylcholine level and disturb the fatty acids composition in plasma

membrane of the yeast form of *P. brasiliensis*, and they suggested that the antifungal effects of ajoene might associated with the disturbance of fungal membrane (San-Blas et al., 1997).

Cysteine residues of proteins were also suggested to be one of the targets of ajoene since addition of cysteine to the ajoene containing fungal growth medium caused a decline in ajoene concentration, and the inhibitory effect of ajoene on *P.brasiliensis* was reduced by addition of cysteine (Naganawa et al., 1996). Garlic derivatives that include ajoene were suggested to achieve their biological activity by reacting with the cysteine residues in proteins because the sulfhydryl group on cysteine can easily be modified by disulfide structures (Jacob et al., 2012). When ajoene was tested on cancer cells, the mitosis of the cells were blocked and apoptosis was induced by ajoene, which was suggested to be due to the oxidation of cysteine, inhibition of microtubule assembly and ROS (reactive oxygen species) induced by the disulfide group of ajoene (Dirsch et al., 1998; Jacob et al., 2012; Kaschula et al., 2012; Li et al., 2002). *C. albicans* cell division, which is a mitosis process, was possibly blocked by ajoene via the modification of cysteines on tubulin and blockage of microtubule assembly.

When *C. albicans* switches to the hyphal growth form and generates germ tubes, the role of microtubules was also suggested to be important for both germ tube formation and growth. Barton and Gull (1998) stained both the yeast form and germ tubes of *C. albicans* using immunofluorescence and they found that mitotic spindles in germ tubes were much longer than the ones in yeast form of *C. albicans*. They suggested that microtubules were responsible for positioning the nuclei in the center of the germ tubes (Barton & Gull, 1988). Blockage of microtubule assembly by ajoene could also result in the reduction of germ tube length in *C. albicans.*

Radial extension of the ascomycete *N. crassa* and the oomycete *A. bisexualis* mycelia on agar plates were both inhibited by ajoene. The diameters of the *N. crassa* colony on plates which contained 5µg/ml ajoene were almost 50% smaller than that of control plates. *A. bisexualis* was less sensitive to ajoene than *N. crassa* but still had a significant decline in radial extension. When individual hyphal extension was

observed on cellophane under the microscope, the pattern agreed with the on plate pattern. The individual hyphal extension rate of *N. crassa* was reduced by 20μg/ml ajoene. Again, the response of *A. bisexualis* hypha extension rate to ajoene treatment was less than that with *N. crassa*.

As mentioned above, the antifungal activity of ajoene was possibly due to the disturbance of cell membrane or inhibition of microtubules. Composition of cell membrane presents a wide deviation among microorganisms. Tylicki and co-workers compared the fatty acids profiles of *Malassezia pachydermatis*, *Candida albicans* and *Saccharomyces cerevisiae* and the fatty acid content varied among the species, which may therefore influence the responses of the microorganisms to drug (Tylicki et al., 2012). Mu's group compared β-tubulin encoding cDNAs between the ascomycete *Pestalotiopsis microspora* and the oomycetes *Pythium ultimum*, and the responses of the two microorganisms to taxol. The author suggested that a sequence difference in β-tubulin resulted in the distinct pattern of responding to taxol (Mu, Bollon, & Sidhu, 1999).

A. bisexualis belongs to oomycetes, a group that are phylogenetically distant from the kingdom Fungi (Förster, Coffey, Elwood, & Sogin, 1990). Oomycetes were considered to belong to Chromalveolata along with algae, and are believed to be some of the most distantly related eukaryotes to fungi (Richards, Dacks, Jenkinson, Thornton, & Talbot, 2006). The distant phylogenetic relationship between *A.bisexualis* and *N. crassa* may result in the difference in composition of cell membrane or in tubulin sequence. Moreover, it was suggested that hyphae growth rate correlated with the microtubule dynamics. *N. crassa* had one of the fastest microtubule polymerization rate and growth rate in filamentous fungi (Uchida, Mouriño-Pérez, Freitag, Bartnicki-García, & Roberson, 2008), which may also played a part in the greater response to the microtubule inhibitor ajoene.

. Due to time constrain and availability of ajoene amount, the concentrations of ajoene and the time in the above experiments were limited. For example, only 35 μg/ml was used in germ tube experiments, and the hyphae radial extension was done only on small plates thus the growth of *N. crassa* and *A. bisexualis* were not able to be

investigated further than 24 hours. In a future study, more concentrations of ajoene could be tested on these organisms and the effects of ajoene on the cytoskeleton could be assessed in depth details by suitable biochemical techniques.

Conclusion

C. albicans cell division was inhibited by ajoene at 5 µg/ml or higher concentrations. The length of ajoene treated *C. albicans* germ tubes was significantly shorter than non-treated ones. Ajoene was also able to inhibit the radial extension and individual hyphal extension of *N. crassa* and *A. bisexualis* but the response of *A. bisexualis* to ajoene was less marked than *N. crassa.* The effect of ajoene may be due to its effect on membrane lipids or the microtubule cytoskeleton.

Appendix

Appendix 3.1. Ingredients of PYG media

Components	Concentration
Glucose (Merck)	3 g/L
Bacterial peptone (Sigma)	1.25 g/L
Yeast extract (Sigma)	1.25 g/L
Agar (Sigma ltd)	20 g/L

Appendix 3.2. Ingredients of PDA media and PDB broth

Components	Concentration
BD Difco™ potato dextrose broth	24 g/L
Agar	20 g/L for PDA or 0 for PDB

Appendix 3.3. *C.albicans* was treated with various concentrations of ajoene. Volume of 1GE and $5x10^4$ cells/ml cell solution added for each concentration group is listed below.

	Control	5µg/ml	10µg/ml	20µg/ml	40µg/ml	60µg/ml	80µg/ml
1mg/ml 1GE	-	-	-	4 µl	8µl	12 µl	16 µl
500µg/ml 1GE	-	2µl	4µl	-	-	-	-
Solution/well	200 µl	200 µl	200 µl	200 µl	200 µl	200 µl	200 µl

Appendix 3.4. *A. bisexualis* and *N. crassa* were treated with various concentrations of ajoene. Volumes of 1GE and media for making up PYG plates contained various concentrations of ajoene are listed below.

	Control	5µg/ml	10µg/ml	20µg/ml
1mg/ml 1GE	0	12.5 µl	25 µl	50 µl
Media/PYG plate	2.5 ml	2.5 ml	2.5 ml	2.5 ml

Appendix 3.5.

Unpaired t test of C.albicans control wells vs 5µg/ml ajoene treated wells	
P value	0.0345
P value summary	*
Significantly different? (P < 0.05)	Yes
One- or two-tailed P value?	Two-tailed
t, df	t=3.151 df=4
How big is the difference?	
Mean ± SEM of column A	100.0 ± 0.0 N=3
Mean ± SEM of column B	97.33 ± 0.8474 N=3
Difference between means	-2.670 ± 0.8474
95% confidence interval	-5.023 to -0.3173
R square	0.7128

Unpaired t test of C.albicans control wells vs 10 µg/ml ajoene treated wells	
P value	0.1281
P value summary	ns
Significantly different? (P < 0.05)	No
One- or two-tailed P value?	Two-tailed
t, df	t=1.914 df=4
How big is the difference?	
Mean ± SEM of column A	100.0 ± 0.0 N=3
Mean ± SEM of column C	84.73 ± 7.979 N=3
Difference between means	-15.27 ± 7.979
95% confidence interval	-37.43 to 6.881
R square	0.4781

Unpaired t test of C.albicans control wells vs 20 µg/ml ajoene treated wells	
P value	< 0.0001
P value summary	****
Significantly different? (P < 0.05)	Yes

One- or two-tailed P value?	Two-tailed
t, df	t=28.47 df=4
How big is the difference?	
Mean ± SEM of column A	100.0 ± 0.0 N=3
Mean ± SEM of column D	18.93 ± 2.848 N=3
Difference between means	-81.07 ± 2.848
95% confidence interval	-88.98 to -73.17
R square	0.9951

Unpaired t test of C.albicans germ tube length compared between control and 35µg/ml ajoene treated group	
P value	< 0.0001
P value summary	****
Significantly different? (P < 0.05)	Yes
One- or two-tailed P value?	Two-tailed
t, df	t=16.52 df=4
How big is the difference?	
Mean ± SEM of column A	100.0 ± 0.0 N=3
Mean ± SEM of column B	46.76 ± 3.224 N=3
Difference between means	-53.24 ± 3.224
95% confidence interval	-62.19 to -44.29
R square	0.9855

Unpaired t test of N. crassa colony diameter compared between control and 5µg/ml ajoene treated groups	
P value	0.0006
P value summary	***
Significantly different? (P < 0.05)	Yes
One- or two-tailed P value?	Two-tailed
t, df	t=9.691 df=4
How big is the difference?	
Mean ± SEM of column A	100.0 ± 0.0 N=3
Mean ± SEM of column B	53.76 ± 4.771 N=3
Difference between means	-46.24 ± 4.771
95% confidence interval	-59.48 to -32.99
R square	0.9592

Unpaired t test of A. bisexualis colony diameter compared between control and 5µg/ml ajoene treated groups	
P value	0.0071
P value summary	**
Significantly different? (P < 0.05)	Yes
One- or two-tailed P value?	Two-tailed
t, df	t=5.066 df=4
How big is the difference?	
Mean ± SEM of column A	100.0 ± 0.0 N=3
Mean ± SEM of column B	86.49 ± 2.667 N=3
Difference between means	-13.51 ± 2.667
95% confidence interval	-20.91 to -6.106
R square	0.8652

Unpaired t test of A. bisexualis on slide hypha growth rate compared between control and 20µg/ml ajoene treated group	
P value	0.0021
P value summary	**
Significantly different? (P < 0.05)	Yes
One- or two-tailed P value?	Two-tailed
t, df	t=7.082 df=4
How big is the difference?	
Mean ± SEM of column D	100.0 ± 0.0 N=3
Mean ± SEM of column E	36.51 ± 8.964 N=3
Difference between means	-63.49 ± 8.964
95% confidence interval	-88.38 to -38.60
R square	0.9261

Chapter 4 – Antitumor activity of ajoene

Introduction

Endometrial cancer is the most common gynecologic cancer (Roque et al., 2013), and it accounts for almost 5% of female cancers in the world with a high incidence rate in western countries (Mileshkin & Jamil, 2012). In the U.S, it is estimated that there are 47,130 new cases and 8010 deaths annually (Fader, Santin, & Gehrig, 2013). Endometrial tumors are solid tumors, and according to the clinical behavior and histopathology, endometrial cancer can be divided into several stages (Chitcholtan, Sykes, & Evans, 2012; Roque et al., 2013). 80% of women with endometrial cancer are diagnosed at an early stage with low grade tumors, and the 5 year survival rate of this type is higher than 80% (Fader et al., 2013; Purdie & Green, 2001; Roque et al., 2013). Advanced stage endometrial cancers, especially uterine serous carcinoma, are in contrast aggressive and have very poor prognosis (Fader et al., 2013; Roque et al., 2013).

The treatment for early stage endometrial cancer includes surgery, radiotherapy or a combination of these two. For advanced stage cancers, chemotheraphy and hormonal therapy plays an important role in management of the disease. Cytotoxic drugs such as paclitaxel, doxorubicin and cisplatin are heavily used to treat the advanced endometrial cancer as a single agent or in combinations (Markman, 2007; Steer & Harper, 2001).

Paclitaxel was originally extracted from leaves of *Camptotheca acuminata* Decne in 1966. It binds to polymerized tubulin, promotes and stablizes polymerized microtubules and thus arrests cells in mitosis (Cragg & Newman, 2004). Today, paclitaxel is widely used as a chemotherapeutic agent and is used as a first-line treatment for all stages of many cancers and is very commonly used in advanced and metastatic endometrial cancer treatment (Mileshkin & Jamil, 2012; Vilos et al., 2013). However, the toxicity of paclitaxel is quite excessive. Adverse side effects include

peripheral neuropathy, myelosuppression, arthralgias, myalgias and skin problems. Therefore, clinical doses of palcitaxel are limited to achieve good responses due to the severity of adverse effects (Cella, Peterman, Hudgens, Webster, & Socinski, 2003).

Novel targeted drugs, which target the dysfunctional signaling pathways that may underlie malignancy have attracted increasing attention, and have the potentiality to be used as second or third line treatments for endometrial cancers, as beneficial results have been noticed by combining targeted drugs with cytotoxic drugs in clinical trials (Cortes & Roché, 2012; Dedes, Wetterskog, Ashworth, Kaye, & Reis-filho, 2011; Dizon, 2010). In endometrial cancer, the most common mutations are on the cell cycle regulator gene *p53* or on phosphatase and tensin homologue (*PTEN*), which regulates the PI3K/AKT/mTOR pathway. Dysfunction of p53 protein results in uncontroled cell progression and dysfunctioning of PTEN results in enhanced cell proliferation (Albitar, Carter, Davies, & Leslie, 2007) (Fig.4.1). Therefore, a drug that can target on molecules associating with the PI3K/AKT/mTOR pathway or its upstream pathway would have a potential in the clinical appication. For example, gefitinib and canertinib are targeted inhibitors for the upstream signalling molecules EGFR/HER2, and everolimus is a mTOR (mammalian target of rapamycin) inhibitor. These targeted drugs exhibit anti-tumour effects on cell proliferation through the PI3K/AKT/mTOR pathway. In addition to the PI3K/AKT/mTOR pathway, the activation of vascular endothelial growth factor (VEGF) via its receptors (VEGFRs) is also crucial for tumour survial. Blocking this conconical VEGF-VEGFRs axis is proven to be good target for cancer treatments. The targeted agent such as sorafenib is shown to have efficacy in tumours that have VEGF-VEGFRs dependent survival (Dedes et al., 2011).

Researchers have also made efforts to search for treatment that produce less adverse effects on patients. The rationale of the use of natural food products as adjuvant therapy in cancer is gaining popularity. Many bioactive food compounds have been isolated, and this includes an active comound from garlic. The garlic derivative ajoene (Scheme 1) has been found to be able to inhibit tumor progression *in*

vitro and *in vivo*. Its antitumor effects have been tested on various cell lines, such as HL-60 and PtK2 (Dirsch et al., 1998; Li et al., 2002), and it is also able to reduce the growth of primary metastasis of B16/BL6 melanoma tumor in mice (Taylor et al., 2006). Furthermore, patients with basal cell carcinoma were treated with ajoene by applying 0.4% ajoene cream on a tumor site, and 17/21 had a reduction in the size of tumor. To reveal the underlying mechanism of ajoene's effects, the authors then tested ajoene on basal cell cancer cell lines, cancer cell death (apoptosis) was detected by flow cytomety analysis (Tilli et al., 2003). Induction of apoptosis by ajoene was also suggested by other groups. Dirsch's group reported that when HL-60 cells were treated with ajoene, reactive oxgen species (ROS) were generated and nuclear factor *k*B (NF-*k*B) was activated (Dirsch et al., 1998). However, there is also evidence of disruption of the cell cycle by ajoene. Xu's group reported that the amount of cytosolic proteasome was increased when HL-60 cells were treated with ajoene, and cells were arrested in the G2/M phase and proteasome activity was inhibited by ajoene (B. Xu, Monsarrat, Gairin, & Girbal-Neuhauser, 2004). Li's group suggested that ajoene inhibited tumor cell growth by inhibition of microtubule assembly and the subsequent interruption of the cell cycle (Li et al., 2002). Structure-activity studies have also been performed and the anti-proliferative effect of ajoene is suggested to be due to the vinyl disulfide site of ajoene (Scheme 4.1). The vinyl disulfide structure is believed to be responsible for the reaction with microtubule cysteine residues and anti-polymerization of microtubules, caspase 3 and ROS activation (Erkoc et al., 2003; Jacob et al., 2012; Kaschula et al., 2012).

In this study, for the first time, ajoene combined with paclitaxel and the selected targeted drugs will be tested on an endometrial adenocarcinoma cell line to investigate the antitumor effects of ajoene and in combination with other drugs to determine if there is any additive/synergistic effects among these compounds. A 3D spheroid model of endometrial cancer cells grown on non-adherent surface, will be employed for cell culture and treatment. The traditional method of testing drugs on cancer cell *in vitro* is using a 2D cell monolayer. Cells are grown on an adherent surface and drugs

are directly added to the cell monolayer. However this cell model may not reliably mimic the *in vivo* cell growth due to the lack of tissue-specific functions, morphological organization and extra- cellular matrix proteins (ECM) which are crucial for differentiation, normal growth, and maintenance of homoeostasis of cells (Chitcholtan et al., 2013). Therefore, effects of drugs received on a 2D monolayer cell culture may differ significantly from the effects *in vivo*. By contrast, the 3D spheroid model reflects more tumourigenic characteristics of cells and signaling in the microenvironment of spheroids is more likely to be related to that of a real tumor. For example, in colorectal cell lines, gene expression of EGFR and the impact of inhibition of EGFR are significantly different in lrECM 3D spheroid culture as compared to 2D cultures (Luca et al., 2013). Cell proliferation, differentiation and EGFR activation is also altered in 3D cell culture when endometrial cancer cells are cultured on ECM (Chitcholtan et al., 2013). The pattern in which pancreatic carcinoma spheroids respond to drugs differs significantly from 2D culture due to the matrix structure and their distinct physiological properties (Longati et al., 2013). Thus, the advantages of using 3D spheroid cultures have driven us to study the antitumor properties of ajoene and synergistic effects between drugs with this model.

Antitumor activity and synergistic effects of paclitaxel and target drugs were initially screened on endometrial cell line Ishikawa cell spheroids. In the first screening experiments, spheroids were treated with paclitaxel, sorafinib, gefitinib, canertinib and everolimus and the drug effects were screened by measuring the growth activity of spheroids. Growth activity, metabolic activity and morphology of spheroids were further investigated in the second round after treatment with paclitaxel and everolimus. These experiments also served as precusor experiments for understanding the drug response patterns of Ishikawa 3D spheroids, and provided information for the later ajoene experiments. To analyze the effects of ajoene and its combination with cancer drugs on Ishikawa cells, growth activity, metabolic activity, morphology, cytoskeletons, cell proliferation and apoptotic activity of Ishikawa cells were analyzed after treatment with the drugs.

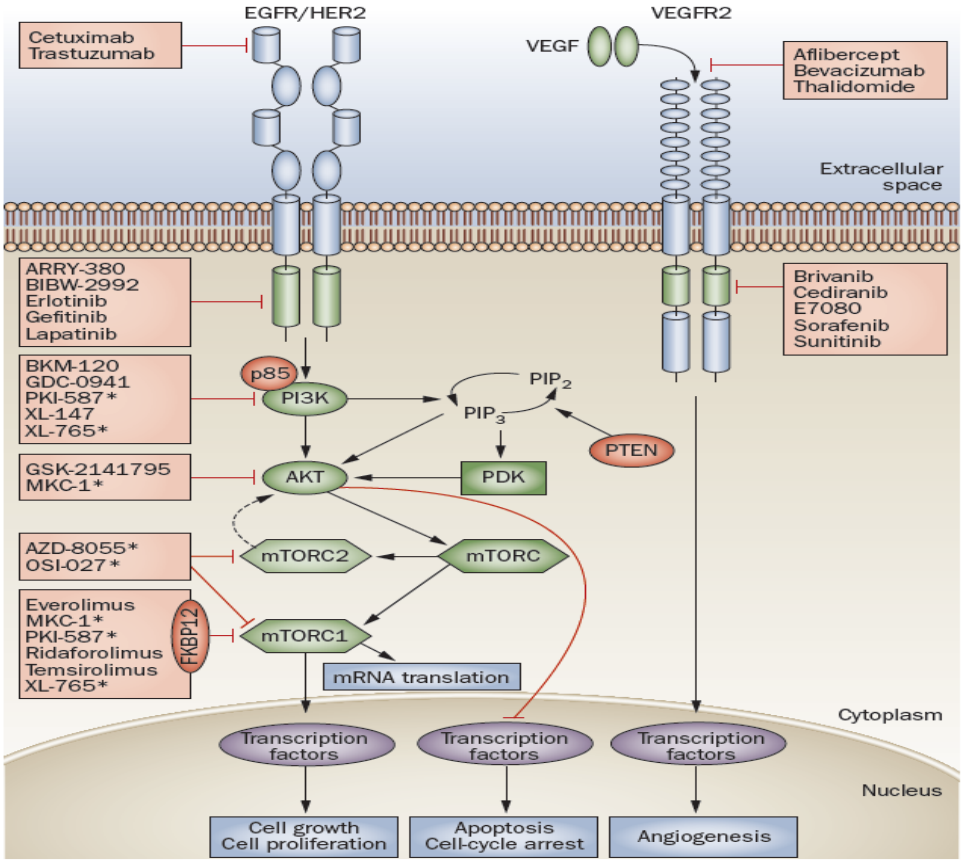

Figure 4.1. Possible targeted pathways for the treatment of endometrial cancer. Current drugs under clinical investigation for the treatment of endometrial cancer and their target molecules in the PI3K/AKT/mTOR and VEGF signaling pathways are displayed. Proteins, ligands and tyrosine kinase domains positively regulating the pathways are displayed in green while proteins with a negative regulatory role are displayed in red. Arrows indicate the activation of a molecule or a process while blunt headed arrows indicate inhibition of a protein or process. The dashed arrow shows the positive feedback from mTORC2 on AKT resulting from the inhibition of mTORC1 alone. Asterisks indicate dual-targeting drugs. Abbreviation: FKBP12, FK506-binding protein 12; mTOR, mammalian target of rapamycin; mTORC1, mammalian target of rapamycin complex 1; mTORC2, mammalian target of rapamycin complex 2; PDK, phosphoinositide-dependent kinase; PI3K, phosphatidylinositol 2 kinase; PIP_2, phosphatidylinositol 4,5-bisphosphate; PIP_3, phosphatidylinositol (3,4,5)-trisphosphate; PTEN, phosphatase and tensin homologue deleted on chromosome 10. Fig. is reproduced from Dedes et al, 2011 (Dedes et al., 2011).

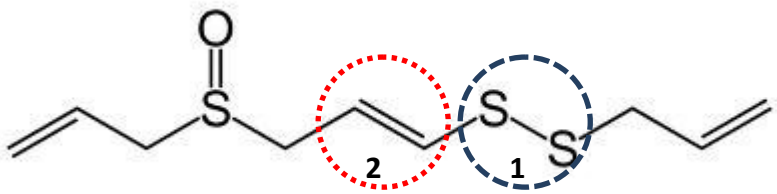

Scheme 4.1. Skeletal structure of ajoene (4,5,9-thrithiadodeca-1,6,11-triene 9-oxide, $C_9H_{14}OS_3$). The disulfide group (1) was suggested to be reponsible for ajoene's activity and the double bond (2) is thought to enhance the activity of the disfulfide.

Materials and Methods

Cell line and growth medium

The endometrial cancer cell line, Ishikawa (grade 1 with *PTEN* and *p53* mutations) was gifted by Dr Masato Nishida, Kasumigaura National Hospital, Tsuchiura-shi, Ibaraki-ken, Japan.

Cells were maintained and grown in DMEM-F12 medium (Catalogue number 12500-096. Invitrogen, New Zealand) supplemented with 10% FBS, 500 units/ml of penicillin/streptomycin and 1mM glutamax.

Drugs

Drugs and their characteristics are listed in Table 4.1.

Table 4.1. Anticancer drugs used in this study.

Drug	**Characteristics of drug**	**Purchased from**
Paclitaxel	Cytotoxic, microtubule inhibitor	Sigma -Aldrich LTD, New Zealand
Everolimus	mTOR inhibitor	LC laboratories, MA, USA
Sorafenib	VEGFR inhibitor	LC laboratories, MA, USA
Gefitinib	EGFR inhibitor	LC laboratories, MA, USA
Canertinib	EGFR/HER-2 inhibitor	LC laboratories, MA, USA
Ajoene	Inhibit microtubule and induce apoptosis	Extracted from garlic (1GE,3GE and 4GE)

Growth and treatment of Ishikawa cells

Coating plates and culturing Ishikawa cells and spheroids

Sterile low melting point agar (Roche, New Zealand) was mixed with nanopure water and autoclaved. Prior to using, agar was completely melted and 400 µl of the melted warm agar was added to each well of a 24 well plates (BD Falcon, New Zealand). The agar in each well was allowed to cool and polymerize and the plates were kept at 4^{o}C prior to further use.

Endometrial cancer cell line, Ishikawa cell line, was cultured in a cell culture flask and was used after it reached 80% confluent. Firstly, the growth medium in a cultural flask was discarded and 10 ml of 1xPBS (components are shown in Appendix 4.1) was added in order to wash cell media. After discarding the PBS, 5 ml of 1xtrypsin- EDTA (Invitrogen, New Zealand) was added and the flask was incubated at 37^{o}C in a humidified 5% CO_2 atmosphere for 10-15 minutes until the cell monolayer was detached from the flask.

The cell suspension was then transferred to a sterile 15 ml tube, and 7 ml of 1xPBS was added and mixed. The tube was then centrifuged at 1500 rpm for 5 min and the supernatant was discarded. 3 ml of pre-warmed growth medium was added to the cell pallet and mixed thoroughly with a pipette, and then 7 ml medium was added and mixed again so the total volume was 10 ml.

The cell concentration was then determined with a haemocytometer, and calculated volumes of the original cell solution was added to each well of the coated 24 well plates which contained 1 ml of growth medium to achieve 2x10^{4} cells/well. 1 ml of the cell solution was also added to the cultural flask which contained 6 ml of growth medium to prepare a new flask. The flask and plates were incubated at 37^{o}C in a humidified 5% CO_2 atmosphere and the flask was subcultured again once it reached 80% confluent.

The cells growing on coated plates formed spheroids and the spheroids were allowed to grow for 6 days before treatment. The medium was replaced every two days.

Treatment with anticancer drugs

Spheroids were treated with either a single drug or combination of drugs. In combination of drugs, paclitaxel was combined with each one of targeted drugs to make up a toxic + non-toxic combination. In addition to being combined with paclitaxel, ajoene was also combined with everolimus to test efficacy. The drug combinations are listed in Table 4.2.

Table 4.2. Drug combination groups for treating Ishikawa spheroids

Drug combination to reveal synergy ("toxic"+"nontoxic")	**Concentrations**
Paclitaxel + Ajoene	Paclitaxel 100 nM or 50 nM with 5 and 10 µg/ml of ajoene
Paclitaxel + Sorafenib	Paclitaxel 100 nM with 2 µM sorafinib
Paclitaxel + Everolimus	Paclitaxel 100 nM or 50 nM with 2 µM Everolimus
Paclitaxel + Gefitinib	Paclitaxel 100 nM with 2 µM Gefitinib
Paclitaxel + Canertinib	Paclitaxel 100 nM with 2 µM Canertinib
Everolimus +ajoene	2 µM or 1µM Everolimus with 10 µg/ml ajoene

When spheroids were treated with single drug listed in Table 4.1 and drugs were replaced every two days. Then, the spheroids were allowed to have 2 days off from drugs, and then the spheroids were incubated with or without the same drug for the following 4 days. In combination treatments, paclitaxel or everolimus was added to the spheroids for the first 2-4 days and one of the other drugs was added to the spheroids for four days after the rest period. Fig.4.2 shows the method of drug treatment. The detailed treatment duration and doses will be explained further in the results section. On the 17^{th} day, spheroids were analyzed with various assays and images of spheroids were taken with a stereomicroscope.

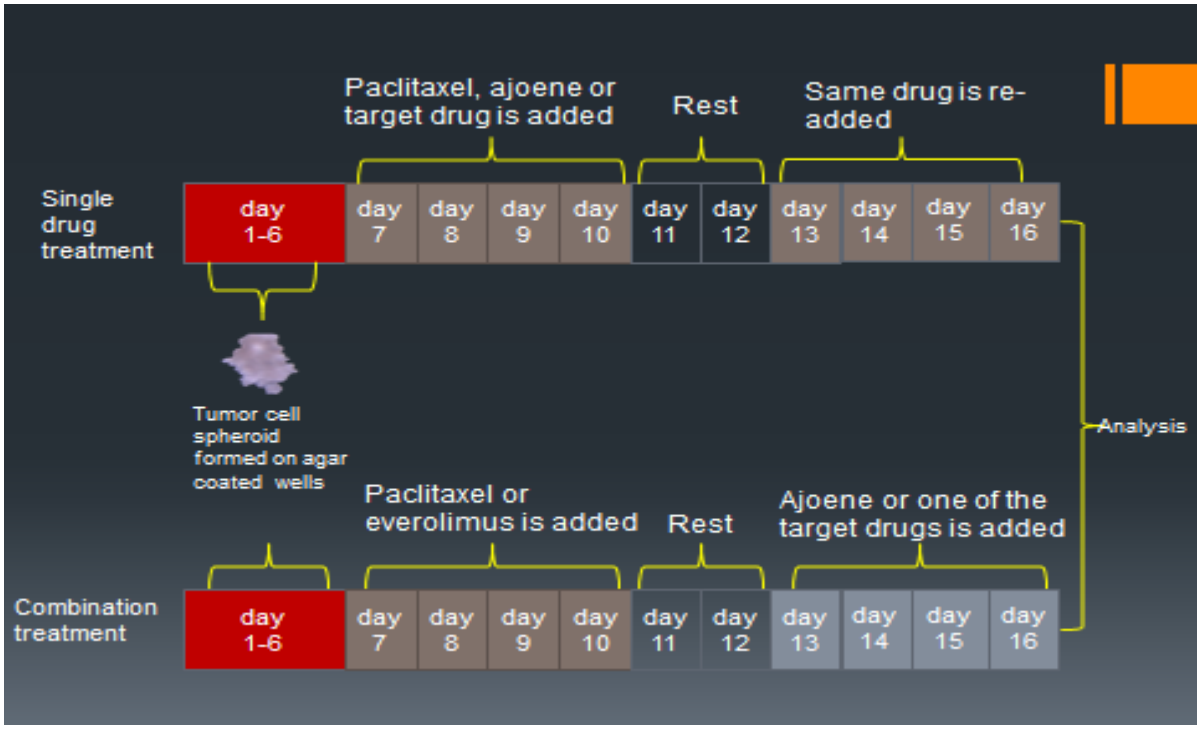

Figure 4.2. Method of drug administration on 3D spheroids. Drugs were added to the cells on Day 7 after the spheroids formed. 2 days drug free interval allowed the model to mimic the recovery period in clinical trials. Various analyses were carried out on Day 17.

Growth activity experiments (Crystal violet assay)

The crystal violet assay was employed to analyze the relative growth activity of Ishikawa spheroids.

Spheroid from each well was added to a microtube and the growth medium was removed with a pipette. 700 µl of 1xPBS and 300 µl of 10xtrypsin-EDTA was added to each tube and mixed. The tubes were then incubated at 37^{o}C for 30 minutes and centrifuged at 1500 rpm for 5 minutes after incubation. The supernatant was discarded and 50 µl of crystal violet (Sigma-Aldrich LTD, New Zealand) was added to each tube and the tubes were left at room temperature for 10 minutes. Then 1 ml of distilled water was added to each tube and mixed well to wash off any unbound crystal violet. The tubes were then centrifuged again at 1500 rpm for 5 minutes. The water washing step was repeated 3 times. After washing, 600 µl of 2% SDS (Sigma-Aldrich LTD, New Zealand) was added to the tubes and the tubes were mixed using a vortex. 200 µl of the solution from each tube was added to each well of 96 well plates and the plates were read at 570 nm for absorbance.

Metabolic experiments (Alamar Blue assay)

Spheroid with 0.5 ml of medium from each well was added to a sterile 4 ml tube. 50 µl of AlamarBlue (Invitrogen, New Zealand) was added to each tube and gently mixed. The tubes were then incubated at 37^{o}C in a humidified 5% CO_2 atmosphere for 24 hours and the absorbance of each tube was read at 570 nm and 600 nm. Metabolic activity was calculated by deducting the 600 nm absorbance from the 570 nm absorbance.

Immunoblotting analysis

Cell proliferation and apoptotic activities were analyzed by Western blotting experiments. The proliferation markers PCNA, Akt, p-Akt, cell cycle marker cyclin-D2 and apoptotic markers caspase-3 and PARP were immunoblotted.

Components of the solutions used in Western blot experiments are shown in Appendix 4.2. The antibodies used are listed in Appendix 4.3.

SDS -PAGE Sample preparation

Spheroids from each group were added to a microtube on ice and 200 µl of RIPA lysis buffer was added to each tube (the volume was adjusted depending on the size of spheroids). The lysate was then kept on ice for 20 minutes. 20 µl of 5x loading sample buffer was added to the lysate. The lysates were mixed thoroughly with the loading sample buffer and were heated at 100^{o}C for 10 minutes and then kept on ice until cooled down. Before loading the gels, lysates were spun at 12000 rpm for 7 minutes and kept on ice.

Gel preparation

After the gel station was assembled, 4 ml of 10% SDS gel solution (12% was used for caspase-3 detection) was added to the gel holder and the holder was topped up with milli Q water. The station was then incubated at 37^{o}C for 1 hour. The stacking gel was prepared by adding the stacking gel solution on top of the solid SDS gel to the top of the glass holder after the water was discarded. Combs were inserted and the station was left in room temperature for 30 minutes. After the incubation, combs were removed and the gel holders were removed from the station and installed in the electrophoresis chamber. Running buffer was added to the chamber and the wells in stacking gel were cleaned with a pipette thoroughly before loading the samples.

Sample loading

Supernatant of cell lysate was loaded in to each well of the stacking gel after cleaning of wells. Samples were loaded as shown in Table 4.3.

Table 4.3. Volume of samples added to Western blotting gel wells.

	well1	well2	well3	well4	well5	well6	well7	well8
Content	Marker	Control	Cancer drug 1	Cancer drug 2	Ajoene	Combination 1	Combination 2	Loading sample buffer
Volume	Fermentous 5 µl + Magic 2 µl	5 µl	10 µl	10 µl	5 µl	10 µl	10 µl	10 µl

* The volume of lysate added to wells was adjusted depending on the total volumes of cell lysates we harvested. After the samples were loaded, electrophoresis was run at 120 V for 2 hours.

* Due to the limited amount of spheroids and cell lysate obtained, there was no sufficient sample for doing a total protein assay for adjusting the protein concentrations. The house keeping protein GAPDH was used as an indicator for protein concentration for each group. GAPDH is used as an internal standard protein since the expression of GAPDH is constant at different times and after experimental manipulations (Mori, Wang, Danenberg, Pinski, & Danenberg, 2008).

Preparation of blocking solution and membrane

Nitrocellulose membranes were cut the same size as the sponge, and the "transfer sandwich" was made as shown in Fig.4.3.

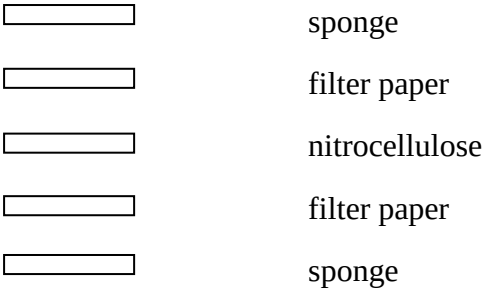

Figure 4.3. Arrangement of the "Transfer sandwich" for transferring proteins from SDS gel to membrane.

The layers were immersed in a box of transfer buffer (with 10% methanol) in a 4^{o}C room. When using a PVDF membrane, PVDF was soaked in 95% methanol for 5 minutes with shaking. The membrane was then washed with milli Q water before it was inserted into the filter paper and sponge and soaked in transfer buffer (without methanol).

Transfer of protein from the gel to the membrane

After electrophoresis, the gel holder was disassembled and the gel was placed in between the membrane and the filter paper. The layers were placed on the cassette and the cassette was sealed after the position of the layers was adjusted. The cassette was inserted into the electrophoresis chamber and a piece of ice was put in the chamber. The electrophoresis was run at 120 V for 1 hour after the transfer buffer was added.

Blocking and primary antibody binding

The membrane was carefully removed after the completion of the transfer. The membrane was cut to keep the protein and it was soaked in a small container with 10 ml of blocking solution. The container was then shaken on a shaker at room temperature for 1 hour. The blocking solution was varied for different proteins (I.e. BSA was used for PARP and ThermoFisher blocking buffer was used for cyclin-D2). After the blocking solution in the membrane container was discarded, 10 ml of diluted primary antibody (1:1000) was poured into the container and the container was left at 4^{o}C overnight.

.

Washing off of the excess antibody, secondary antibody binding and washing

After the overnight incubation in the primary antibody, the solution in the container was discarded. 20 ml of TBS-T was added and the container was shaken on a shaker at room temperature for 10 minutes. The TBS-T was discarded after the wash. The washing step was repeated 4 times. 13 ml of diluted secondary antibody solution (1:5000) was added to the container on the membrane. The container was then shaken for 90 minutes.

After binding, the solution was discarded and the membrane was washed again in the same manner as washing for the primary antibody, finally the membrane was washed with 20 ml of milli Q water for 5 minutes at the end.

Developing and imaging

After the final wash the membrane was taken out of the container and was laid on a piece of transparent plastic sheet. Approximately 1 ml of developing solution (GE Healthcare ECL plus western blotting detection system, New Zealand) was added to each membrane and they were allowed to develop at room temperature for 7 minutes. After developing, excess solution was removed and the membrane was covered with the other piece of plastic and then ready for imaging. Detection was done with Uvitec, Cambridge with Alliance 4.7 software.

Frozen sectioning and immunofluorescence

Cell proliferation and the cytoskeletal protein markers were analysed with immunofluorescence experiments. Cell proliferation markers PCNA, p-Akt and cytoskeletal proteins tubulin (α) and actin were stained with immunofluorescence tagged antibodies using frozen sections of spheroids.

Sample preparation

Spheroids were harvested from 24 well plates and gathered in eppendorf tubes. Spheroids from the same treatment group were combined in the same tube respectively. Medium was removed after a brief centrifugation. 0.5 ml of a 50%/50% methanol-acetone solution at -20 ^{o}C was added to each tube. The tubes were kept at 4°C for further analysis

Spheroids staining and freezing

The tubes were centrifuged at 2500 rpm for 5 min and the supernatant was removed. 1 ml of 1xPBS was added to each tube and the tubes were centrifuged again

at 2500 rpm for 5 min. After removal of the PBS, 50 µl of aniline blue (Sigma -Aldrich LTD, New Zealand) was added to each tube and the tubes were left in room temperature for 20 minutes. 1 ml of water was added to each tube and mixed and the tubes were centrifuged at 2500 rpm for 5 minutes. The supernatant was discarded after centrifugation.

The above step was repeated 3 times to wash off the excess color. After washing, CryO-Z-T (Ted Pella, INC, USA) was added to the pre-labeled plastic square plate and evenly covered the plate area. 1 ml of CryO-Z-T was added to the spheroids in each eppendorf tube and spheroids in CryO-Z-T was laid on the CryO-Z-T covered plate. Plates were kept at -80°C for further cutting.

Cutting

Chunks and brushes were kept at -80°C to maintain the temperature of the sections. One frozen block of sample was entirely removed from the plastic container and fixed on a chunk with CryO-Z-T. Then the sample on chunk was fixed on the sample station of cryostat and frozen section with spheroids was cut with microtome piece by piece. The pieces were removed with brushes and laid on a pre-labeled clean polysine slide (Labserv, New zealand). The slides were kept at -20°C prior to further analysis.

Staining frozen section slides with fluorescence tagged antibodies

Prior to observation, the slides were taken out from -20 °C and left at 4 °C overnight. The next day, 300 µl of 1xPBS was added to each slide and the PBS was absorbed with paper tissue. Slides were left at 37 °C until completely dry. And then superpap pen was used to circle the staining area in order to block the liquid. 300 µl of blocking solution was added to each slide and the slides were left at 4 °C for 1 hour.

After blocking, 1xPBS was used to wash the slides. 300 µl of 1xPBS was added to each slide and the PBS was again absorbed with paper tissue. 300 µl of primary antibody (1:200 in dilution solution which was 2% BSA in 1xPBS) was added to each

slide. The slides were then incubated at 4 °C overnight.

The next day, the antibody solution was drawn with paper tissue after incubation, and the slides were washed with 1xPBS. The slides were inserted in a slide holder in a glass container which was topped up with 1xPBS, with a magnetic stirrer stirring in the bottom of the container. 30 minutes later, the PBS was discarded. This washing step was repeated once.

After the PBS was discarded, the slides were taken out and gently dried with paper tissue. Secondary antibody solution (1:500 in same dilution solution) was added to each slide. The slides were incubated at 37 ^{o}C for 90 minutes.

After incubation, 300 µl of 20 µg/ml Hoechst 33342 (Invitrogen, New Zealand) was added to each slide and slides were kept in the dark place for 20 minutes. Then the slides were washed twice in a glass container with 1xPBS 0.1% tween 20. Slides were gently dried after washing and a drop of anti-fading solution 2g/L p-phenylenediamine (Sigma -Aldrich LTD, New Zealand) in 80% glycerol was added to each slide and the slide was covered with coverslip, slides were observed with an epifluorescence microscope (AxioVision 4.5. Apotome software, Carl Zeiss, Oberkochen, Germany).

Statistical analysis

Data were statistically analyzed with Prism statistical software using Student's *t*-test and $P<0.05$ was used to determine statistical significant. All data were presented as mean+SEM.

Morphology

The morphology of spheroids were observed and imaged using transmitted light with a Leica stereo microscope

Results

The growth activity and metabolic activity results presented in each section below were the combined and analysed results of three independent experiments unless otherwise specified. Images of spheroids, immunofluorescence and Western blotting shown below were representative photos selected from one of the 3 experiments.

Anticancer drug screening

Growth activities of spheroids treated with paclitaxel and target drugs

The anticancer drugs sorafenib, everolimus, gefitinib and canertinib were tested on Ishikawa spheroids alone and in combination with paclitaxel. In the first round, the drugs were added to the spheroids in the manner as shown in Table 4.4. Growth activity was analysed with crystal violet assay after the end of the treatment period. The results of crystal violet are shown in Fig.4.4 and Fig.4.6. Photos of spheroids after treatment are shown in Fig.4.5 and Fig.4.7.

Table 4.4. Duration and concentration of drug treatment for the target drugs screening.

Treatment	Drug concentration	Duration
Paclitaxel	100 nM	4days+2days off+4days
Sorafenib	2 μM	4days+2days off+4days
Everolimus	2 μM	4days+2days off+4days
Gefitinib	2 μM	4days+2days off+4days
Canertinib	2 μM	4days+2days off+4days
Combination	100 nM Paclitaxel +2 μM one of the other drugs	4days paclitaxel+2days off+4days one of the other drugs

The crystal violet assay is a simple assay which is used to determine cell viability. Crystal violet (Triphenylmethane dye) stains DNA of cells and the intensity of color, which is depending on the amount of the dye taken up by cells, is directly proportional to cell number (Vega-Avila & Pugsley, 2011).

The growth activity of spheroids had a significant reduction in 100 nM paclitaxel and 2 μM everolimus treated groups (Fig.4.4), which agreed with sizes of spheroids shown on the photos in Fig.4.5. When everolimus was combined with paclitaxel to treat spheroids, the growth activity and spheroid size were reduced even further than paclitaxel alone (Fig.4.4 and Fig.4.5), but the further reduction was not statistically significant. The VEGFR inhibitor sorafenib alone did not show any inhibitory effect over Ishikawa spheroids (Fig.4.4 and Fig.4.5), but its combination with paclitaxel gave lower growth activity than control although the result was not statistically significant due to the noticeable high variation among experiments.

A similar pattern was observed in canertinib and gefitinib treatment (Fig.4.6 and Fig.4.7). Single use of 100 nM paclitaxel or 2 μM canertinib significantly reduced growth activity of spheroids than control, and 2 μM gefitinib alone did not show any inhibitory effect on spheroids. The combinations, paclitaxel +canertinib or paclitaxel + gefitinib had significant lower growth activity than control, but the combinations were not able to inhibit the spheroids growth further than paclitaxel alone.

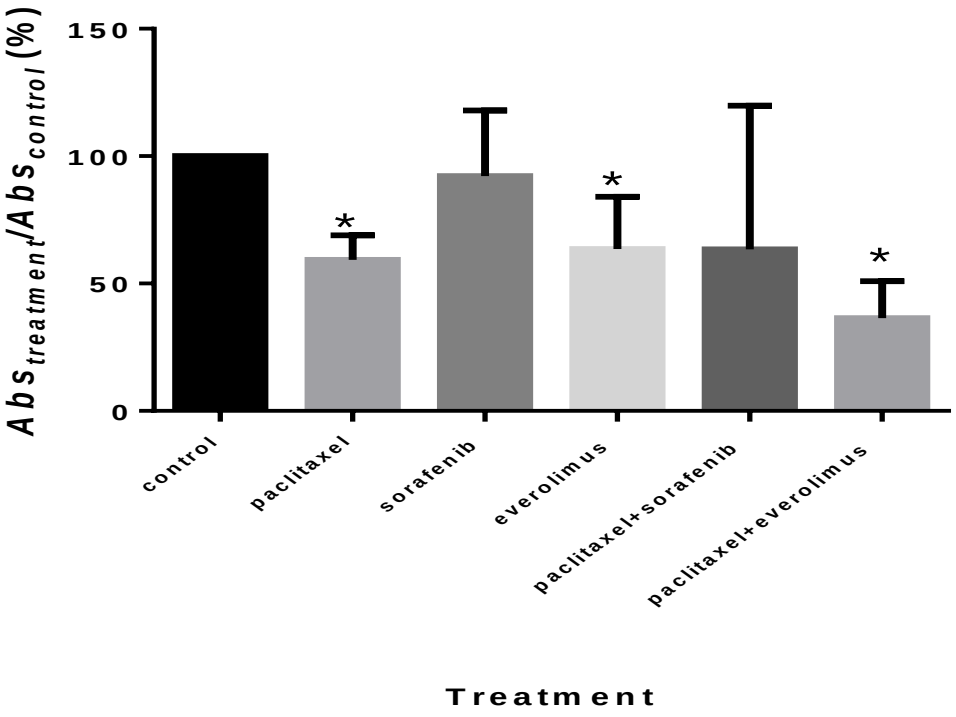

Figure 4.4. Growth activities of spheroids treated with various drugs. Growth activity was measured by reading the absorbance of crystal violet stained DNA solution. Data was normalized by dividing the average absorbance of each treatment group by the average absorbance of the control group. Paclitaxel, everolimus and paclitaxel+everolimus treated spheroids had significantly reduced growth activity (*t* test, $P<0.05$), but the difference between single drug and combination groups was not significant (*t* test, $P>0.05$).

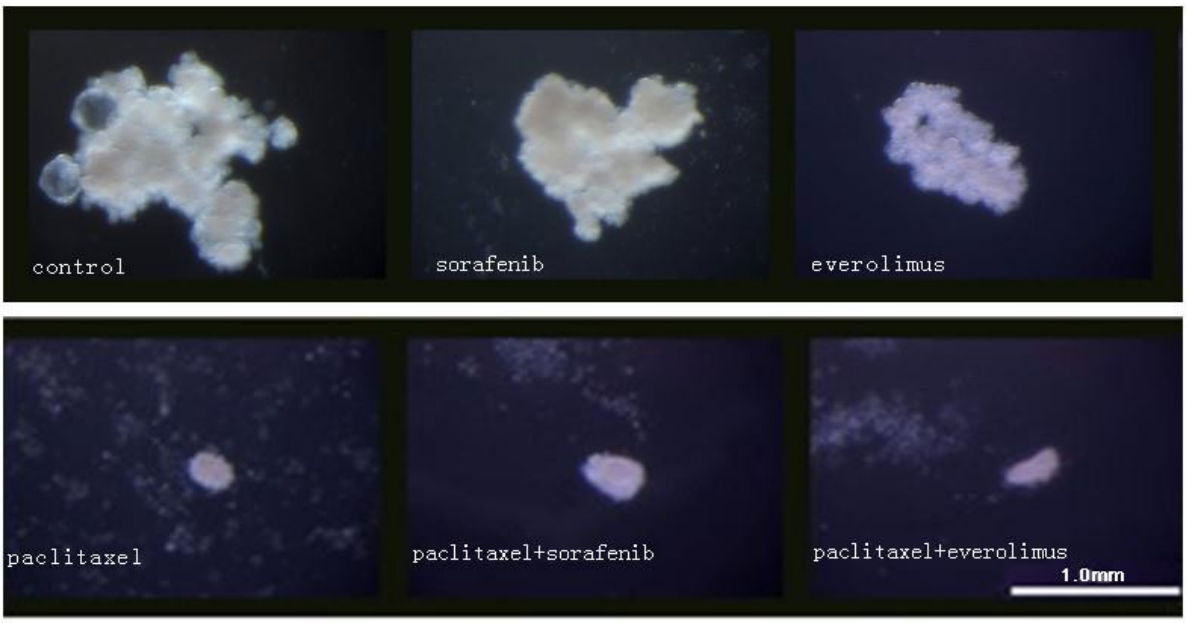

Figure 4.5. Images of Ishikawa spheroids after exposure to drugs. Paclitaxel treated spheroids had significant smaller spheroids than others treatment and structures of spheroids were also more compact than other groups.

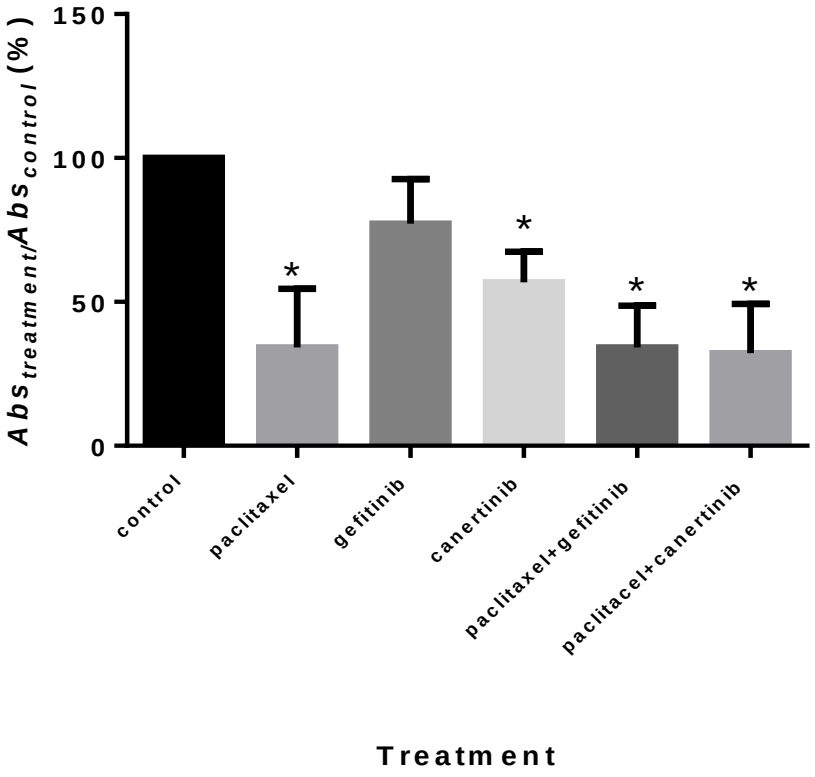

Figure 4.6. Growth activity of spheroids treated with various drugs. Data was normalized by dividing the average absorbance of each treatment group by the average absorbance of the control group. Paclitaxel, canertinib and the combination drugs treated spheroids had significantly reduced growth activity (*t* test, $P<0.05$), but the difference between the single drug treatments and combination groups was not significant (*t* test, $P>0.05$).

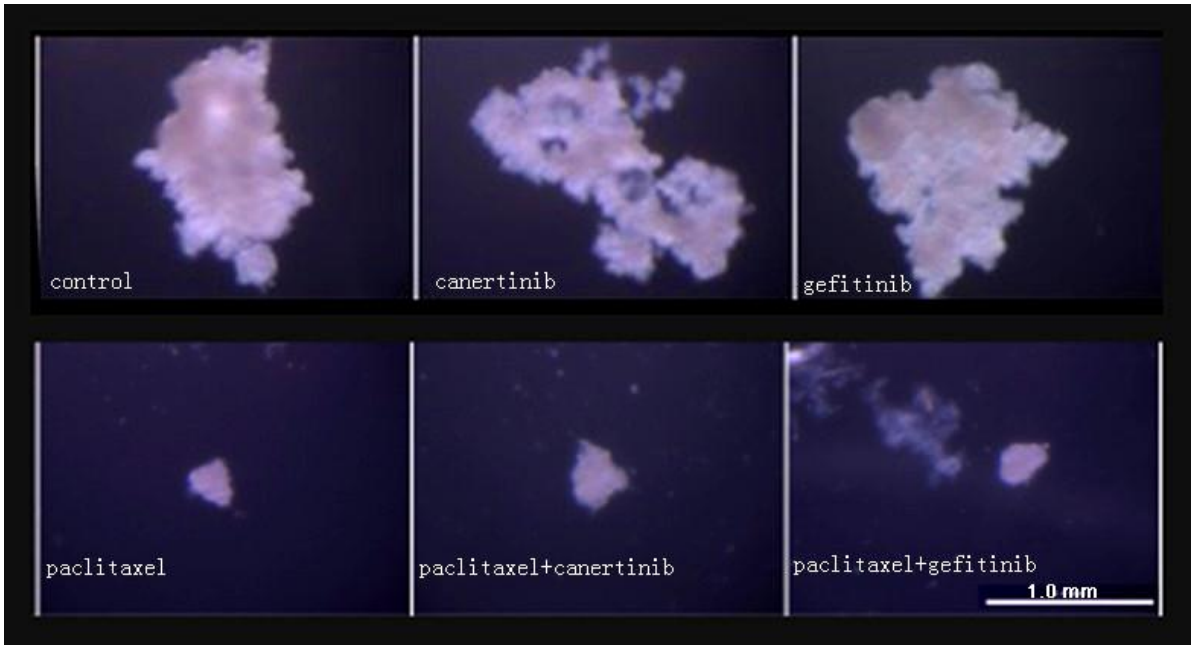

Figure 4.7. Images of spheroids after treatment. Again paclitaxel treated groups had significant smaller and more compact spheroids than the control.

Effects of everolimus and paclitaxel on Ishikawa spheroids

In the targeted drugs screening, paclitaxel alone and the combinations showed significant inhibitory effects on the growth activity of spheroids. Everolimus alone was able to inhibit the growth activity of the cancer cells and it also enhanced the effects of paclitaxel (Fig.4.4). In order to further analyze the effects of everolimus and its combination with paclitaxel, metabolic activities of spheroids treated with paclitaxel, everolimus or the combinations were analyzed using an Alamar Blue assay. The concentrations and durations of paclitaxel and everolimus treatments used in metabolic activity assessments are listed in Table 4.5. Results and comparisons are shown in Fig.4.9.

Table 4.5. Duration and concentration of paclitaxel+everolimus treatment for metabolic activity experiments.

Treatment	Drug concentration	Duration
Paclitaxel	50 nM	4days treatment+2days off+ 4days treatment
Paclitaxel	100 nM	4days treatment+2days off+ 4days treatment
Everolimus	2 µM	4days treatment+2days off+ 4days treatment
Combination1	50 nM Paclitaxel +2 µM everolimus	4days paclitaxel+2days off+4days everolimus
Combination2	100 nM Paclitaxel +2 µM everolimus	4days paclitaxel+2days off+4days everolimus

Alamar blue (Resazurin sodium salt) is a colometric REDOX indicator for detecting metabolic activity of cells. When cells are proliferating and metabolic activity is maintained, a reduced microenvironment is produced and the indicator is remains blue. Once the metabolic activity is inhibited, the indicator is oxidized and it turns to red (Invitrogen). The absorbance difference at 570 nm and 600 nm represents the metabolic activity of cells.

Before the metabolic activity of drug treated spheroids were measured, metabolic activities and diameters of standard spheroids were measured by growing 6 groups spheroids on 24 well plates and one group of them was withdrawn from the plates in every 2 days. The change of metabolic activity and spheroid diameter are shown in Fig.4.8. The figure showed that the pattern of metabolic activity changed by time is not the same as the size change. Metabolic activity tended to become stable after a certain time of incubation although the sizes of spheroids were still increasing due to the expansion of cell numbers in spheroids. Comparison of metabolic activity between spheroids treated with different drugs is not going to be significantly affected by the size of spheroids.

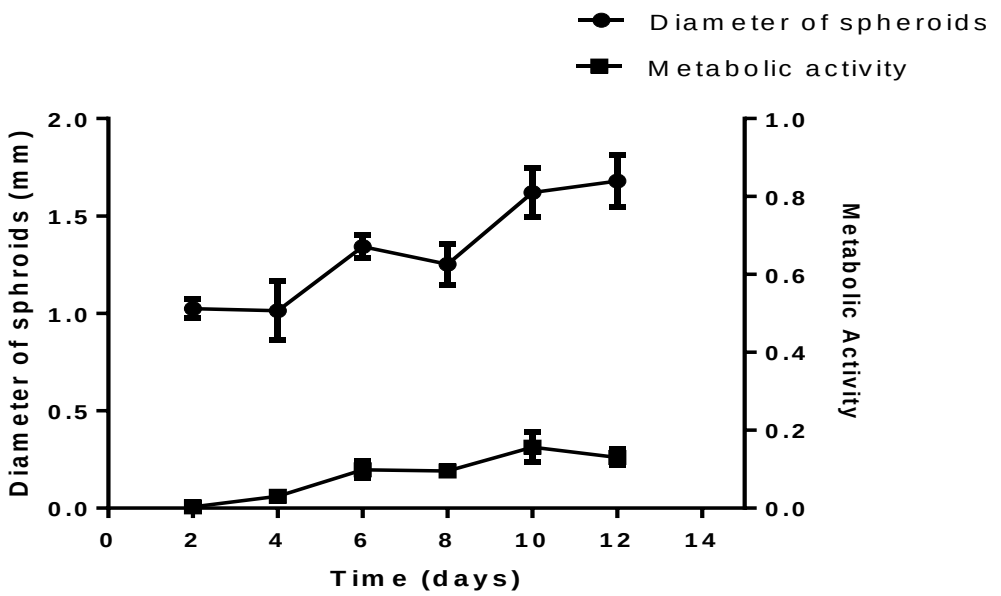

.

Figure 4.8. Growth pattern of Ishikawa cell spheroids. The left side Y axis and upper graph are representing the diameters of spheroids, and the right side Y axis and lower graph are representing the metabolic activity. Metabolic activity was calculated through Absorbance 570 nm –Absorbance 600 nm

When spheroids metabolic activity was analyzed after treatment, 50 nM paclitaxel, 100 nM paclitaxel and 2 µM everolimus treated spheroids had significantly lower metabolic activity than the control (Fig.4.9). 50 nM and 100 nM paclitaxel treated spheroids did not have significantly different metabolic activity, suggesting that the cytotoxic effect of paclitaxel is still high even when the dose was reduced to 50 nm. When everolimus was used in conjunction with paclitaxel, metabolic activity of the spheroids had a further reduction. Again the further reduction was not statistically significant due to the relatively high variations among the experiments. The metabolic activity experiment results agreed with the growth activity experiments of paclitaxel and everolimus.

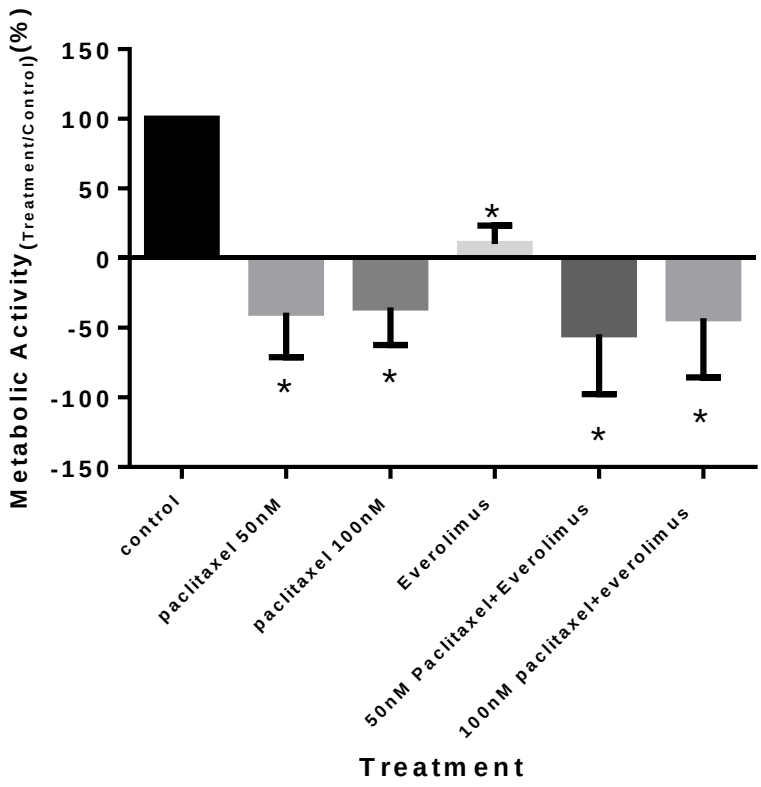

Figure 4.9. Results of metabolic activity experiments for paclitaxel and everolimus treated spheroids. In the paclitaxel and combination groups, paclitaxel was added to the spheroids in the first 4 days. Paclitaxel was again added to spheroids in the last 4 days of the paclitaxel treatment groups whereas everolimus was added to the combination groups in the last 4 days. Since the results were Absorbance 570 nm-Absorbance 600 nm, negative results represent low metabolic activities. Data was normalized by dividing the results of treatment groups by the result of the control. Drug treated spheroids had significantly lower metabolic activity than the control group (*t* test, $P<0.05$), but the difference between single treatments and combination treatments was not significant. (*t* test, $P>0.05$)

Since the growth activity and metabolic activity in paclitaxel+everolimus combination groups were not significantly lower than paclitaxel alone treated groups, and lower dose paclitaxel still exhibited high inhibitory effects, there is a possibility that the cytotoxic effects of the 4 day paclitaxel treatment was too high and the growth of spheroids was still inhibited by the earlier paclitaxel treatment in the next 6 days, thus the effects of everolimus were revealed.

Therefore, in order to test if everolimus had the ability to maintain and enhance the effect of a shorter treatment of paclitaxel, the duration of paclitaxel treatment was reduced to 2 days in the second round of crystal violet assays. Comparison was made between paclitaxel+everolimus group and the group with only 2 days of paclitaxel treatment. Drug doses used in the second round crystal violet experiments are shown in Table 4.6. Crystal violet results are shown in Fig.3.10 and images of spheroids are shown in Fig. 3.11.

Table4.6. Duration and concentration of paclitaxel and everolimus for the second growth activity experiments.

Treatment	**Drug concentration**	**Duration**
Paclitaxel	50 nM	2days treatment+8days off
Paclitaxel	100 nM	2days treatment+8days off
Everolimus	2 μM	2days treatment+2days off+6days treatment
Combination1	50 nM Paclitaxel +2 μM everolimus	2days paclitaxel+2days off+6days everolimus
Combination2	100 nM Paclitaxel +2 μM everolimus	2days paclitaxel+2days off+6days everolimus

The growth activity pattern remained similar to the previous experiments even when the duration of paclitaxel was reduced to 2 days. Spheroids treated with 2 days of paclitaxel had significantly reduced growth activity and sizes compared to control, even after 8 days of resting period (Fig.4.10 and Fig.4.11). Again the addition of everolimus tended to further reduce the growth activity and sizes of paclitaxel treated spheroids, but the enhancement of inhibitory effect was not statistically significant.

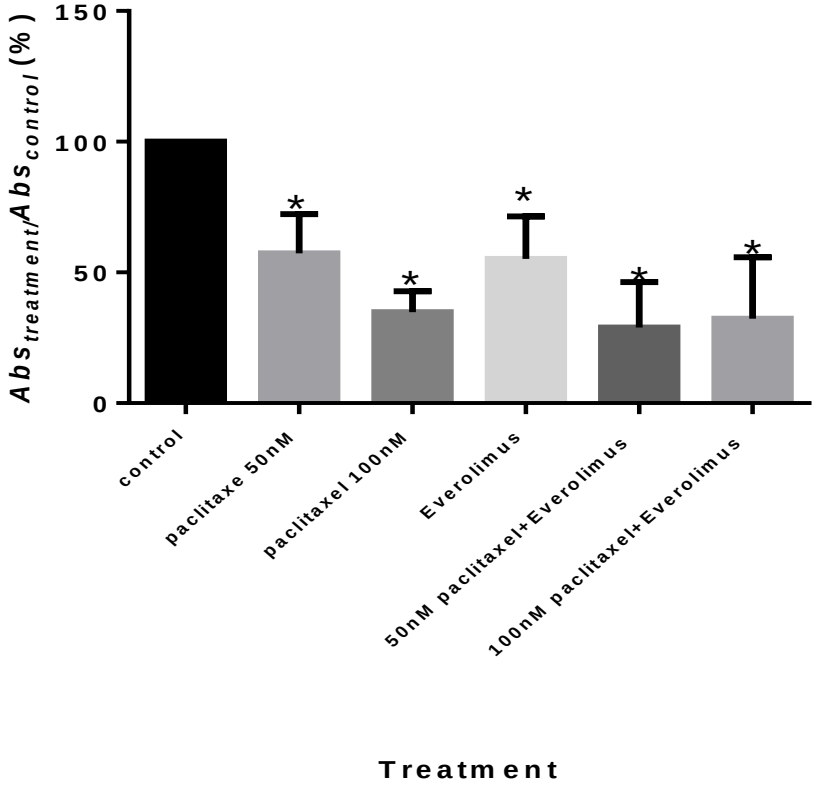

Figure 4.10. Growth activity of spheroids treated with paclitaxel and everolimus. In these experiments, the spheroids were only treated with paclitaxel for 2 days in the single paclitaxel and combination groups. The spheroids had significantly reduced growth activity in all the drug treated groups (*t* test, $P<0.05$) but the difference between single and combination groups was not significant (*t* test, $P>0.05$).

Figure 4.11. Images of spheroids after treatment with the respective drugs. The sizes of spheroids in the drug treated groups were smaller than in the control group. The 100 nM paclitaxel+everolimus treated spheroids was smaller than the 100 nM paclitaxel treated spheroid. Combination groups tended to have noticeably smaller spheroids than the corresponding single groups.

Antitumor experiments with ajoene

Paclitaxel and ajoene

1GE (see chapter 1 garlic extraction) was tested on spheroids alone or with paclitaxel and the growth activity of 1GE treated spheroids was assessed by the crystal violet assay. Table 4.7 below shows the duration and concentration of paclitaxel and ajoene used in this experiment. Fig.4.12 shows the results of crystal violet experiments.

Table 4.7. Duration and concentration of paclitaxel and ajoene treatment for the first growth activity experiments.

Treatment	Drug concentration	Duration
Paclitaxel	100 nM	4days treatment+2days off+ 4days treatment
Ajoene	5 µg/ml	4days treatment+2days off+ 4days treatment
Ajoene	10 µg/ml	4days treatment+2days off+ 4days treatment
Combination	100 nM Paclitaxel +5 µg/ml ajoene	4days paclitaxel+2days off+4days ajoene

5 µg/ml and 10 µg/ml of ajoene alone did not inhibit the growth activity of spheroids (Fig.4.12). A combination of 5 µg/ml ajoene and paclitaxel reduced the growth activity of spheroids further than paclitaxel alone, but this was not statistically significant.

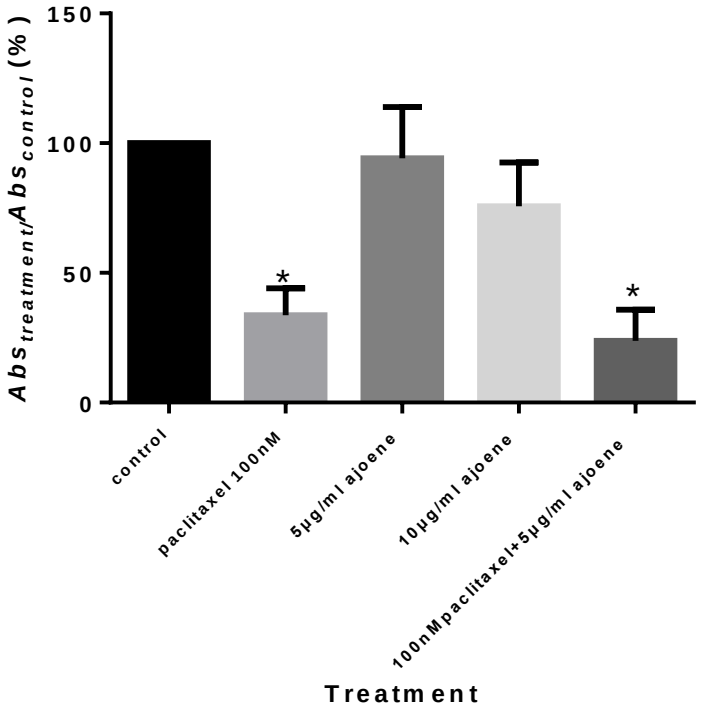

Figure 4.12. Growth activities of spheroids treated with paclitaxel and ajoene. Ajoene treated spheroids did not show any significant difference from control groups. Paclitaxel and the combination groups had lower results than the control. Treatments using combinations tended to inhibit spheroid growth activity further than using paclitaxel alone. The paclitaxel and combination groups had significantly reduced growth activities (*t* test, $P<0.05$) but the difference between these two groups was not significant (*t* test, $P>0.05$).

Again, in order to exclude the possibility that the inhibitory effects were solely due to the prior paclitaxel treatment, the duration and dose of paclitaxel and ajoene treatment was altered in the second round of experiments. Besides growth activity, metabolic activity, cell proliferation, cytoskeletons and apoptotic activities were also analyzed for the spheroids. 3GE and 4GE (see chapter1 garlic extraction) was used in this round of experiments.

Table 4.8. The duration and concentration of paclitaxel and ajoene used in second round of antitumor experiments.

Treatment	Drug concentration	Duration
Paclitaxel	50 nM	4days treatment+6days off
Paclitaxel	100 nM	4days treatment+6days off
Ajoene	10 μg/ml	4days treatment+2days off+4days treatment
Combination1	50 nM paclitaxel +10 μg/ml ajoene	4days paclitaxel+2days off+4days ajoene
Combination2	100 nM paclitaxel +10 μg/ml ajoene	4days paclitaxel+2days off+4days ajoene

Growth activity, metabolic activity and sizes of spheroids did not show any significant change in the 10 μg/ml ajoene treated groups (Fig.4.13, Fig.4.14 and Fig.4.15). Four days of 50 nM or 100 nM paclitaxel alone treated groups had significantly reduced growth activity, metabolic activity and sizes. Addition of 10 μg/ml ajoene for the later 4 days of treatment after paclitaxel did not bring any further reduction in growth activity, metabolic activity and sizes of spheroids.

Immunofluorescent staining of the cell proliferation markers PCNA and p-Akt was elevated in single paclitaxel and paclitaxel+ajoene treated spheroids (Fig.4.18 and Fig.4.19). Ajoene alone enhanced PCNA but not p-Akt expression (Fig.4.18 and Fig.4.19).

Immunofluorescent images of the cytoskeletal protein tubulin showed higher expression of tubulin in paclitaxel and ajoene treated groups than the control (Fig.4.16). The pattern of actin staining did not show significant difference among groups (Fig.4.17).

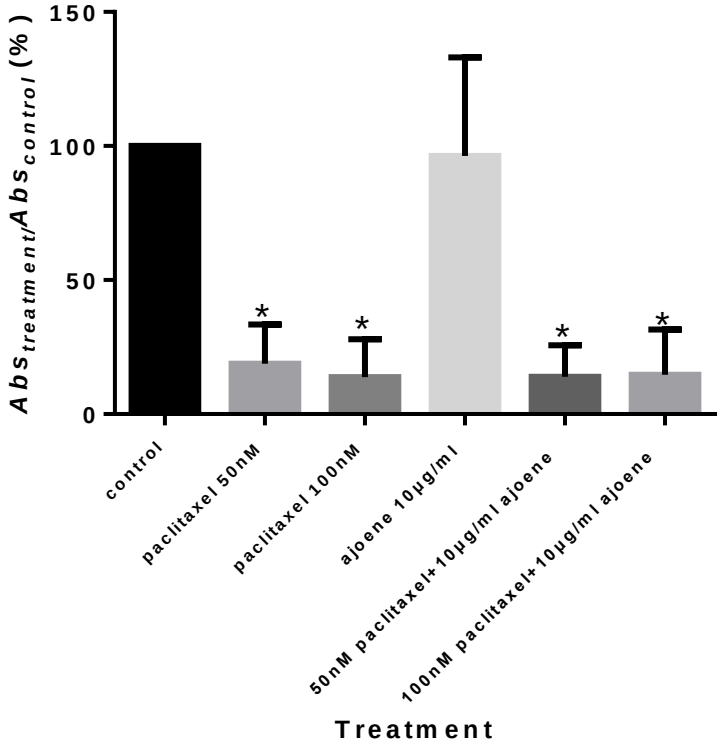

Figure 4.13. Growth activities of spheroids treated with paclitaxel and ajoene. For these experiments paclitaxel was only added to the single paclitaxel treatment groups in the first 4 days and spheroids were left untreated for the rest of the incubation time. Again 10 µg/ml ajoene treated spheroids did not have any significant difference from control groups. The single drug paclitaxel groups and combination groups had significantly reduced growth activities compared to the control (*t* test, $P<0.05$) but the difference between the correspondent single and combination groups was not significant (*t* test, $P>0.05$).

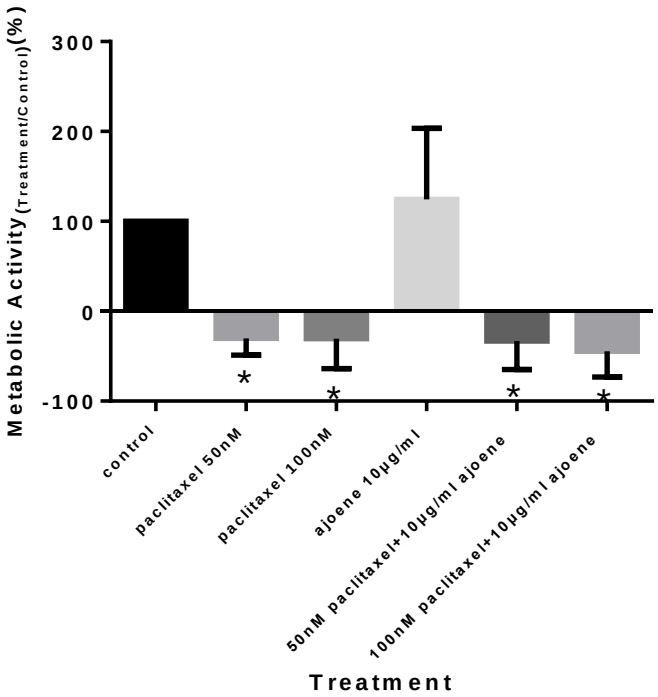

Figure 4.14. Results of metabolic activity (Alamar Blue) experiments for paclitaxel and ajoene treated spheroids. In the paclitaxel and combination groups, paclitaxel was only added to the spheroids for the first 4 days. Then spheroids were left untreated in the single paclitaxel group whereas ajoene was added to the combination groups in the last 4 days. Again negative results represent low metabolic activities. 10 µg/ml ajoene treated spheroids did not show any significant reduction in metabolic activity. Paclitaxel containing groups had significantly lower metabolic activity than the control group (*t* test, $P<0.05$). Combinations of paclitaxel and ajoene groups tended to have lower metabolic activities than their correspondent single paclitaxel groups but the difference was not significant. (*t* test, $P>0.05$)

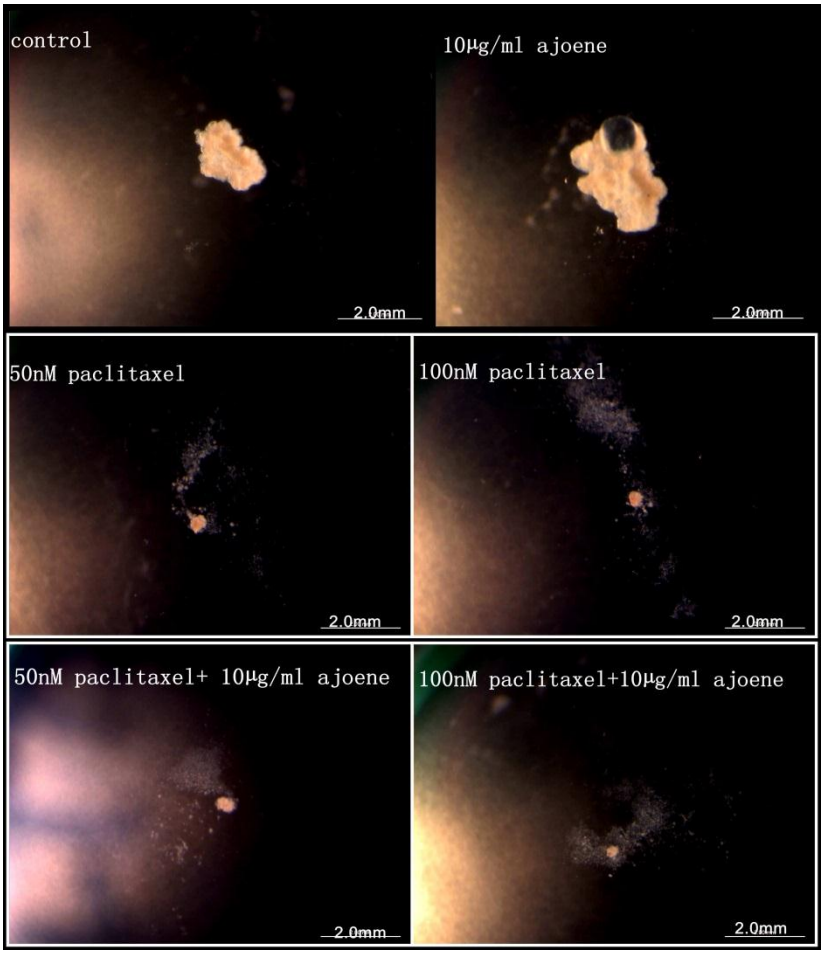

Figure 4.15. Images of spheroids treated with paclitaxel and ajoene. 10 μg/ml ajoene treated spheroids did not have any reduction in size. Paclitaxel involved groups had significantly reduced spheroids sizes and the structures of spheroids in these groups were compacter than control and ajoene groups.

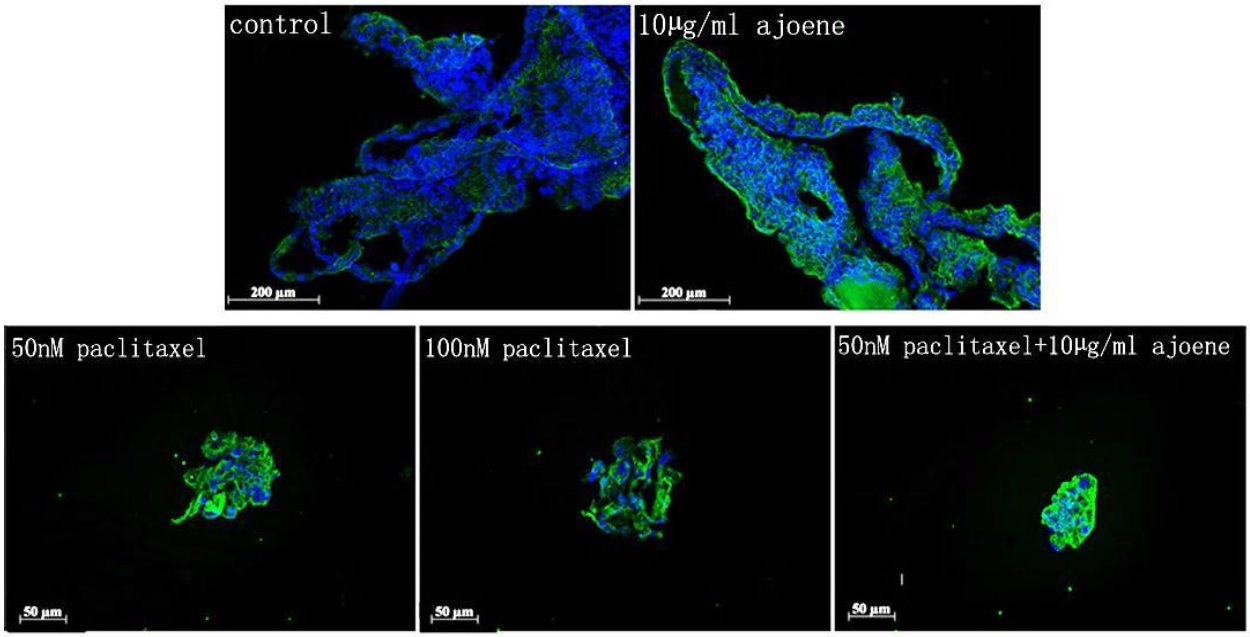

Figure 4.16. Immunofluorescent images of tubulin in frozen cut sections of spheroids treated with paclitaxel and ajoene. Tubulin was stained green and nuclei were stained blue.

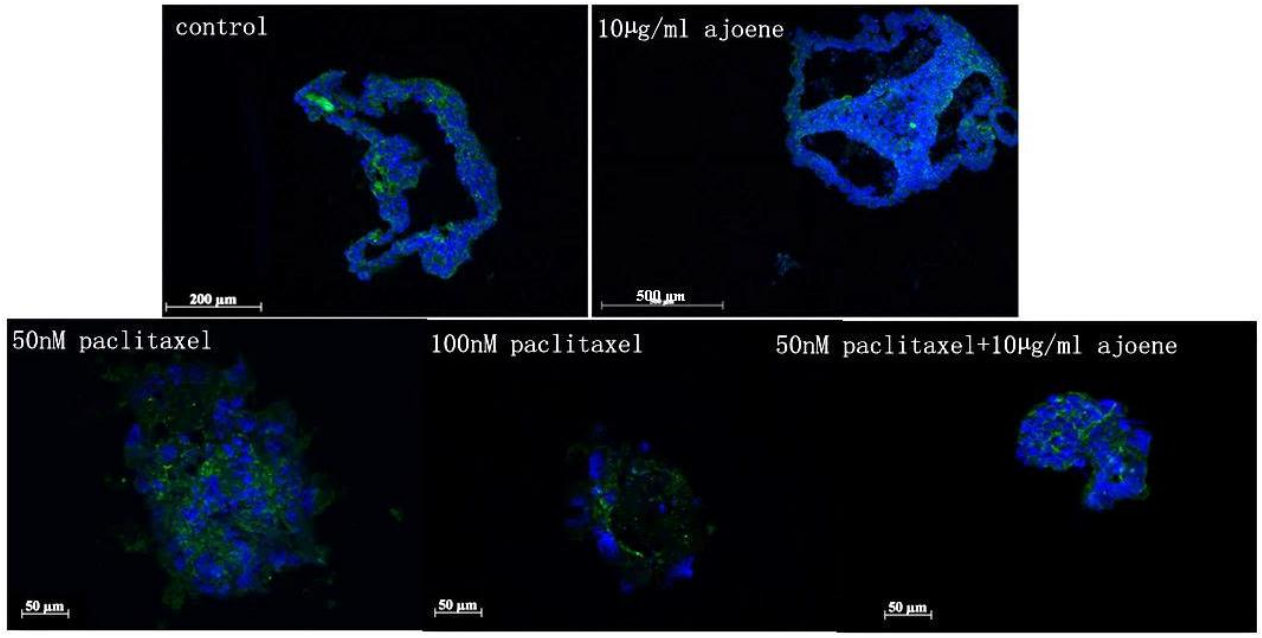

Figure 4.17. Immunofluorescent images of actin in frozen cut sections of spheroids treated with paclitaxel and ajoene. Actin was stained green and nuclei were stained blue.

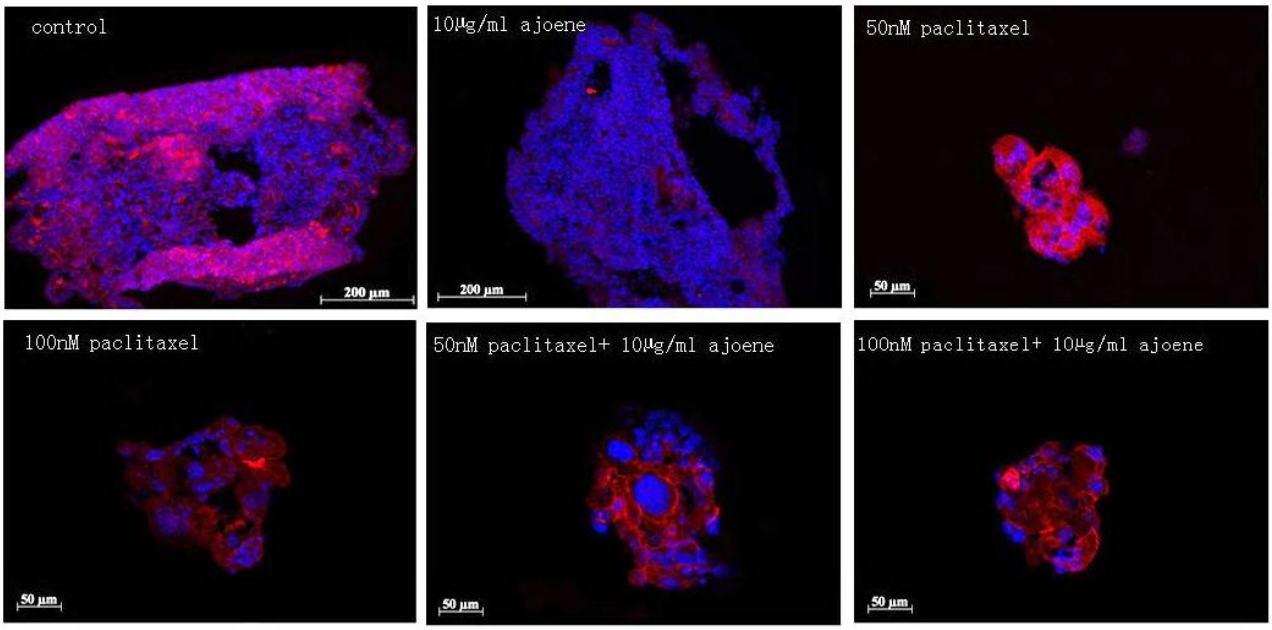

Figure 4.18. Immunofluorescent images of p-Akt in frozen cut sections of spheroids treated with paclitaxel and ajoene. P-Akt was stained red and nuclei were stained blue.

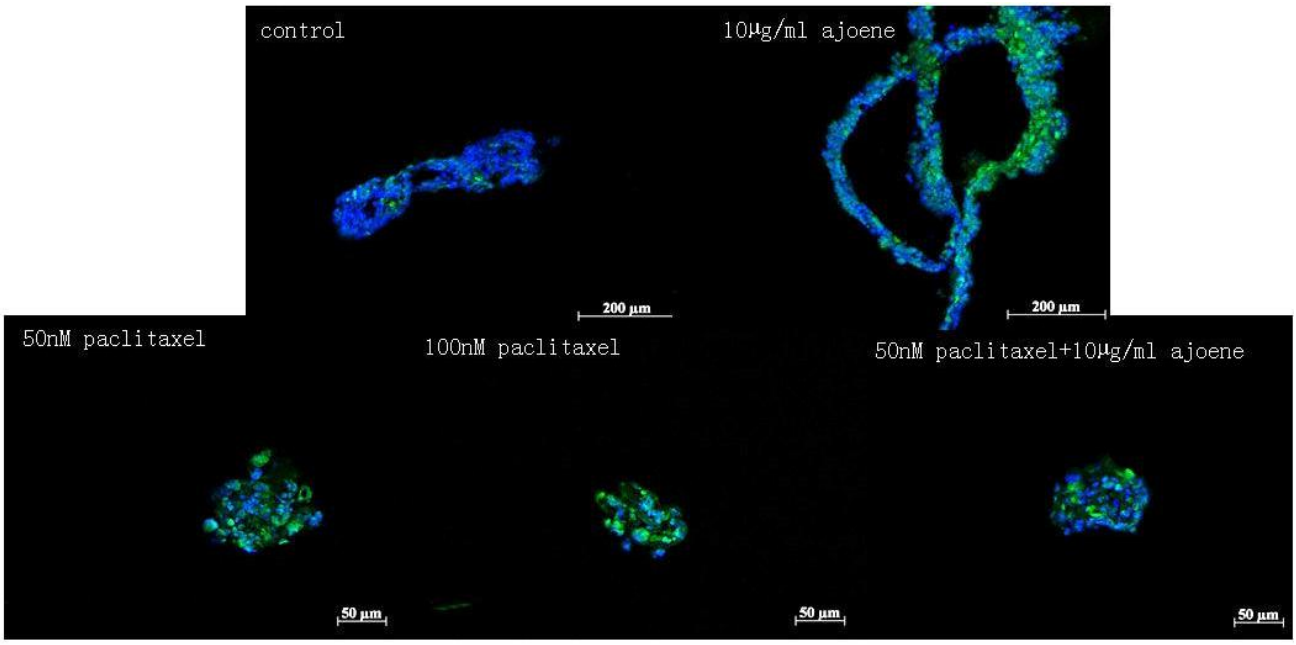

Figure 4.19. Immunofluorescent images of PCNA in frozen cut sections of spheroids treated with paclitaxel and ajoene. PCNA was stained green and nuclei were stained blue.

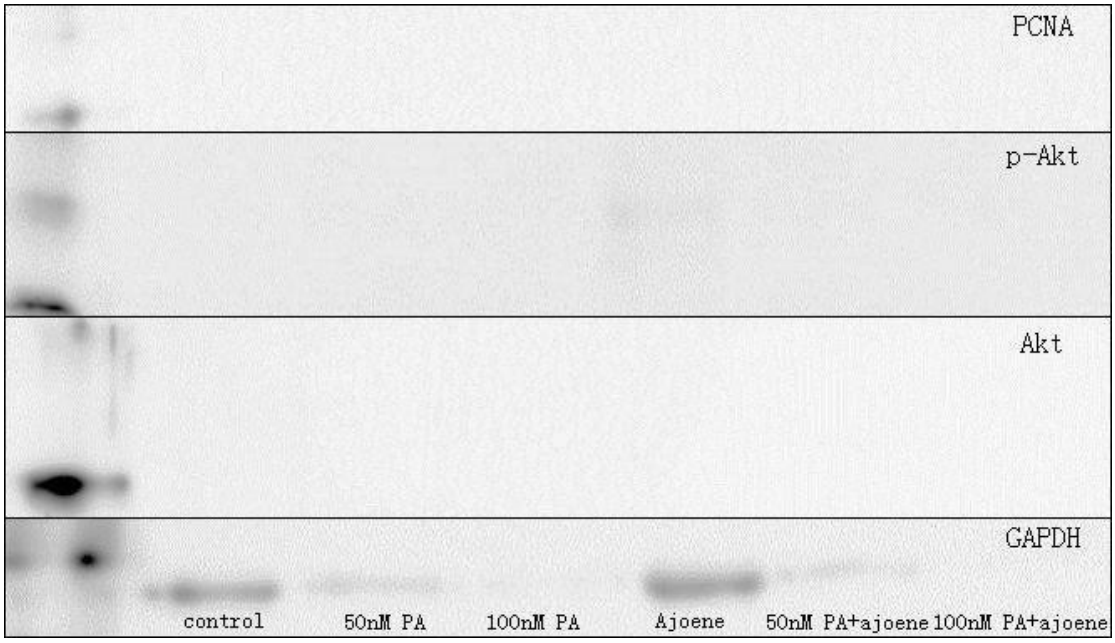

Figure 4.20. Results of a Western blotting for GAPDH, PCNA, Akt and p-Akt of spheroids treated with paclitaxel and ajoene. PA stands for paclitaxel on this Fig.. Several attempts were made using spheroids from each individual experiment. The results above were the best images from all of the attempts. Since the spheroids were tiny and volume of protein solution added to Western blotting wells were limited, there was not enough protein to be shown on the PCNA, Akt AND p-Akt western blotting images. The Housekeeping protein GAPDH bands appeared on the image but this protein from paclitaxel and combination treated groups was not enough to be clearly displayed. As such conclusive result could be generated from this western blotting result.

Everolimus and ajoene

Everolimus was tested along with paclitaxel in the antitumor drug screening experiments stated in the earlier paragraphs. The drug has shown its ability to inhibit the growth and metabolic activities of spheroids. In order to investigate any additive/synergistic effect between everolimus and ajoene, spheroids were treated with ajoene, everolimus and their combinations, and growth activity, metabolic activity, cell proliferation, cytoskeletons and apoptotic activities was analyzed with crystal violet assay, Alamar Blue, frozen section immunofluorescence staining and western blotting. The duration and doses of everolimus and ajoene used in this round of experiments are listed in Table 4.9.

Table 4.9. The Duration and doses of everolimus and ajoene used in antitumor experiments

Treatment	Drug concentration	Duration
Everolimus	1 µM	4days treatment+2days off+ 4days treatment
Everolimus	2 µM	4days treatment+2days off+ 4days treatment
Ajoene	10 µg/ml	4days treatment+2days off+4days treatment
Combination1	1 µM Paclitaxel +10 µg/ml ajoene	4days everolimus+2days off+4days ajoene
Combination2	2 µM Paclitaxel +10 µg/ml ajoene	4days everolimus+2days off+4days ajoene

Growth activity and metabolic activity of spheroids did not show any significant change in everolimus and ajoene treated groups (Fig.4.21 and Fig.4.22). The size of spheroids was reduced in 2 μM everolimus and 2 μM everolimus+ajoene treated groups (Fig. 4.23).

Immunofluorescent staining and an immunoblotting of the cell proliferation marker PCNA was slightly elevated in everolimus and ajoene treated groups (Fig.4.26), and p-Akt was elevated in everolimus but not the ajoene treated groups (Fig.4.25). Western blot results showed that the cell cycle marker cyclin D2 was elevated by everolimus and ajoene (Fig.4.28).

Immunofluorescent images of the cytoskeletal proteins tubulin and actin did not show significant difference among groups (Fig.4.27 and Fig.4.24). The apoptotic marker cleaved caspase 3 protein at 17 kDa was not shown by any group on Western blotting results, but PARP (Poly ADP ribose polymerase) and cleaved PARP was observed in everolimus treated groups on western blotting image (Fig.4.28).

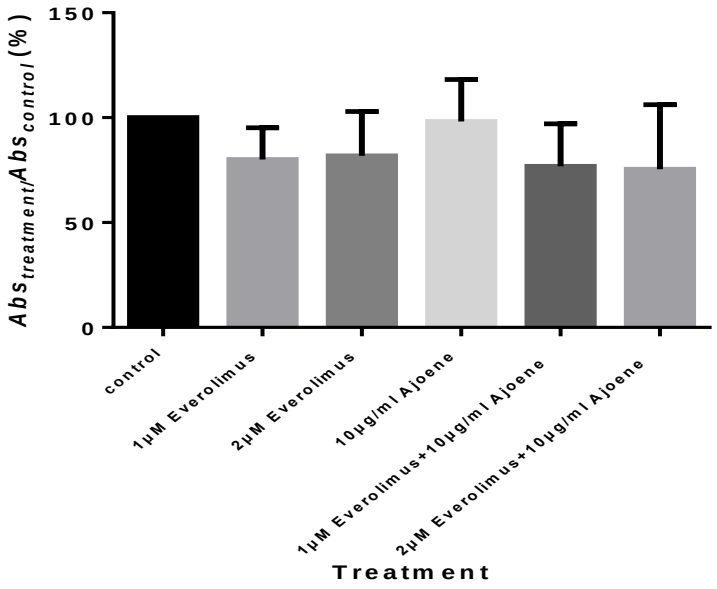

Figure 4.21. Growth activities of spheroids treated with everolimus and ajoene. Everolimus involved groups tended to have lower growth activities than control, but the differences among groups are not significant. (*t* test, $P>0.05$)

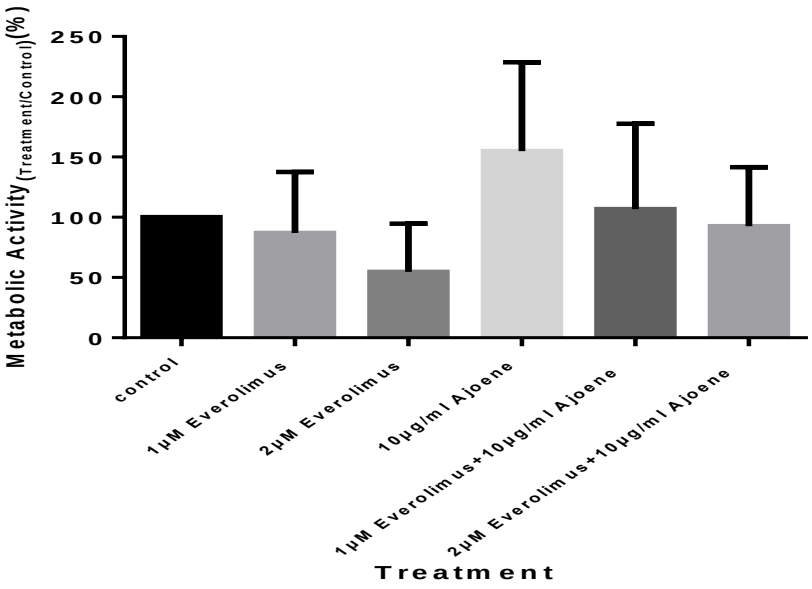

Figure 4.22. Results of metabolic activity experiments for everolimus and ajoene treated spheroids. Differences among groups are not significant. (*t* test, *P*>0.05)

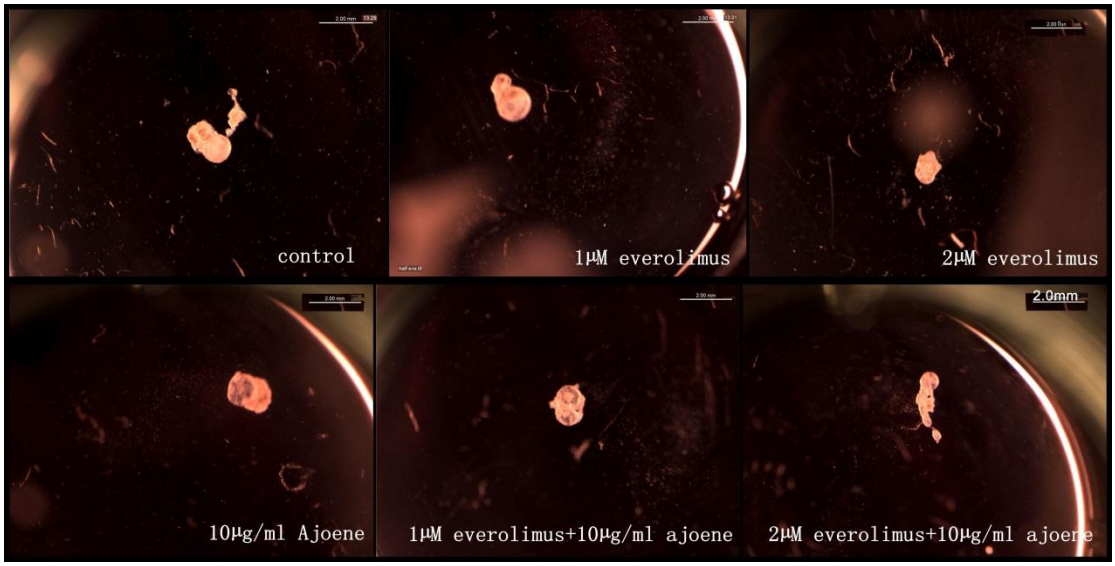

Figure 4.23. Images of spheroids treated with everolimus and ajoene. Spheroids had a reduction in size in the 2 μM everolimus and 2 μM everolimus +ajoene groups.

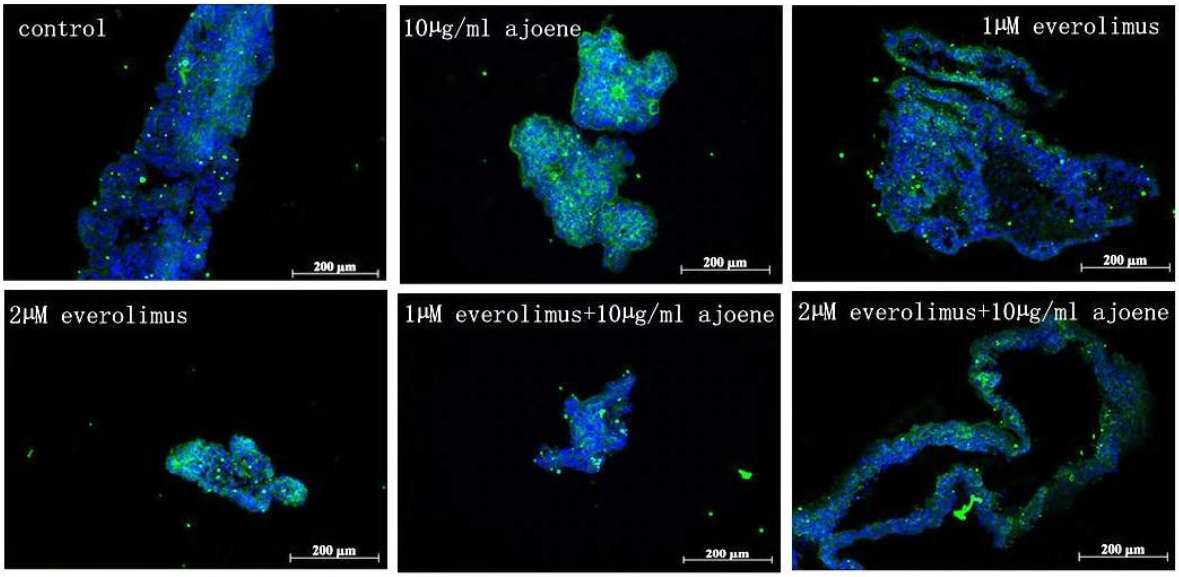

Figure 4.24. Immunofluorescent images of actin in spheroids treated with everolimus and ajoene. Actin was stained green and nuclei were stained blue.

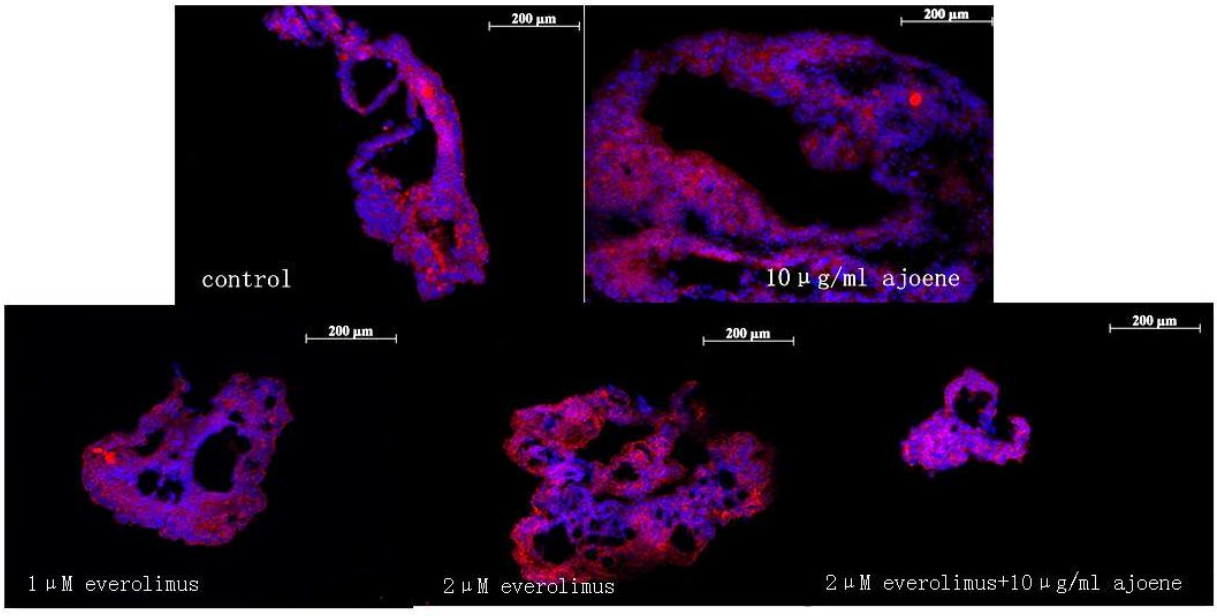

Figure 4.25. Immunofluorescent images of p-Akt in spheroids treated with everolimus and ajoene. P-Akt was stained red and nuclei were stained blue.

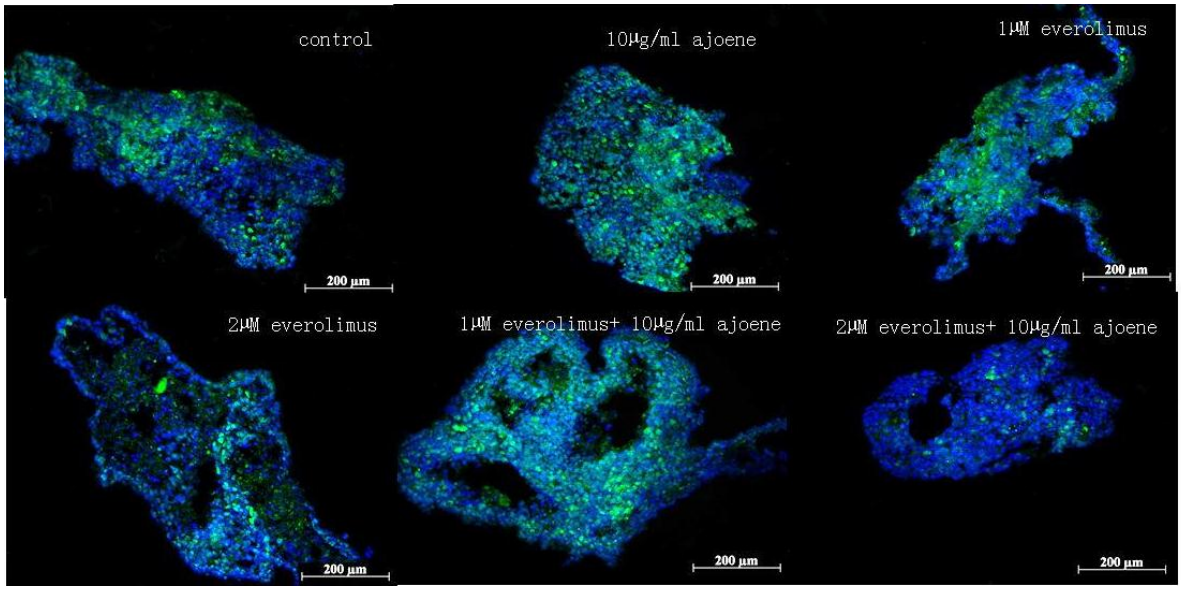

Figure 4.26. Immunofluorescent images of PCNA in spheroids treated with everolimus and ajoene. PCNA was stained green and nuclei were stained blue.

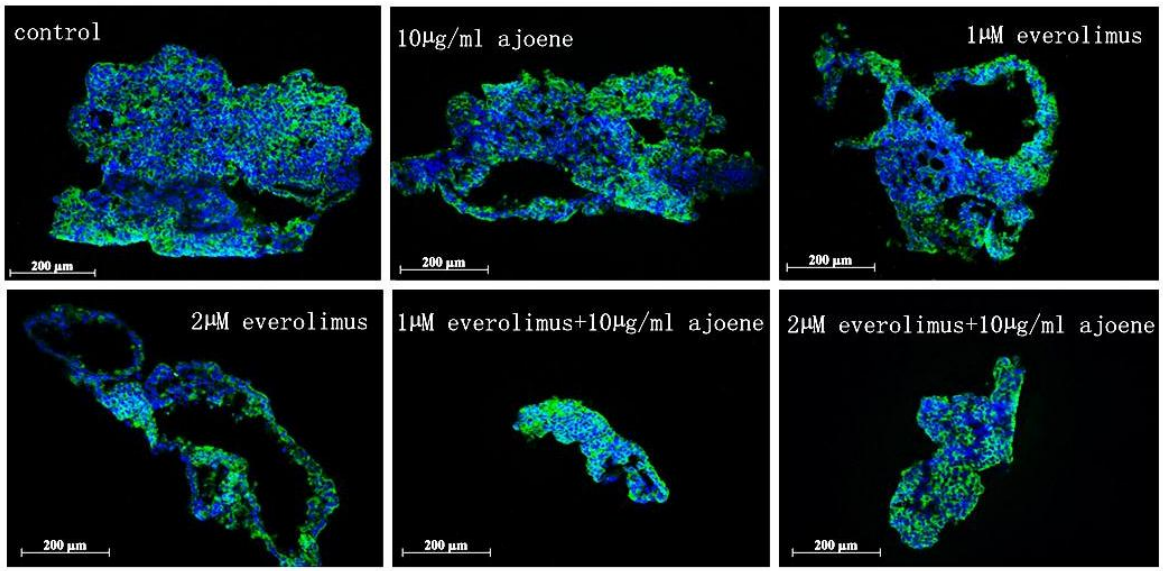

Figure 4.27. Immunofluorescent images of tubulin in spheroids treated with everolimus and ajoene. Tubulin was stained green and nuclei were stained blue.

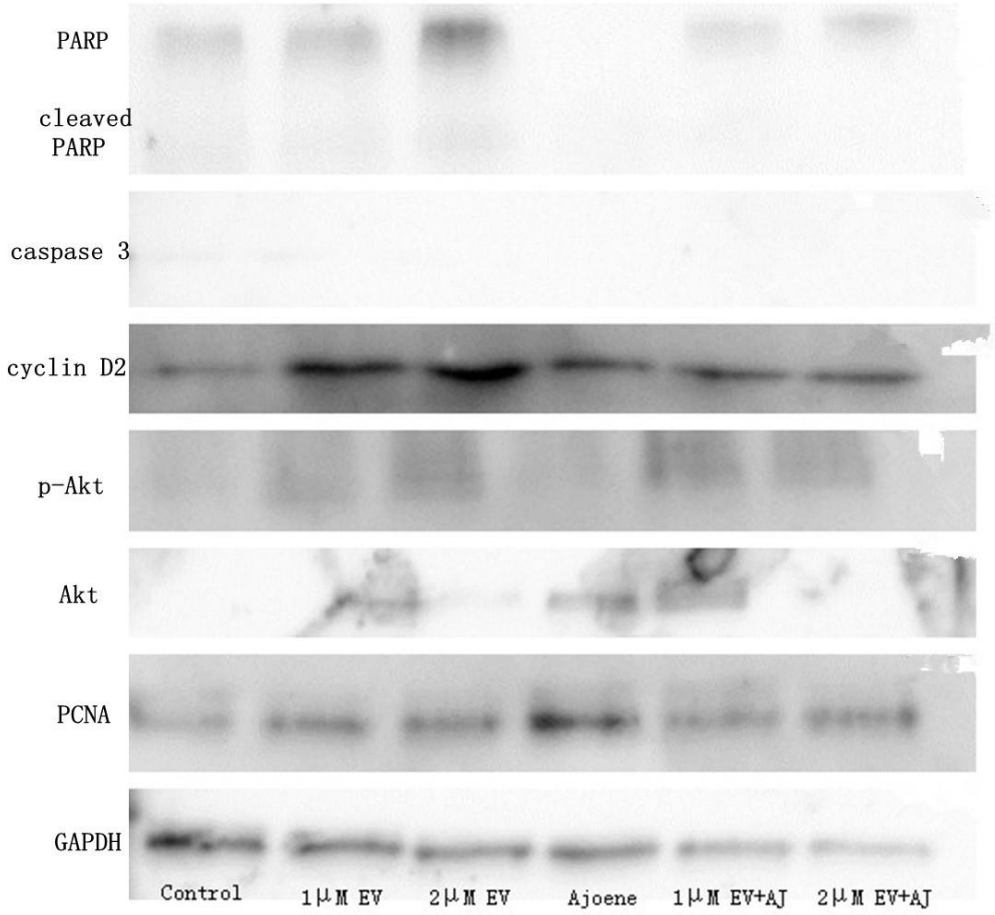

Figure 4.28. Results of Western blotting for GAPDH, PCNA, cyclin D2, caspase 3, Akt, p-Akt and PARP from spheroids treated with everolimus and ajoene. There was no band visible for caspase 3 and Akt. The housekeeping protein GAPDH bands appeared and suggesting the relative amount of protein in each group. “EV” stands for everolimus and “AJ” stands for ajoene.

.

Discussion

Growth activities of spheroids treated with paclitaxel and targeted drugs

Sorafenib has been suggested to be a multikinase inhibitor. It inhibits several kinases including Raf-1, tyrosine kinase receptors and vascular-endothelial growth factors (VEGF). It has shown inhibitory effects on endometrial cancer previously using a monolayer cell culture. Liobet's group treated Ishikawa cell monolayers and endometrial carcinoma tissue monolayers with sorafenib for 24 or 48 hours, and they found that sorafenib was able to induce cytotoxicity and mitochondrial apoptosis to the cancer cells in a dose and time dependent manner (Llobet et al., 2010). Gefitinib is a small molecule inhibitor of EGFR, and it binds to the ATP binding site of the EGFR kinase domain and inhibits the activation of the growth factor and results in the inhibition of cell proliferation (Fig. 4.1). It has shown therapeutic effects on various cancer cells, which have an active EGFR pathway (Albitar et al., 2007; Dedes et al., 2011). Albitar's group suggested that Ishikawa cells with *PTEN* mutations are more sensitive to gefitinib than the cells with a *p53* mutation (Albitar et al., 2007). Recently, Meng's group xenotransplanted human endometrial cancer cells on mice and cells were withdrawn from mice after growth. Gefitinib and paclitaxel was then tested on the tumor cells *in vitro* on monolayers. Gefitinib alone does not show significant effect on the cells but addition of gefitinib reduces the IC_{50} of paclitaxel from 14.7 nM to 1.3 nM (Meng et al., 2013).

In our study, a 3D spheroid culture of Ishikawa cells with *p53* and *PTEN* mutation was used in sorafenib and gefitinib treatments, and neither of these two drugs showed an inhibitory effect on growth of Ishikawa spheroids, nor any synergistic effect with paclitaxel. Previous studies suggested that the secretion of VEGF was highly suppressed in Ishikawa 3D spheroids and the influence of EGFR on cell growth was reduced in 3D cell cultures (Chitcholtan et al., 2013). Down regulated EGFR and reduced EGFR inhibitor efficacy is observed in 3D culture of colorectal cancer cells (Luca et al., 2013). The reduced VEGF and EGFR influence in 3D spheroids may be an explanation of the resistance to VEGF and EGFR inhibitors

sorafenib and gefitinib.

EGFR activity can be activated and enhanced by HER-2 overexpression and the inhibition of HER-2 together with EGFR can result in greater inhibition of tumor growth than inhibition of EGFR alone (Reid, Vidal, Shaw, & de Bono, 2007). Canertinib is an irreversible inhibitor and it has inhibitory activity over both EGFR and HER-2 (Rabindran, 2005). It is able to induce apoptosis on breast cancer cell lines which overexpresses HER-2 (Nelson & Fry, 2001).

In our results, canertinib was able to reduce the growth activity of 3D Ishikawa spheroids alone. There was no evidence on synergy between cancertinib and paclitaxel treatment. The inhibitory effect of canertinib on the 3D culture of spheroids may suggest that inhibition of both EGFR and HER-2 is more effective on 3D endometrial cancer culture than inhibition of EGFR alone.

Everolimus targets the mTOR, which is the downstream growth factor of Akt. Akt/mTOR is described as a pair of master switch proteins of cell metabolism and proliferation, and mTOR is also suggested to be apoptosis inhibitor (Castedo, Ferri, & Kroemer, 2002). Inhibition of mTOR by everolimus results in blockage of cell cycle of lymphocyte cell lines in G_1/S phase and apoptosis (Majewski et al., 2000). Everolimus has been tested on HEC-1A endometrial adenocarcinoma cell monolayers in 96 well plates and shown inhibitory effect on cell growth (Treeck, Wackwitz, Haus, & Ortmann, 2006). When everolimus is combined with cytotoxic drug cisplatin to treat A549 human non-small cell lung carcinoma cells in 96 well plates, the sensitivity of cancer cells to cisplatin is increased 10 fold by everolimus (Beuvink et al., 2005).

In this study, everolimus was able to reduce the size, growth activity and metabolic activity of 3D Ishikawa spheroids which had dysfunctioning PTEN. The result agreed with the previous findings that everolimus inhibited both PTEN mutant Ishikawa cell monolayers and xenograft tumors (Shoji et al., 2012), and oral intake of everolimus showed beneficial results in phase II clinical trials for treating endometrial carcinoma (Slomovitz et al., 2010). However, the synergistic effect between paclitaxel and everolimus was not significant which may due to the distinct pattern of signaling and cell-cell interactions in 3D culture from 2D culture used in the previous study

(Beuvink et al., 2005).

Effects of ajoene and paclitaxel on Ishikawa spheroids

Size (Fig.4.15), growth activity (Fig.4.13) and metabolic activity (Fig.4.14) of ajoene treated Ishikawa cell spheroids did not show any reduction when compared to control groups. PCNA but not p-Akt immunostaining was slightly elevated in ajoene and paclitaxel treated groups (Fig.4.18 and Fig.4.19). PCNA is an auxiliary protein of DNA polymerase C and is important in the initiation of cell proliferation. It is mostly used as a marker for evaluation of proliferative activity in cut sections of tumors (Alka & Kumar, 2012). Phosphorylated and activated Akt leads to inhibition of apoptosis and PI3K/Akt/mTOR pathway is up-regulated in *PTEN* mutated endometrial cancer cells (Church, Koppensteiner, Yap, Fink, & Dedes, 2012). The status of Akt may serve as a prognostic marker and the inhibition of PI3K/Akt signaling pathway (Kim et al., 2006). Therefore, these results suggested that ajoene did not inhibit growth of Ishikawa cells and possibly promoted the proliferation of Ishikawa spheroids. The Akt pathway might not be involved in the promotion of cell proliferation by ajoene.

In this study, immunostaining of cytoskeletal protein actin did not show any significant change in ajoene treated spheroids and α-tubulin expression was slightly elevated in ajoene treated spheroids. The cytoskeletal proteins are important for cellular morphology and structure maintenance. Microtubules which are formed by tubulin assembly are essential for intracellular transport, metabolism and cell division. Previous studies on pancreatic cancer cell 3D culture suggested that cytoskeleton protein actin formed less stress fibers in 3D nanoculture and tubulin expression was higher in 3D culture than in 2D culture (Matsuda et al., 2010). Ajoene is thought to be able to inhibit the assembly of microtubules (Li et al., 2002). When ajoene is used to treat 2D culture of leukemic cell line U937 cells in 96 well plates, expression of β-tubulin is increased by ajoene and the expression of α-tubulin is not altered (Li, Shi, Wang, Min, & Cui, 2004). However, in our study, the response of cytoskeletal proteins to ajoene treatment may indicate an inter-cell line difference and the effects

of ajoene on microtubules may not be significant in the 3D spheroid model.

Size (Fig.4.15), growth activity (Fig.4.13) and metabolic activity (Fig.4.14) of paclitaxel treated Ishikawa cell spheroids were significantly reduced. These results agreed with the previous reports of *in vitro* and clinical trials on treating endometrial cancers with paclitaxel (Ball, Blessing, Lentz, & Mutch, 1996; Vilos et al., 2013; C. Xu et al., 2011). Unfortunately, the proliferation markers could not be detected by Western blotting assay due to the significantly reduced cell number in spheroids. When the spheroids were treated with paclitaxel, cell number and spheroid size were very low and there was not enough proteins to be detected by western blotting assay since the volume of cell lysate added to SDS gel was limited. In future study, it will be necessary to increase the concentrations of proteins in cell lysates for loading.

Strong PCNA and p-Akt staining was observed in the cells of the spheroids treated with paclitaxel. These cells have shown strong proliferating ability thus suggested that these cancer cells would be able to divide and reproduce again once the paclitaxel treatment is stopped. This results agreed with the findings that the reoccurrence of endometrial cancer is frequent in the treatment-free interval of paclitaxel treatment (Markman et al., 1999).

Actin staining was not altered in paclitaxel treated groups but strong tubulin staining was observed in paclitaxel treated groups. Polymerized β-tubulin is believed to be the binding site of paclitaxel and paclitaxel kills tumors by inhibit the disassembly of microtubules. More effective paclitaxel treatment is suggested in tubulin overexpressed cancers (Roque et al., 2013). The high expression of tubulin in Ishikawa spheroids could have resulted in the response to paclitaxel treatment.

There was no synergistic effect found between ajoene and paclitaxel. However, the antitumor effects of paclitaxel were not interrupted by ajoene (Fig.4.13- Fig.4.15). Intake of ajoene may be beneficial in other aspects of health such as antimicrobial effects (see chapter 2), and it does not bring disadvantage when patients are treated with paclitaxel.

Effects of ajoene and everolimus on Ishikawa spheroids

Again, ajoene alone did not show inhibitory effect on spheroids but increased the PCNA expression. There was no apoptotic marker (PARP and caspase-3) detected by Western blotting assay in ajoene treated spheroids, suggesting that ajoene alone might not induce apoptosis to Ishikawa spheroids.

Levels of the cytoskeletal proteins actin and tubulin were not altered by everolimus (Fig.4.24 and Fig.4.27). PCNA and p-Akt were slightly elevated in everolimus treated groups in both immunofluorescent and Western blotting results (Fig. 4.25, Fig.4.26 and Fig.4.28). The remaining cells in the spheroids treated with everolimus still appeared to be proliferating. mTOR is the downstream of Akt, and everolimus which inhibits mTOR1 is suggested to be able to activate mTOR2 and increase the phosphorylation of Akt in 2D culture of small intestinal neuroendocrine tumor cells. Therefore, everolimus treatment can be affected by the activation of Akt (Svejda et al., 2011). The elevation of p-Akt by everolimus in our study may provide a clue for the moderate effect of everolimus on Ishikawa spheroids. But in order to confirm this, Akt level should be determined together with p-Akt level in any further study.

Cyclin D2 was increased by everolimus as shown on the Western blotting (Fig.3.28). D-type cyclins are a group of highly conserved cell cycle regulators and cyclin D2 is an important regulator of cell cycle progression from the G1 phase to S phase (Witt et al., 2013). The reason why the cell cycle progression was unregulated is unclear, but it may also suggest that the remaining survival cells in the spheroids are proliferating and quickly progressing through their cell cycles.

The apoptotic markers PARP and cleaved PARP were present on the Western blotting of everolimus treated spheroids but there was no caspase 3 shown (Fig.4.28). PARP catalyzes the poly(ADP-ribosyl)ation of nuclear proteins and its substrate was suggested to be NAD. PARP contributes to cell death by depleting NAD and ATP. Cleavage of PARP occurs when cell apoptosis is induced by drug treatment and this cleavage is believed to be mostly done by caspase 3, which is a central apoptotic mediator (Boulares et al., 1999). Therefore, cleavage of PARP should accompanied by

the activation of caspase 3. We did not detect any cleaved caspase 3 and this may be due to the low amount of proteins present in cell lysates.

Again there was no synergistic effect found between ajoene and everolimus since ajoene did not significantly further inhibit the everolimus treated spheroids. Intake of ajoene may be beneficial in other aspects of health as ajoene did not interrupt the treatment when spheroids were treated with everolimus.

Conclusion

The targeted drugs sorafenib and gefitinib did not show inhibitory effect or synergistic effect with paclitaxel on 3D spheroids of Ishikawa cells. Canertinib was able to inhibit growth activity of Ishikawa spheroids but it was not synergistic with paclitaxel. Everolimus was able to inhibit the growth and metabolic activity of the spheroids and induce apoptosis but its synergistic effect with paclitaxel was not significant.

Ajoene alone did not inhibit growth of 3D spheroids, and it did not induce cell death. Paclitaxel showed strong anticancer activity over 3D Ishikawa cell spheroids but the survival cells showed strong proliferation ability. There was no synergistic effect detected between ajoene and paclitaxel or between ajoene and everolimus. Intake of ajoene is still beneficial as it did not interrupt paclitaxel or everolimus treatment.

Appendix

Appendix 4.1. Components of 10xPBS

Components	Amount
Na_2HPO_4	7.1g
NaH_2PO_4	For pH adjustment
NaCl	45g
KCl	1g
Water	500ml

Appendix 4.2. Components of solutions used in western blot experiments.

Components of RIPA lysis buffer

components	concentration
Tris-HCl pH7.4	50mM
NaCl	100mM
EDTA	5mM
NP-40	1%
SDS	0.10%
Sodium deoxycholate	0.50%
Na_3VO_4	1mM
Glycerol	10%
Protease inhibitor tablet	1 tablet in 50ml

Loading sample buffer

Content	**1M Tris-HCl pH6.8**	**50%glycerol**	**10% SDS**	**1% bromophenol blue**	**Water**
Volume	0.6ml	5ml	2ml	1ml	1.4ml

10% or 12% SDS gel solution

Content	**40% Acylamide 0.8% bis-acylamide**	**solution B (75% 2M Tris-HCl pH 8.8 + 4%SDS)**	**10% ammonium persulfate**	**TEMED**	**Milli Q water**
Volume(10%)	4.995ml	3.75ml	75ul	7.5ul	6.255ml
Volume(12%)	4ml	2.5ml	50ul	5ul	3.5ml

7% stacking gel solution

Content	**40% Acylamide 0.8% bis-acylamide**	**solution C (50% 1M Tris-HCl pH 6.8 + 4%SDS)**	**10% ammonium persulfate**	**TEMED**	**Milli Q water**
Volume	1ml	1ml	40ul	5ul	2ml

Running buffer

Content	**Tris**	**Glycine**	**SDS**	**Milli Q water**
Mass or Volume	3g	14.4g	1g	1L

TBS-T

Content	**Tris-HCl pH7.5**	**NaCl**	**0.7% tween 20**
Concentration or Volume	20mM	140mM	0.1%v/v

Transferring buffer

Content	**Tris**	**Glycine**	**Milli Q water**
Mass or Volume	1.93g	9g	1L

Blocking solution

Blocking solution varied in different protein detection. There were 3 types of blocking solution used in this study. They were: 5% skim milk in TBS-T, 4% BSA (Bovine serum albumin, Sigma-Aldrich LTD, New Zealand) in TBS-T or ThermoFisher blocking solution (ThermoFisher scientific LTD, New Zealand).

Appendix 4.3. Protein antibodies used in western blot and immunofluorescence experiments.

Protein antibody	Origin
GAPDH	Santa Cruz Biotechnology, CA, USA
PCNA	Santa Cruz Biotechnology, CA, USA
AKT	Santa Cruz Biotechnology, CA, USA
p-AKT	Santa Cruz Biotechnology, CA, USA
Cyclin D2	Santa Cruz Biotechnology, CA, USA
Caspase 3	Santa Cruz Biotechnology, CA, USA
PARP	Santa Cruz Biotechnology, CA, USA
Alpha-tubulin	Sigma LTD, New zealand
Actin	Santa Cruz Biotechnology, CA, USA
anti-Mouse IgG-HRP	Sigma -Aldrich LTD, New Zealand
anti-Rabbit IgG-HRP	Sigma -Aldrich LTD, New Zealand
Anti-mouse FITC	Sigma -Aldrich LTD, New zealand
Anti-rabbit 594	Sigma -Aldrich LTD, New zealand

Final conclusions

We successfully extracted ajoene from 3 of the 4 independent garlic extractions. The position of ajoene on the thin layer chromatography was confirmed in the first and third extraction and this provided a clue for ajoene detection in the further extractions. In the second extraction, ajoene was not able to be eluted off from the flash chromatography column. The size of column and pressure used in the flash chromatography were concluded to be crucial for successful separation and elution.

Antifungal activity of ajoene was shown against the yeast and germ tube form of *Candida albicans*. Radial extension and individual hyphal extension of a filamentous fungus *Neurospora crassa* and an oomycete *Achlya bisexualis* were also inhibited by ajoene. The possible targets of ajoene are suggested to be either the cell membrane or the microtubules (Li et al., 2002; Naganawa et al., 1996; San-Blas et al., 1997), and cysteine residues are thought to be oxidized during the reaction and played a crucial part in ajoene's bioactivity (Jacob et al., 2012; Kaschula et al., 2012; Naganawa et al., 1996).

The extent of which *Neurospora crassa* responded to ajoene was higher than that for *Achlya bisexualis*. The reason is possibly due to the distant phylogenetic relationship between *Neurospora crassa* and *Achlya bisexualis* (Richards et al., 2006), since cell membrane composition and microtubule sequence may vary between these species (Mu et al., 1999; Tylicki et al., 2012).

Ajoene did not show any antitumor effect on 3D Ishikawa spheroids. No additional or synergistic effect was detected when ajoene was combined with paclitaxel or everolimus to treat 3D Ishikawa spheroids. The signaling, growth pattern and cell differentiation are significantly different when cancer cells are growing in a 3D culture (Chitcholtan et al., 2013). Drug resistance has been suggested to occur in 3D cancer cultures (Longati et al., 2013). Although ajoene has been suggested to be able to inhibit growth of various cancer cell lines *in vitro* and *in vivo* (Dirsch et al., 1998; Taylor et al., 2006; B. Xu et al., 2004), the 3D Ishikawa spheroids were found

to be resistant to ajoene treatment.

Similar patterns were noticed with the targeted drugs sorafenib and gefitinib (drugs which target VEGF and EGFR) treatments, which did not show any inhibitory effect on 3D Ishikawa spheroids. The reduced influence of VEGF and EGFR in 3D cancer cell cultures possibly resulted in the observed drug resistance (Chitcholtan et al., 2013). Additional inhibition of HER-2 together with EGFR showed inhibitory effects on 3D Ishikawa spheroids when the spheroids were treated with canertinib. The mTOR inhibitor everolimus was able to inhibit the growth of *PTEN* mutated Ishikawa spheroids, suggesting that the *PTEN* mutated, mTOR enhanced cell line was susceptible to mTOR inhibitor treatment. However, the synergistic effect between everolimus and cytotoxic drug was not significant, due to the different cell line and cell model used from the previous studies.

In conclusion, the garlic extract ajoene was successfully extracted from fresh New Zealand garlic and it was able to inhibit the growth of *C.albicans*, *N. crassa* and *A. bisexualis*. On 3D Ishikawa spheroids, ajoene showed neither an inhibitory effect nor any synergistic effect with other drugs. The targeted drugs exhibited varied effects on ajoene, and the effects of the targeted drugs were influenced by the 3D cell model.

References

Aala, F., Yusuf, U. K., Jamal, F., & Khodavandi, A. (2010). In vitro antifungal activity of allicin alone and in combination with two medications against Trichophyton rubrum. *World Journal of Microbiology and Biotechnology, 26*(12), 2193-2198.

Alberts, B., Johnson, A., Lewis, J., Raff, M., Roberts, K., & Walter, P. (2002). *Molecular biology of the cell*. New York, NY: Garland Science.

Albitar, L., Carter, M. B., Davies, S., & Leslie, K. K. (2007). Consequences of the loss of p53, RB1, and PTEN: Relationship to gefitinib resistance in endometrial cancer. *Gynecologic Oncology, 106*(1), 94-104. doi: http://dx.doi.org/10.1016/j.ygyno.2007.03.006

Alka, R., & Kumar, R. (2012). PCNA labelling as a proliferative marker in gynaecological tumours. *Journal of Clinical and Diagnostic Research, 5*(6), 1203-1208.

Amant, F., Moerman, P., Neven, P., & Timmerman, D. (2005). Endometrial cancer. *The Lancet, 366*(9484), 491-505.

Ankri, S., & Mirelman, D. (1999). Antimicrobial properties of allicin from garlic. *Microbes and Infection, 1*(2), 125-129.

Araujo, R., Pina-Vaz, C., & Rodrigues, A. G. (2010). Mould infections: A global threat to immunocompromised patients. In I. Ahmad (Ed.), *Combating fungal infections, first problems and remedy* (pp. 1-19). Heidelberg: Springer.

Ball, H. G., Blessing, J. A., Lentz, S. S., & Mutch, D. G. (1996). A Phase II trial of paclitaxel in patients with advanced or recurrent adenocarcinoma of the

endometrium: A gynecologic oncology group study. *Gynecologic Oncology, 62*(2), 278-281. doi: http://dx.doi.org/10.1006/gyno.1996.0227

Barton, R., & Gull, K. (1988). Variation in cytoplasmic microtubule organization and spindle length between the two forms of the dimorphic fungus Candida albicans. *Journal of Cell Science, 91*(Pt 2), 211-220.

Bates, R. C., Edwards, N. S., & Yates, J. D. (2000). Spheroids and cell survival. *Critical Reviews in Oncology/Hematology, 36*(2–3), 61-74. doi: http://dx.doi.org/10.1016/S1040-8428(00)00077-9

Berman, J., & Sudbery, P. E. (2002). Candida albicans: A molecular revolution built on lessons from budding yeast. *Nature Reviews Genetics, 3*(12), 918-930.

Beuvink, I., Boulay, A., Fumagalli, S., Zilbermann, F., Ruetz, S., O'Reilly, T., . . . Thomas, G. (2005). The mTOR inhibitor RAD001 sensitizes tumor cells to DNA-damaged induced apoptosis through inhibition of p21 translation. *Cell, 120*(6), 747-759.

Bhandari, P. R. (2012). Garlic (Allium sativum L.): A review of potential therapeutic applications. *International Journal of Green Pharmacy, 6*(2), 118-129. doi: 10.4103/0973-8258.102826

Block, E., Ahmad, S., Catalfamo, J. L., Jain, M. K., & Apitz-Castrozd, R. (1986). Antithrombotic organosulfur compounds from garlic: Structural, mechanistic, and synthetic studies. *Journal of the American Chemical Society, 108*(22), 7045-7055.

Block, E., Ahmad, S., Jain, M. K., Crecely, R. W., Apitz-Castro, R., & Cruz, M. R. (1984). (E,Z)-ajoene: A potent antithrombotic agent from garlic. *Journal of the American Chemical Society, 106*(26), 8295-8296.

Bolsover, S. R., Shephard, E. A., White, H. A., & Hyams, J. S. (2011). *Cell Biology : A Short Course* Retrieved from http://canterbury.eblib.com.au/patron/FullRecord.aspx?p=675008

Boulares, A. H., Yakovlev, A. G., Ivanova, V., Stoica, B. A., Wang, G., Iyer, S., & Smulson, M. (1999). Role of poly(ADP-ribose) polymerase (PARP) cleavage in apoptosis: Caspase 3-resistant parp mutant increases rates of apoptosis in transfected cells. *Journal of Biological Chemistry, 274*(33), 22932-22940. doi: 10.1074/jbc.274.33.22932

Calderone, R., & Clancy, C. J. (2012). *Candida and Candidiasis.* Retrieved from http://canterbury.eblib.com.au/patron/FullRecord.aspx?p=1039537

Carlile, M. G. (1995). The success of the hypha and mycelium. In N. A. R. Gow & G. M. Gadd (Eds.), *The growing fungus* (pp. 7). London: Chapman and Hall.

Carrero, S., Romero, H., & Apitz-Castro, R. (2009). In vitro inhibitory effect of ajoene on Candida isolates recovered from vaginal discharges. *Revista Iberoamericana de Micología, 26*(3), 189-193.

Castedo, M., Ferri, K. F., & Kroemer, G. (2002). Mammalian target of rapamycin (mTOR): Pro- and anti-apoptotic. *Cell Death and Differentiation, 9*(2), 99-100.

Cavallito, C. J., & Bailey, J. H. (1944). Allicin, the antibacterial principle of Allium sativum. I. Isolation, physical properties and antibacterial action. *Journal of the American Chemical Society, 66*(11), 1950-1951.

Cella, D., Peterman, A., Hudgens, S., Webster, K., & Socinski, M. A. (2003). Measuring the side effects of taxane therapy in oncology. *Cancer, 98*(4), 822-831. doi: 10.1002/cncr.11578

Chitcholtan, K., Asselin, E., Parent, S., Sykes, P. H., & Evans, J. J. (2013). Differences in growth properties of endometrial cancer in three dimensional (3D) culture and 2D cell monolayer. *Experimental Cell Research, 319*(1), 75-87.

Chitcholtan, K., Sykes, P. H., & Evans, J. J. (2012). The resistance of intracellular mediators to doxorubicin and cisplatin are distinct in 3D and 2D endometrial cancer. *Journal of Translational Medicine, 10*(1), 1-16.

Church, D. N., Koppensteiner, R., Yap, T. A., Fink, D., & Dedes, K. J. (2012). PI3K-AKT-mTOR inhibitors for the systemic treatment of endometrial cancer. *Expert Review of Obstetrics and Gynecology, 7*(5), 421-430.

Cortes, J., & Roché, H. (2012). Docetaxel combined with targeted therapies in metastatic breast cancer. *Cancer Treatment Reviews, 38*(5), 387-396. doi: http://dx.doi.org/10.1016/j.ctrv.2011.08.001

Cragg, G. M., & Newman, D. J. (2004). A tale of two tumor targets: topoisomerase I and tubulin. The wall and wani contribution to cancer chemotherapy. *Journal of Natural Products, 67*(2), 232-244.

Das, M. P., Jeyanthi, R. L., & Sharmila, S. (2013). Evaluation of antibacterial and antifungal efficacy of Wedelia chinensis leaf extracts. *Journal of Chemical and Pharmaceutical Research, 5*(2), 265-269.

Deacon, J. W. (2009). *Fungal biology.* Retrieved from http://canterbury.eblib.com.au/patron/FullRecord.aspx?p=428109

Dedes, K. J., Wetterskog, D., Ashworth, A., Kaye, S. B., & Reis-filho, J. S. (2011). Emerging therapeutic targets in endometrial cancer. *Nature Reviews. Clinical Oncology, 8*(5), 261-271.

Deepa, J., Parashurama, T. R., Krishnappa, M., & Nataraja, S. (2013). Antimicrobial efficacy of Blechnum orientale L. *International Journal of Pharma and Bio Sciences*, *4*(2), P475-P479.

Dirsch, V. M., Gerbes, A. L., & Vollmar, A. M. (1998). Ajoene, a compound of garlic, induces apoptosis in human promyeloleukemic cells, accompanied by generation of reactive oxygen species and activation of nuclear factor kB. *The American Society for Pharmacology and Experimental Therapeutics, 53*, 402-407.

Dizon, D. S. (2010). Treatment options for advanced endometrial carcinoma. *Gynecologic Oncology, 117*(2), 373-381. doi: http://dx.doi.org/10.1016/j.ygyno.2010.02.007

Emerson, S. (1964). Slime a plasmodioid variant of Neurospora crassa. *Genetica, 34*(1), 162-182.

Erkoc, S., Sumerb, S., & Erkoc, F. (2003). Structural and electronic properties of ajoene molecule. *Journal of Molecular Structure (Theochem), 631*, 271-276.

Evan, G. I., & Vousden, K. H. (2001). Proliferation, cell cycle and apoptosis in cancer. *Nature, 411*(6835), 342-348.

Förster, H., Coffey, M. D., Elwood, H., & Sogin, M. L. (1990). Sequence analysis of the small subunit ribosomal RNAs of three zoosporic fungi and implications for fungal evolution. *Mycologia, 82*(3), 306-312. doi: 10.2307/3759901

Fader, A. N., Santin, A. D., & Gehrig, P. A. (2013). Early stage uterine serous carcinoma: Management updates and genomic advances. *Gynecologic Oncology, 129*(1), 244-250.

Fischer, R., Zekert, N., & Takeshita, N. (2008). Polarized growth in fungi: Interplay between the cytoskeleton, positional markers and membrane domains. *Molecular Microbiology, 68*(4), 813-826. doi: 10.1111/j.1365-2958.2008.06193.x

Freeman, F., & Kodera, Y. (1995). Garlic chemistry: Stability of S-(2-propenyl) 2-propene-1-sulfinothioate (allicin) in blood, solvents, and simulated physiological fluids. *Journal of Agricultural and Food Chemistry, 43*(9), 2332-2338.

Fuangsawat, W., Abking, N., & Lawhavinit, O. A. (2011). Sensitivity comparison of pathogenic aquatic fungal hyphae to sodium chloride, hydrogen peroxide, acetic acid and povidone iodine. *Kasetsart Journal - Natural Science, 45*(1), 84-89.

Gladfelter, A., & Berman, J. (2009). Dancing genomes: Fungal nuclear positioning. *Nature Reviews: Microbiology, 7*(12), 875-886.

González-Vallinas, M., Molina, S., Vicente, G., de la Cueva, A., Vargas, T., Santoyo, S., . . . Ramírez de Molina, A. (2013). Antitumor effect of 5-fluorouracil is enhanced by rosemary extract in both drug sensitive and resistant colon cancer cells. *Pharmacological Research, 72*(0), 61-68. doi: http://dx.doi.org/10.1016/j.phrs.2013.03.010

Gow, N. A. R., Brown, A. J. P., & Odds, F. C. (2002). Fungal morphogenesis and host invasion. *Current Opinion in Microbiology, 5*(4), 366-371.

Gruhlke, M. C. H., Portz, D., Stitz, M., Anwar, A., Schneider, T., Jacob, C., . . . Slusarenko, A. J. (2010). Allicin disrupts the cell's electrochemical potential and induces apoptosis in yeast. *Free Radical Biology and Medicine, 49*(12), 1916-1924.

Guo, N., Wu, X., Yu, L., Liu, J., Meng, R., Jin, J., . . . Deng, X. (2010). In vitro and in vivo interactions between fluconazole and allicin against clinical isolates of fluconazole-resistant Candida albicans determined by alternative methods. *FEMS Immunology and Medical Microbiology, 58*(2), 193-201.

Heath, I. B., & Steinberg, G. (1999). Mechanisms of hyphal tip growth: Tube swelling amebae revisited. *Fungal Genetics and Biology, 28*(2), 79-93. doi: http://dx.doi.org/10.1006/fgbi.1999.1168

Iciek, M., Kwiecień, I., & Włodek, L. (2009). Biological properties of garlic and garlic-derived organosulfur compounds. *Environmental and Molecular Mutagenesis, 50*(3), 247-265.

Ilić, D. P., Nikolić, V. D., Nikolic, L. B., Stanković, M. Z., Stanojević, L. P., & Cakić, M. D. (2011). Allicin and related compounds: Biosynthesis, synthesis and pharmacological activity. *Facta universitatis series: Physics, Chemistry and Technology, 9*(1), 9-20. doi: 10.2298/FUPCT1101009I

Invitrogen. (n.d.). Alamar blue assay: U.S. Patent No. 5,501,959. from http://tools.invitrogen.com/content/sfs/manuals/PI-DAL1025-1100_TI%20alamarBlue%20Rev%201.1.pdf

Jacob, C., Battaglia, E., Burkholz, T., Peng, D., Bagrel, D., & Montenarh, M. (2012). Control of oxidative posttranslational cysteine modifications: From intricate chemistry to widespread biological and medical applications. *Chemical Research in Toxicology, 25*(3), 588-604.

Kaschula, C. H., Hunter, R., Stellenboom, N., Caira, M. R., Winks, S., Ogunleye, T., . . . Parker, M. I. (2012). Structure–activity studies on the anti-proliferation activity of ajoene analogues in WHCO1 oesophageal cancer cells. *European Journal of Medicinal Chemistry, 50*(0), 236-254. doi:

http://dx.doi.org/10.1016/j.ejmech.2012.01.058

Kay, H. Y., Yang, J. W., Kim, T. H., Lee, D. Y., Kang, B., Ryu, J. H., . . . Kim, S. G. (2010). Ajoene, a stable garlic by-product, has an antioxidant effect through Nrf2-mediated glutamate-cysteine ligase induction in HepG2 cells and primary hepatocytes. *Journal of Nutrition, 140*(7), 1211-1219.

Khodavandi, A., Alizadeh, F., Harmal, N. S., Sidik, S. M., Othman, F., Sekawi, Z., & Chong, P. P. (2011). Expression analysis of SIR2 and SAPs1-4 gene expression in Candida albicans treated with allicin compared to fluconazole. *Tropical Biomedicine, 28*(3), 589-598.

Kim, T. J., Lee, J. W., Song, S. Y., Choi, J. J., Choi, C. H., Kim, B. G., . . . Bae, D. S. (2006). Increased expression of pAKT is associated with radiation resistance in cervical cancer. *British Journal of Cancer, 94*(11), 1678-1682.

Kretschmar, M., Hube, B., Bertsch, T., Sanglard, D., Merker, R., Schröder, M., . . . Nichterlein, T. (1999). Germ tubes and proteinase activity contribute to virulence of Candida albicans in murine peritonitis. *Infection and Immunity, 67*(12), 6637-6642.

Ledezma, E., De Sousa, L., Jorquera, A., Sanchez, J., Lander, A., Rodriguez, E., . . . Apitz-Castro, R. (1996). Efficacy of ajoene, an organosulphur derived from garlic, in the short-term therapy of tinea pedis. *Mycoses, 39*(9-10), 393-395.

Ledezma, E., Marcano, K., Jorquera, A., De Sousa, L., Padilla, M., Pulgar, M., & Apitz-Castro, R. (2000). Efficacy of ajoene in the treatment of tinea pedis: A double-blind and comparative study with terbinafine. *Journal of the American Academy of Dermatology, 43*(5), 829-832.

Leslie, K. K., Thiel, K. W., & Yang, S. (2012). Endometrial cancer: Potential

treatment and prevention with progestin-containing intrauterine devices. *Obstetrics and Gynecology, 119*(2 PART 2), 419-420.

Lew, R. R. (2011). How does a hypha grow? The biophysics of pressurized growth in fungi. *Nature Reviews. Microbiology, 9*(7), 509-518.

Li, M., Ciu, J.-R., Ye, Y., Min, J.-M., Zhang, L.-H., Wang, K., . . . Leung-Tack, J. (2002). Antitumor activity of Z-ajoene, a natural compound purified from garlic: Antimitotic and microtubule-interaction properties. *Carcinogenesis, 23*(4), 573-579.

Li, M., Shi, X. H., Wang, L., Min, J. M., & Cui, J. R. (2004). Mechanism of growth inhibition of Z-ajoene on U937 cells. *Chinese Pharmacological Bulletin, 20*(6), 688-693.

Llobet, D., Eritja, N., Yeramian, A., Pallares, J., Sorolla, A., Domingo, M., . . . Dolcet, X. (2010). The multikinase inhibitor Sorafenib induces apoptosis and sensitises endometrial cancer cells to TRAIL by different mechanisms. *European Journal of Cancer, 46*(4), 836-850. doi: http://dx.doi.org/10.1016/j.ejca.2009.12.025

Lo, H. J., Köhler, J. R., Didomenico, B., Loebenberg, D., Cacciapuoti, A., & Fink, G. R. (1997). Nonfilamentous C. albicans mutants are avirulent. *Cell, 90*(5), 939-949.

Longati, P., Jia, X., Eimer, J., Wagman, A., Witt, M. R., Rehnmark, S., . . . Heuchel, R. L. (2013). 3D pancreatic carcinoma spheroids induce a matrix-rich, chemoresistant phenotype offering a better model for drug testing. *BMC Cancer, 13*.

Luca, A. C., Mersch, S., Deenen, R., Schmidt, S., Messner, I., Schäfer, K. L., . . .

Stoecklein, N. H. (2013). Impact of the 3D Microenvironment on Phenotype, Gene Expression, and EGFR Inhibition of Colorectal Cancer Cell Lines. *PLoS ONE, 8*(3).

Majewski, M., Korecka, M., Kossev, P., Li, S., Goldman, J., Moore, J., . . . Wasik, M. A. (2000). The immunosuppressive macrolide RAD inhibits growth of human Epstein-Barr virus-transformed B lymphocytes in vitro and in vivo: A potential approach to prevention and treatment of posttransplant lymphoproliferative disorders. *Proceedings of the National Academy of Sciences of the United States of America, 97*(8), 4285-4290.

Maluf, M. L. F., Takahachi, G., Svidzinski, T. I. E., Xander, P., Apitz-Castro, R., Bersani-Amado, C. A., & Cuman, R. K. N. (2008). Antifungal activity of ajoene on experimental murine paracoccidioidomycosis. *Revista Iberoamericana de Micologia, 25*(3), 163-166.

Markman, M. (2007). Chemotherapy in the management of endometrial cancer. *CME Journal of Gynecologic Oncology, 12*(1), 29-32.

Markman, M., Kennedy, A., Webster, K., Kulp, B., Peterson, G., & Belinson, J. (1999). Persistent chemosensitivity to platinum and/or paclitaxel in metastatic endometrial cancer. *Gynecologic Oncology, 73*(3), 422-423. doi: http://dx.doi.org/10.1006/gyno.1999.5407

Matsuda, Y., Ishiwata, T., Kawamoto, Y., Kawahara, K., Peng, W.-X., Yamamoto, T., & Naito, Z. (2010). Morphological and cytoskeletal changes of pancreatic cancer cells in three-dimensional spheroidal culture. *Medical Molecular Morphology, 43*(4), 211-217. doi: 10.1007/s00795-010-0497-0

Meng, X., Laidler, L. L., Kosmacek, E. A., Yang, S., Xiong, Z., Zhu, D., . . . Leslie, K. K. (2013). Induction of mitotic cell death by overriding G2/M checkpoint in

endometrial cancer cells with non-functional p53. *Gynecologic Oncology, 128*(3), 461-469. doi: http://dx.doi.org/10.1016/j.ygyno.2012.11.004

Mileshkin, L., & Jamil, S. (2012). The adjuvant management of endometrial cancer: A review of the role of systemic therapy. *European Journal of Clinical and Medical Oncology, 4*(4), 1-11.

Milner, J. A., & Romagnolo, D. F. (2010). *Bioactive compounds and cancer* Retrieved from http://canterbury.eblib.com.au/patron/FullRecord.aspx?p=603666

Money, N. P., & Harold, F. M. (1993). Two water molds can grow without measurable turgor pressure. *Planta, 190*(3), 426-430.

Mori, R., Wang, Q., Danenberg, K. D., Pinski, J. K., & Danenberg, P. V. (2008). Both β-actin and GAPDH are useful reference genes for normalization of quantitative RT-PCR in human FFPE tissue samples of prostate cancer. *Prostate, 68*(14), 1555-1560.

Mu, J. H., Bollon, A. P., & Sidhu, R. S. (1999). Analysis of β-tubulin cDNAs from taxol-resistant Pestalotiopsis microspora and taxol-sensitive Pythium ultimum and comparison of the taxol-binding properties of their products. *Molecular and General Genetics, 262*(4-5), 857-868.

Munin, E., Giroldo, L. M., Alves, L. P., & Costa, M. S. (2007). Study of germ tube formation by Candida albicans after photodynamic antimicrobial chemotherapy (PACT). *Journal of Photochemistry and Photobiology B: Biology, 88*(1), 16-20. doi: http://dx.doi.org/10.1016/j.jphotobiol.2007.04.011

Naganawa, R., Iwata, N., Ishikawa, K., Fukuda, H., Fujino, T., & Suzuki, A. (1996). Inhibition of microbial growth by ajoene, a sulfur-containing compound

derived from garlic. *Applied and Environmental Microbiology, 62*(11), 4238-4242.

Nelson, J. M., & Fry, D. W. (2001). Akt, MAPK (Erk1/2), and p38 act in concert to promote apoptosis in response to ErbB receptor family inhibition. *Journal of Biological Chemistry, 276*(18), 14842-14847.

Pérez-Blanco, M., Valles, R. H., Zeppenfeldt, G. F., & Apitz-Castro, R. (2003). Ajoene and 5-fluorouracil in the topical treatment of Cladophialophora carrionii chromoblastomycosis in humans: A comparative open study. *Medical Mycology, 41*(6), 517-520.

Purdie, D. M., & Green, A. C. (2001). Epidemiology of endometrial cancer. *Best Practice & Research Clinical Obstetrics & Gynaecology, 15*(3), 341-354. doi: http://dx.doi.org/10.1053/beog.2000.0180

Rabindran, S. K. (2005). Antitumor activity of HER-2 inhibitors. *Cancer Letters, 227*(1), 9-23. doi: http://dx.doi.org/10.1016/j.canlet.2004.11.015

Reid, A., Vidal, L., Shaw, H., & de Bono, J. (2007). Dual inhibition of ErbB1 (EGFR/HER1) and ErbB2 (HER2/neu). *European Journal of Cancer, 43*(3), 481-489. doi: http://dx.doi.org/10.1016/j.ejca.2006.11.007

Reimann, M., & Schmitt, C. (2007). Apoptosis and cancer therapy. In R. Srivastava (Ed.), *Apoptosis, Cell Signaling, and Human Diseases* (pp. 303-320): Humana Press.

Richards, T. A., Dacks, J. B., Jenkinson, J. M., Thornton, C. R., & Talbot, N. J. (2006). Evolution of filamentous plant pathogens: Gene exchange across eukaryotic kingdoms. *Current Biology, 16*(18), 1857-1864. doi: http://dx.doi.org/10.1016/j.cub.2006.07.052

Roque, D. M., Bellone, S., English, D. P., Buza, N., Cocco, E., Gasparrini, S., . . . Santin, A. D. (2013). Tubulin-β-III overexpression by uterine serous carcinomas is a marker for poor overall survival after platinum/taxane chemotherapy and sensitivity to epothilones. *Cancer, Epub ahead of print*. doi: 10.1002/cncr.28017

Rufatto, L. C., Finimundy, T. C., Roesch-Ely, M., & Moura, S. (2013). Mikania laevigata: Chemical characterization and selective cytotoxic activity of extracts on tumor cell lines. *Phytomedicine, Epub ahead of print*. doi: http://dx.doi.org/10.1016/j.phymed.2013.03.016

Ruiz-Herrera, J. (2012). *Dimorphic fungi : Their importance as models for differentiation and fungal pathogenesis* Retrieved from http://canterbury.eblib.com.au/patron/FullRecord.aspx?p=976645

San-Blas, G., San-Blas, F., Gil, F., Marino, L., & Apitz-Castro, R. (1989). Inhibition of growth of the dimorphic fungus Paracoccidioides brasiliensis by ajoene. *Antimicrobial Agents and Chemotherapy, 33*(9), 1641-1644.

San-Blas, G., Urbina, J. A., Marchán, E., Contreras, L. M., Sorais, F., & San-Blas, F. (1997). Inhibition of Paracoccidioides brasiliensis by ajoene is associated with blockade of phosphatidylcholine biosynthesis. *Microbiology, 143*(5), 1583-1586.

Scharfenberg, K., Wagner, R., & Wagner, K. G. (1990). The cytotoxic effect of ajoene, a natural product from garlic, investigated with different cell lines. *Cancer Letters, 53*(2-3), 103-108.

Shadkchan, Y., Shemesh, E., Mirelman, D., Miron, T., Rabinkov, A., Wilchek, M., & Osherov, N. (2004). Efficacy of allicin, the reactive molecule of garlic, in inhibiting Aspergillus spp. in vitro, and in a murine model of disseminated

aspergillosis. *Journal of Antimicrobial Chemotherapy, 53*(5), 832-836.

Sherr, C. J. (1996). Cancer cell cycles. *Science, 274*(5293), 1672-1677. doi: 10.2307/2890939

Shin, D. B., Yoo, M. y., Seog, H. M., Ha, J. H., Lee, S. H., & Cho, Y. S. (2012). *U.S. Patent No. 20120282334 A1*. Washington, DC: U.S. Patent and Trademark Office.

Shoji, K., Oda, K., Kashiyama, T., Ikeda, Y., Nakagawa, S., Sone, K., . . . Taketani, Y. (2012). Genotype-dependent efficacy of a Dual PI3K/mTOR inhibitor, NVP-BEZ235, and an mTOR inhibitor, RAD001, in endometrial carcinomas. *PLoS ONE, 7*(5).

Slomovitz, B. M., Lu, K. H., Johnston, T., Coleman, R. L., Munsell, M., Broaddus, R. R., . . . Wolf, J. (2010). A phase 2 study of the oral mammalian target of rapamycin inhibitor, everolimus, in patients with recurrent endometrial carcinoma. *Cancer, 116*(23), 5415-5419.

Soeberg, M. (2012). *Cancer trends: Trends in cancer survival by ethnic and socioeconomic group, New Zealand, 1991-2004* Retrieved from http://www.health.govt.nz/publication/cancer-trends-trends-cancer-survival-ethnic-and-socioeconomic-group-new-zealand-1991-2004

Steer, C., & Harper, P. (2001). Is there any place for cytotoxic chemotherapy in endometrial cancer? *Best Practice and Research: Clinical Obstetrics and Gynaecology, 15*(3), 447-467.

Svejda, B., Kidd, M., Kazberouk, A., Lawrence, B., Pfragner, R., & Modlin, I. M. (2011). Limitations in small intestinal neuroendocrine tumor therapy by mTor kinase inhibition reflect growth factor–mediated PI3K feedback loop

activation via ERK1/2 and AKT. *Cancer, 117*(18), 4141-4154. doi: 10.1002/cncr.26011

Taylor, P., Noriega, R., Farah, C., Abad, M.-J., Arsenak, M., & Apitz, R. (2006). Ajoene inhibits both primary tumor growth and metastasis of B16/BL6 melanoma cells in C57BL/6 mice. *Cancer Letters, 239*(2), 298-304. doi: http://dx.doi.org/10.1016/j.canlet.2005.08.022

Tilli, C. M. L. J., Stavast-Kooy, A. J. W., Vuerstaek, J. D. D., Thissen, M. R. T. M., Krekels, G. A. M., Ramaekers, F. C. S., & Neumann, H. A. M. (2003). The garlic-derived organosulfur component ajoene decreases basal cell carcinoma tumor size by inducing apoptosis. *Archives of Dermatological Research, 295*(3), 117-123.

Treeck, O., Wackwitz, B., Haus, U., & Ortmann, O. (2006). Effects of a combined treatment with mTOR inhibitor RAD001 and tamoxifen in vitro on growth and apoptosis of human cancer cells. *Gynecologic Oncology, 102*(2), 292-299. doi: http://dx.doi.org/10.1016/j.ygyno.2005.12.019

Tylicki, A., Siemieniuk, M., Dobrzyn, P., Ziolkowska, G., Nowik, M., Czyzewska, U., & Pyrkowska, A. (2012). Fatty acid profile and influence of oxythiamine on fatty acid content in Malassezia pachydermatis, Candida albicans and Saccharomyces cerevisiae. *Mycoses, 55*(3), e106-e113. doi: 10.1111/j.1439-0507.2011.02152.x

Uchida, M., Mouriño-Pérez, R. R., Freitag, M., Bartnicki-García, S., & Roberson, R. W. (2008). Microtubule dynamics and the role of molecular motors in Neurospora crassa. *Fungal Genetics and Biology, 45*(5), 683-692. doi: http://dx.doi.org/10.1016/j.fgb.2007.10.013

University of Arizona. (2013). Introduction to Mass spectrometry. Retrieved

08/06/2013, from http://www.chem.arizona.edu/massspec/intro_html/intro.html

Van Deemter, J. J., & Zuiderweg, F. J. (1956). Longitudinal diffusion and resistance to mass transfer as causes of non ideality in chromatography. *Chem. Engng Sci., 5*, 271-289.

Vega-Avila, E., & Pugsley, M. K. (2011). An overview of colorimetric assay methods used to assess survival or proliferation of mammalian cells. *Proceedings of the Western Pharmacology Society, 54*, 10-14.

Vilos, C., Morales, F. A., Solar, P. A., Herrera, N. S., Gonzalez-Nilo, F. D., Aguayo, D. A., . . . Velasquez, L. A. (2013). Paclitaxel-PHBV nanoparticles and their toxicity to endometrial and primary ovarian cancer cells. *Biomaterials, 34*(16), 4098-4108.

Wellmer, A., & Bernhardt, H. (1997). Adherence on buccal epithelial cells and germ tube formation in the continuous flow culture of clinical Candida albicans isolates. *Mycoses, 40*(9-10), 363-368.

Witt, D., Burfeind, P., von Hardenberg, S., Opitz, L., Salinas-Riester, G., Bremmer, F., . . . Kaulfuß, S. (2013). Valproic acid inhibits the proliferation of cancer cells by re-expressing cyclin D2. *Carcinogenesis, 34*(5), 1115-1124. doi: 10.1093/carcin/bgt019

Xu, B., Monsarrat, B., Gairin, J. E., & Girbal-Neuhauser, E. (2004). ORIGINAL ARTICLE Effect of ajoene, a natural antitumor small molecule, on human 20S proteasome activity in vitro and in human leukemic HL60 cells. *Fundamental & Clinical Pharmacology, 18*(2), 171-180. doi: 10.1111/j.1472-8206.2004.00219.x

Xu, C., Li, X., Li, T., Wang, X., Yang, Y., Xiao, L., & Shen, H. (2011). Combination effects of paclitaxel with signaling inhibitors in endometrial cancer cells. *Asian Pacific Journal of Cancer Prevention, 12*(11), 2951-2957.

Yamada, Y., & Azuma, K. (1977). Evaluation of the in vitro antifungal activity of allicin. *Antimicrobial Agents and Chemotherapy, 11*(4), 743-749.

Yoshida, H., Iwata, N., Katsuzaki, H., Naganawa, R., Ishikawa, K., Fukuda, H., . . . Suzuki, A. (1998). Antimicrobial activity of a compound isolated from an oil-macerated garlic extract. *Biosci. Biotechnol. Biochem., 62*(5), 1014-1017.

Yoshida, S., Kasuga, S., Hayashi, N., Ushiroguchi, T., Matsuura, H., & Nakagawa, S. (1987). Antifungal activity of ajoene derived from garlic. *Applied and Environmental Microbiology, 53*(3), 615-617.

Zlotogorski, A., Dayan, A., Dayan, D., Chaushu, G., Salo, T., & Vered, M. (2013). Nutraceuticals as new treatment approaches for oral cancer: II. Green tea extracts and resveratrol. *Oral Oncology, 49*(6), 502-506. doi: http://dx.doi.org/10.1016/j.oraloncology.2013.02.011